Quantum Interference of Force: Anomalous Forces in a Quantum Interferometric Context.

Marina Frauendorf Branco Cenni

2016

Universidade Federal de Minas Gerais - UFMG

Instituto de Ciências Exatas - ICEx

Programa de Pós Graduação em Física

Quantum Interference of Force: Anomalous Forces in a Quantum Interferometric Context.

Marina Frauendorf Branco Cenni

Orientador: Pablo Lima Saldanha

Dissertação apresentada ao departamento de Física da Universidade Federal de Minas Gerais, para a obtensão de Título de Mestre em Física

2016

""Throughout the narrative you will find many statements that are obviously nonsensical and quite at variance with common sense. For the most part these are true." ***- Robert Gilmore, Alice in Quantumland: An Allegory of Quantum Physics***"

Agradecimentos

Agradeço primeiramente a Deus, que em todos os dias da minha vida e do meu mestrado não deixou que eu desistisse, e que com certeza é o motivo maior de este texto estar sendo entregue. Ao prof. Pablo Lima Saldanha, pela orientação, apoio, disponibilidade e imensa paciência que teve comigo nos últimos meses - todos estes fatores fundamentais para a conclusão deste trabalho. Ao Raul, que participou mais de perto da criação e evolução do tema da dissertação, por sua ajuda nas nossas reuniões, por todas as suas dicas e sugestões. A todos os meus professores na UFMG, no mestrado e na graduação, que de alguma forma contribuíram para a minha formação. Ao CNPQ e à CAPES, pelo apoio financeiro tão importante durante meus estudos no mestrado. Agradeço também aos meus pais, Marcos e Denise, por sempre apoiarem minhas decisões e me suportarem em tempos difíceis. Sem seu apoio e amor iancondicional eu não teria chegado até onde cheguei. Ao Gustavo e Tainá, minha segunda família, não seria a pessoa que sou hoje se não fosse por vocês!

Resumo

Propriedades físicas associadas aos fenômenos de superposição e interferência quântica têm, ao passar dos anos, se mostrado em direta oposição com a nossa intuição clássica. Neste trabalho, à parte de uma breve revisão sobre as peculiaridades associadas aos fenômenos de superposição quântica e suas consequências, apresentamos e propomos um experimento original no contexto de interferência quântica com o qual introduzimos pela primeira vez a noção de 'Forças Anômalas' existentes em um contexto quântico. Em particular, discutimos como se torna possível que um objeto físico quântico adquira momento linear em um sentido 'errado', após ter interagido ou não com outro sistema físico conhecido dentro de um interferômetro. Mostramos como, nesse contexto, o efeito de superposição de uma força positiva (em um braço do interferômetro) e uma força nula (no braço alternativo) *'gera uma força resultante negativa'* sobre um objeto físico. Quando essa noção é aplicada para dois elétrons dentro de um interferômetro, torna-se então possível simular uma *atração elétrica entre dois elétrons* em um contexto quântico. O trabalho aqui apresentado foi inspirado em um artigo publicado em 2013 por *Aharonov et. al.* [1], no qual os autores discutem a existência de uma *pressão de radiação negativa* de fótons em um espelho quântico. Nesse texto, argumentamos em como esse fenômeno aparentemente ilógico é possível, sendo derivado diretamente de propriedades contra intuitivas da interferência quântica, e propomos uma versão do experimento usando interferência com elétrons com o qual acreditamos que resultados análogos possam ser observados em laboratório.

Palavras-chave: Superposição e Interferência Quântica, Fundamentos de Mecânica Quântica

Abstract

Physical properties concerning the phenomena of quantum superposition and quantum interference have throughout the years been found in direct opposition to our classical every day physical intuition. In this work, together with a brief review on the peculiarities concerning the phenomena of quantum superposition and it's consequences, we present and propose an original experiment in the context of quantum interference in which we first introduce the notion of 'Anomalous Forces' existing in a quantum interferometric context. In particular, we discuss how it becomes possible for a quantum physical object to acquire a physical linear momentum in a 'wrong' direction, after having interacted or not with some other known physical system inside a two-paths interferometer. We show how, in this context, it is as if the superposition of a positive force (in one arm of the interferometer) and a null force (in the alternative arm) '*generated an interferometric negative force*' acting on the interfering physical object. When this notion is applied to two traveling electrons inside the interferometer it becomes possible to simulate an *electric attraction between electrons* in a quantum context. The present work was inspired by a paper published in the year of 2013 by *Aharonov et. al.* [1], in which the authors discuss the existence of a *negative radiation pressure* of photons in a quantum mirror. In this text, we argue on how this seemingly illogical phenomenon comes about, being derived directly from the counter intuitive properties of quantum interference, and propose a version of the experiment using interfering electrons with which we believe that analogous results can be observed in the laboratory.

Keywords: Quantum superposition, Quantum interference, Fundamentals of Quantum Mechanics

Contents

List of Figures

Chapter 1

Introduction

It is reported that, when Einstein sent out his theory of relativity to be published, "he warned them that there were not more than twelve persons in the whole world who would understand it" [12]. On that regard, physicist Richard Feynman remarked, during a lecture opening, that "there was a time when the newspapers said that only twelve men understood the theory of relativity. I do not believe there ever was such a time. There might have been a time when only one man did, because he was the only guy who caught on, before he wrote his paper. But after people read the paper a lot of people understood the theory of relativity in some way or other, certainly more than twelve. On the other hand, I think I can safely say that nobody understands quantum mechanics". He proceeded: "I am going to tell you what nature behaves like. If you will simply admit that maybe she does behave like this, you will find her a delightful, entrancing thing. Do not keep saying to yourself, if you can possible avoid it, "But how can it be like that?" because you will get 'down the drain', into a blind alley from which nobody has ever escaped. Nobody knows how it can be like that".

Of course, it is a bold move to affirm that nobody understands or has ever understood quantum mechanics. And of course, saying something seems incomprehensible is not to say that it is false. But the dilemma surrounding the world presented by quantum mechanics, with all its nuances and although it has already proved itself successful in many ways as a physical theory, is indeed a real one. If quantum mechanics represents the truth about the behavior of the physical world as much as it seems to, it seems to be also possible to affirm that our human minds are simply not naturally 'tuned in' to the way the world is, or to the logic it seems to follow. In this dissertation, we are not interested in discussing in depth the roll of interpretations that the strange world of quantum mechanics suggests, but instead address some of the poignant peculiarities pertaining this theory, and how they seem to oppose our standard every day classical intuition. In particular, in this work we propose an original experiment in the context of quantum interference in which the result that the quantum mechanical formalism yields, although being derived by application of basic concepts, opposes directly our classical logic. In it we show how, in a quantum context, it becomes possible for a quantum physical object to acquire a physical linear momentum in a 'wrong' direction, after having interacted or not with some other known physical system. The two existing and here presented versions of our experiment make use of the quantum superposition phenomena applied to electrons in a two-paths interferometer, and were firstly inspired by the contents of a paper published in the year of 2013 by physicists *Yakir Aharonov, Alonso Botero, Shmuel Nussinov, Sandu Popescu, Jeff Tollaksen and Lev Vaidman*, named "The classical limit of quantum optics: not what it seems at first sight" [1], in which the authors present and discuss a rather astounding existing difference concerning the interpretation of a physical phenomenon when looked at in classical or quantum regimes. This difference in possible physical interpretations in the scenario presented by the *Aharonov et. al.* paper arises from the strange conclusion that the traveling light beam responsible for an existing momentum transfer inside a certain system do not coincide between the two regimes - and that, in the quantum context, the photons found responsible for this momentum transfer are the ones that *could not intuitively be accounted as responsible for it.* In this context it becomes possible to introduce the notion of 'anomalous forces' inside a interferometer. Both discussions, the one contained in *Aharonov et. al.* paper and the one contained in our present dissertation and original proposed experiments, serve well as to enrich and further exercise our knowledge of what can or can not be possible in a world ultimately led by quantum mechanics. Also, we believe that at least one version of our proposed experiment, as opposed to the thought experiment discussed by the authors in the aforementioned paper, is in this day within experimental reach.

In Chapter 2, we start our discussion with a brief exposure of the quantum superposition phenomena, showing some of its peculiar characteristics in order to obtain some intuition pertaining the notion of quantum interference. This chapter is not in any way essential for understanding the original results presented in this dissertation, and a reader familiar with its contents would find no problem in skipping it if they please. Following this first discussion, in Chapter 3, we present a more in-depth overview of the paper of *Aharonov et. al.*, presenting and describing their interferometric thought experiment with light, deriving their results and showing how these results derive in the quantum context directly from a quantum superposition, which is the essential physical phenomenon we are in exploring in this text. Finally, in Chapter 4, we present the discussion concerning our original interferometric experiment with electrons, where we first introduce the notion of 'quantum interferometric anomalous forces', which accounts for our studied possible 'wrong momentum gains' inside a physical system when treated in a context of quantum interference. This central chapter serves as presenting both a new discussion about the seemingly strange effects of quantum interference and superposition and a more viable way of experimentally observing the unusual results of anomalous momentum gain of a physical object due to the phenomenon of quantum interference.

A manuscript containing the here presented original results is currently under preparation and should be submitted for publication soon [13].

Chapter 2

What is Quantum Interference?

For the most part of science history, interference was regarded as a purely classical phenomenon. It is the result of the physical principle of superposition applied to the propagation of waves in a linear medium: the net response at a given point in space-time caused by two or more different incoming disturbances is the sum of the responses that would be generated by each disturbance individually. Mathematically speaking, it is nothing more than the addition of two or more wave functions - functions that satisfy the wave equation - to build the shape of a final wave.

In the year of 1801 Thomas Young performed a double-slit light interference experiment that demonstrated that light had a wave nature, as opposed to the corpuscular theory of light put forward by many philosophers and upheld by Newton in the 18th century [14]. The idea that light could consist of a large number of fast moving particles was then nearly abandoned, and today's classical theory of light, a very fruitful area of physics that culminated in today's Electromagnetic theory, was taking its first steps. It was not until the year of 1900, when Max Planck presented his paper "On the Law of Distribution of Energy in the Normal Spectrum" [15], that the discussion between the two points of view arose again and took a central part in the scientific scenario. Trying to solve a mathematical thermodynamic problem of radiation equilibrium, Planck proposed that the expected results on the black body radiation could be obtained if it could be considered that a light source emits its radiation not continuously, but in equal finite "packs" of energy, the *quanta*. Five years later, Albert Einstein, making use of Planck's *quanta* of light, successfully explained the photoelectric effect [16]. An uneasy question, however, prevailed: if a black body emits discontinuously, in the form of *quanta*, was the radiation not expected too to behave like *quanta* in times past its emission? Is light, after all, not a wave form but is it composed by small separated *grains*, or particles, of light?

Throughout the history of what we now call the “old quantum theory”, which one may say had its beginning with Planck's paper, the fact that light seemed to present a ‘mixture’ of wave-like and particle-like natures brought physicists more questions than answers. At the same time, while the particle theory of light could be used to explain new phenomena, it also obscured what scientists thought they knew about the ‘old’ phenomena. In this dissertation, we are concerned with the physical long-known phenomenon of interference, and how it is understood in the context of Quantum Mechanics, the branch of physics born at the confusing times we briefly described. Interference is no longer regarded as a only classical phenomenon, but the concepts of quantum wave functions and quantum superposition have a richness of their own. Within this new and exciting context, a simple phenomenon such as wave interference can bring us quite counterintuitive results - so much that the famous physicist Richard Feynman, confronted by those, went so far as to call the characteristics of quantum superposition the Quantum Mechanic's "only mystery" [3].

2.1 The Quantum Double Slit Experiment with Light

The principle of the classical ‘double-slit’ interference of light is one easy to follow and is discoursed in detail in elemental text books on Electromagnetism [17]: a light beam, a wave consisting of varying electromagnetic fields, is split in two by an optical device like a semitransparent mirror or a screen with two small apertures, as in the case of the famous Young's double slit experiment. These beams take the two different spatially separated paths and are then reunited in a second screen to form an interference pattern. The light splitting has an important role, since to form the fringes it is necessary that the incoming beams be coherent with each other. The difference in path length is then what generates the light and dark areas on the screen in the form of an interference pattern, as is depicted

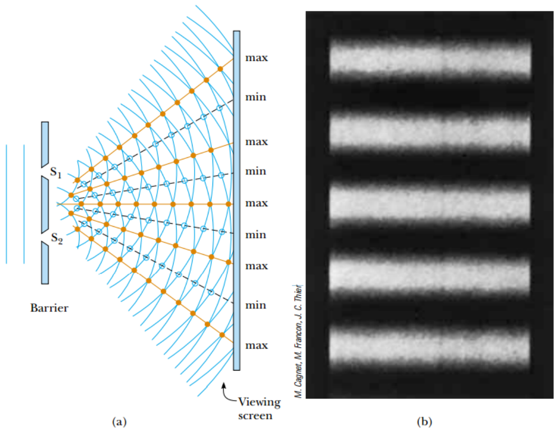

Figure 2.1: An schematic diagram of Young's double slit experiment with light beams. (a) The beam is directed towards a dividing screen containing two small slits S_1 and S_2 that act as coherent sources of light waves and produce alternate light and dark regions on the final screen. (b) Piece on the center of interference fringes formed on the viewing screen. *Image extracted from ref. [2].*

in Fig. 2.1. The total intensity is proportional to the square modulus of the *total* electric field $\vec{E} = \vec{E_1} + \vec{E_2}$, which is the superposition of the electric fields of the wave fronts coming through aperture 1 and aperture 2, at any point x of the screen:

$$I_1 = |\vec{E_1}|^2, I_2 = |\vec{E_2}|^2, \tag{2.1}$$

$$\begin{aligned} I_T &= |\vec{E_1} + \vec{E_2}|^2 = |\vec{E_1}|^2 + |\vec{E_2}|^2 + 2|\vec{E_1}||\vec{E_2}|\cos\delta \\ &= I_1 + I_2 + 2\sqrt{I_1 I_2}\cos\delta, \end{aligned} \tag{2.2}$$

where δ is the phase difference between the electric fields and a function of x, and I_1 and I_2 the wave intensities due to each source individually. If the difference on the path length of light coming from the different apertures is an integer multiple of the light's wavelength, then $\delta = n2\pi$ (where n is an integer) and we have a constructive interference point which results in a light area on the screen. These light areas are then surrounded by dark areas where the opposite situation occurs: the difference on path length is an odd integer multiple of *half* the light's wavelength and the waves interfere destructively. The complete interference pattern is therefore made of these alternating light and dark areas representing high and low wave intensities.

What happens, however, if we lower the intensity of light to the point that only one *particle* of light, or photon, arrives per unity time at the screen containing the apertures? It appears that the light splitting referred above has lost its meaning entirely, as it is expected that, as an indivisible particle, the photon will take one and only one of the two routes possible for it, even if we can not predict exactly what route it would take. The very idea of a light beam is obscured here, and in this new context we can only talk about the probability that the photon will arrive at some given point x on the screen as a function of x. If we kept sending photons to the screen in this way to try to visualize the probability distribution of photon arrival, and had some way to detect each photon as it hits the screen, what we would expect is that we would get a larger number of photons arriving at the center of the receiving screen, and that this number would become lower as the position x drew away from the center. This is, in fact, only what we would get by adding up the probabilities that the photon would arrive at point x with either aperture 1 or 2 closed. That is to say, *we do not expect that the probability of arrival at some point x for the photon coming through one of the apertures would 'interfere' in any way with the analogous probability for the photon coming through the other.* We expect that they will arrive following a classical probability theory, the one followed by billiard balls or any other solid 'particles' we can have direct experience of. This probability distribution, including the *partial probabilities* that are expected with each aperture closed - that intuitively consists of two curves with peaks right in front of each aperture - is represented in Fig 2.2. We can visualize how the curves representing the situations where the photon has only one of the apertures open to it simply add together to a final probability distribution.

Strangely enough, that is not the way photons go. In fact, the probability distribution in x that we would get by doing this experiment in the way just described would be very much alike the intensity curve as a function of x in our classical experiment with a light beam. Even if we can still talk about the partial probabilities of a photon arriving at the receiving screen having passed by a certain one of the two apertures, is it clear now that these probabilities *do not* simply add together. By waiting until many photons have arrived at the screen, what we get is an *interference pattern*, with fringes just like shown in Fig 2.1, and this pattern is again dependent on the difference in length between the two possible paths. This new situation is depicted in Fig 2.3. But how can we understand the formation of this pattern in the photons picture? It does not in principle seem illogical that we can say for sure that the photon has passed through only *one* of the two apertures. Consequently we could as well assume that one photon could only "know" about the length of one of the two paths - but how then can the photons arrive in a pattern that depends on the *difference of length* between these paths? One can argue that, indeed, the interference pattern can be formed only by a collection of photons arriving after a long exposure time, and this collection as a whole could have all the available "knowledge" about the paths. That would imply the interference effect to have some large dependance on the intensity that we sent the photons through the screen: by lowering this intensity, at some point the interference pattern would start to become blurry and then, by the time each photon became spatially separated from all other photons in the experiment so that no information from one could reach another, it would not exist at all. But that isn't what happens. The 'visibility' v, $v = (I_{max} - I_{min})/(I_{max} + I_{min})$, where I_{max} and I_{min} are the maximal and minimum 'intensities' (proportional to the probability of photon arrival) of the fringes, is not dependent on the intensity we send the photons in. Experiments at very low light intensities have already been performed and confirmed this in the twentieth century [18, 19].

It is now known that *the probability of photon detection doesn't just add together classically, but mathematically it behaves exactly like the classical electromagnetic fields*:

$$
\begin{aligned}
P_1 &= |\varphi_1|^2, P_2 = |\varphi_2|^2, &\quad (2.3)\\
P_T &= |\varphi_1 + \varphi_2|^2 = |\varphi_1|^2 + |\varphi_2|^2 + 2|\varphi_1||\varphi_2| \cos\delta \\
&= P_1 + P_2 + 2\sqrt{P_1 P_2}\cos\delta, &\quad (2.4)
\end{aligned}
$$

where φ_1 and φ_2 are the *wave functions* associated to the existing possible paths for the photons, and δ the phase shift between them.

This is a mathematical result that can't be obtained by any simple classical method that considers single photons traveling through one aperture or the other. And yet that is the probability curve we can test in the laboratory, had we performed the above experiment. We should note, however, as much mathematically alike these results are, that there is an important difference here in what concerns the interpretations of the two theories, the quantum and the classical, in the double-slit experiment and in any context when speaking about interference in physics. The *wave functions* φ_1 and φ_2, the actual mathematical

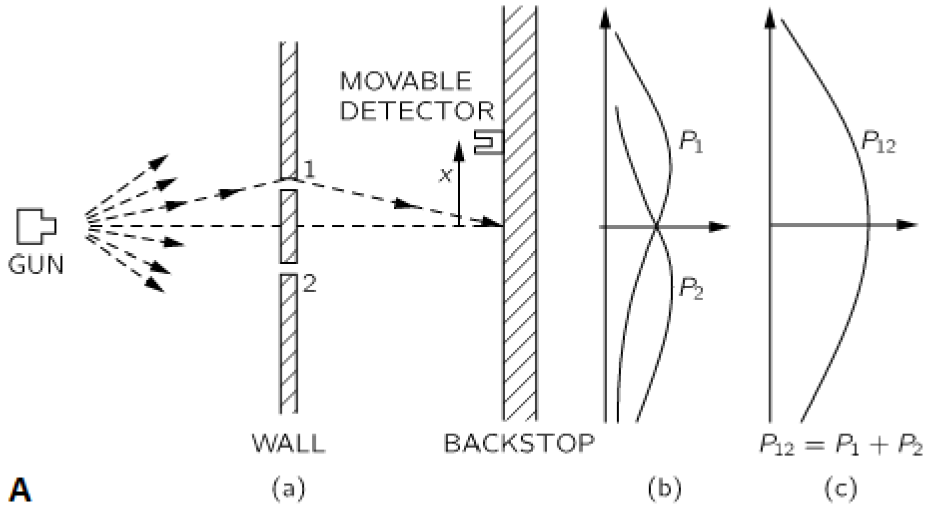

Figure 2.2: Classical particles are sent through a dividing wall (a) containing two apertures of enough size. A second wall works as a backstop for the incoming particles, and a movable detector is introduced to measure the rate that these particles arrive as a function of the position on the backstop wall. In (b), it is shown the partial probabilities P_1 and P_2 that the particles will arrive at the backstop wall having passed through aperture 1 OR 2, respectively. These partial probability curves can be achieved by closing one of the apertures at the first wall so that the particles can only go through the other during the experiment. In (c), there is the total probability curve for the arrival of the classical particles. This curve can be achieved by the simple sum of the partial probability curves, so that $P_{12} = P_1 + P_2$. *Image from ref. [3].*

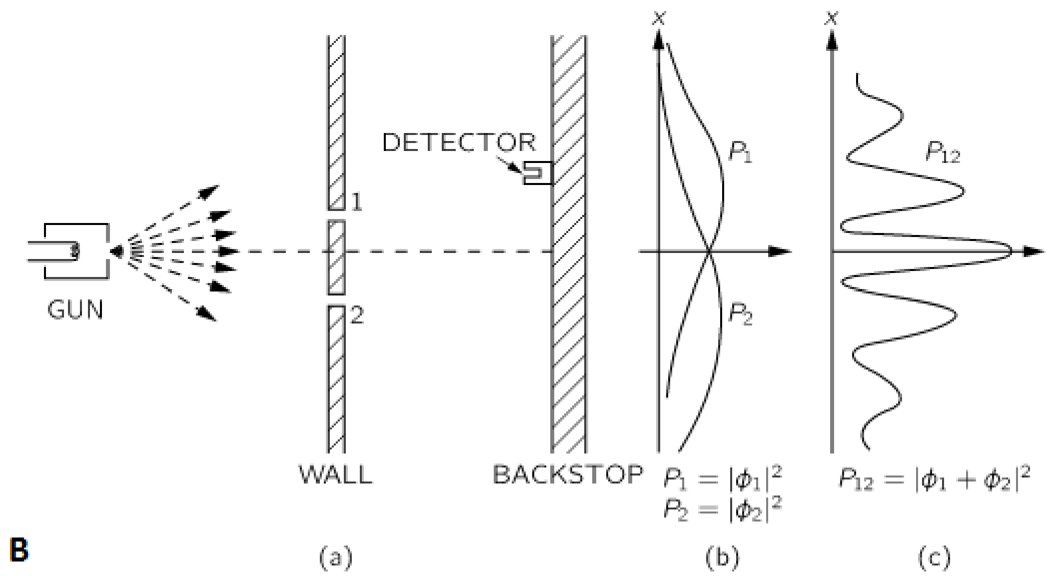

Figure 2.3: Young's double slit experiment with single photons. It is clear here that the photons do not behave as classical particles. The partial probabilities for the photon to have passed through a given aperture (b) don't simple add together to a final arrival probability (c), and $P_{12} \neq P_1 + P_2$. However, the *probability amplitudes* corresponding to each possible indistinguishable path for the photons are additive and the total probability of photon arrival as a function of the position at the final screen is the square of the absolute value of the total probability amplitude. *Image from ref. [3].*

amplitudes that arrive at the final screen and are what we can indeed associate with each path, are now *complex* functions of time and space variables. In general we can't work only with the real parts of these amplitudes, and, differently from the case of the classical electromagnetic fields, *we cannot really regard this functions as real disturbances in space-time*. Due to this, in spite of the equivalent mathematical results, there is an essential difference between the two phenomenons, or between the same phenomenon in the two regimes, the quantum and the classical. We can only use and talk about the "wave functions" of the photons as what they are: *quantum probability amplitudes*, that do not exist in space-time. Within this scenario we can say that the photons, arriving one by one at highly localized points in our final screen are detected discretely and thus behave like particles, however that the probability amplitude's of detecting each photon interfere like waves.

As about the common question of 'what if we tried to track the photons to see which route it has taken inside the interferometer before its detection?', it is a frustrating but well known fact to physicists that there is no way to do so and at the same time maintain our interference pattern. In the case of the double-slit experiment, anything that can be used to measure the complete 'which-way' information of the photon disturbs its path in such a random way that a photon that could be going to end up in a peak of arrival probability actually ends up in a minimum of arrival probability, and this randomness acts as to mimic classical probability distributions and destroy the fundamental quantum interference effect we wish to observe. The 'principle' invoked by physicist Niels Bohr to to explain this feature of quantum behavior was the Heisenberg's *uncertainty relations*, more precisely the uncertainty relations applied to the conjugate pair of the position and momentum operators. They state that the product of the 'uncertainty' of the dynamical variables associated to these two operators has a lower bound, and as a result it fundamentally says that, even at the most perfect laboratory conditions, there is a limit of what we can know about one without essentially altering the other. As a result, measuring the position of the photon just after it has passed through a slit alters its momentum just enough so that we lose the interference. In fact, as we now know, the complete theory of quantum mechanics depends so much on the correctness of these relations that, if they were proven wrong, and there was no essential limit on the knowledge about two conjugate quantities, we would need a throughout reformulation of the theory.

To see how the interference pattern is intrinsically dependent on the which-way information of the photon, and how this is a result that comes naturally in the context of quantum mechanics, we will discuss briefly a thought experiment [3] used by Richard Feynman to introduce quantum mechanics and quantum behavior. Let us imagine that behind each aperture of the first screen in our interference experiment there is some imaginary system that accuses the photon to have passed through it. The result does not depend on the specifics of this system, so it could be anything that marks the way of the photon - lets say it scatters some particle at a detector near it with some fixed probability. We do the exact same behind the other aperture. Also, we don't want our path marking to be perfect, and to add a source of error we include another probability, small compared to the first, that the detector behind one aperture will trigger even though the photon has taken the other way. (See Fig 2.4.)

As before, we write the amplitude that a photon sent by a source S will arrive at the position x of the screen having passed through aperture 1 as φ_1, and the analogous amplitude for aperture 2 as φ_2. Those would be the final amplitudes if there was nothing behind the first screen. We consider now the existence of the detectors D_1 and D_2 as our 'flawed' path-markers. What is now the amplitude that the photon will be emitted by source S, pass through aperture 1, trigger the "correct" detector D_1, and arrive at the second screen at position x? If a is the probability amplitude that a photon coming through aperture 1 will trigger the detector D_1, the total amplitude in this case is the product of the two probability amplitudes, $a\varphi_1$. If b is the smaller probability amplitude that the photon coming through aperture 2 would "wrongly" trigger detector D_1, the analogous amplitude in this case would be $b\varphi_2$. So the total probability amplitude that detector D_1 will be triggered by a passing photon is the sum of these two probability amplitudes, and the total probability of this event is the square of the sum of the amplitudes:

$$P_{D1}(x) = |a\varphi_1 + b\varphi_2|^2. \tag{2.5}$$

Following this line, analogous amplitudes exist for the cases where detector D_2, not detector D_1, is triggered. If we assume for simplicity that the system is symmetric, and we can use amplitudes a and b in an analogous manner, the total probability of this event is then calculated as:

$$P_{D2}(x) = |b\varphi_1 + a\varphi_2|^2. \tag{2.6}$$

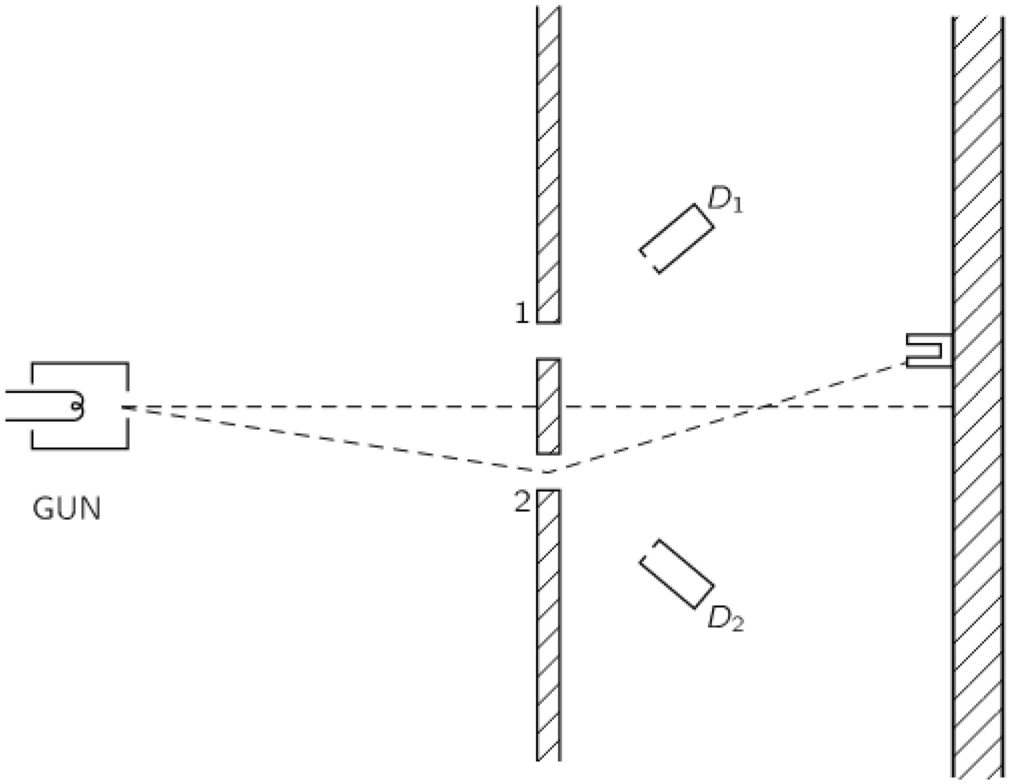

Figure 2.4: Two detectors, D_1 and D_2, are placed behind the dividing screen of a double-slit interference experiment of single photons. The detectors are placed in the vicinity of the apertures 1 and 2 of the dividing screen, and can 'detect' the passage of the photons via any third physical system that can accuse a photon to have passed through it. The probabilities of detection in the various situations can be fixed at will for the purposes of this imaginary experiment. *Image from ref. [3].*

Finally, the total probability that the photon sent by source S will arrive at a certain position x of the second screen and in its way trigger *any one* of the two detectors is:

$$P_T(x) = |a\varphi_1 + b\varphi_2|^2 + |b\varphi_1 + a\varphi_2|^2, \tag{2.7}$$

where φ_1 and φ_2 are both (complex) functions of x.

Here, we do not add all the existing probability amplitudes and then take the square at the end because the events where D_1 and D_2 are triggered are *distinguishable events*, and we only add up amplitudes for events that are *indistinguishable*, for those are the events that can interfere in accord to the quantum formalism.

Taking a look at this expression we can see what happens if, for example, $a = 1$ and $b = 0$. This is the specific case where a passing photon always trigger a detector, and it is always the "correct" one. This represents a perfect marking of the photon's path. In this case the probability is just the sum $|\varphi_1|^2 + |\varphi_2|^2$ of partial probabilities, which is just the expected classical result, representing no interference pattern. Even if a differs from unity (but still we keep $b = 0$, $a < 1$), this probability is then just reduced by a factor $|a|^2$ and still we get no interference for the photons that have triggered the detector. We say that the detection at D_1 has reduced the 'visibility' of the interference. But if a is practically equal to b, and the "wrong" and "right" detectors have nearly the same chance to be triggered whenever a photon enters the interferometer, then the final probability distribution becomes $|\varphi_1 + \varphi_2|^2$ (multiplied by the factor $|a|^2$), the result we would get in the case where we have no detectors at all. In the intermediate cases, where the detection is partially effective, we get more complicate forms for the final probability at the screen and therefore intermediate forms of the interference pattern. It is clear by this example that the dependence of the existence of quantum interference on path marking is something very intrinsic to the indeed 'mysterious', but very successful quantum mechanical formalism.

In talking consistently about probabilities, we have thus implied that probabilities are all the information quantum mechanics can give us, and this is actually absolutely right. As opposed to classical mechanics, where, if given all information, in principle *everything* can be predicted, in quantum mechanics we get only the outcome's probabilities, sometimes even in the more perfect scenarios. It is in general impossible to predict exactly what would happen in a given situation, and, as we have discoursed in this section, it is in general impossible to know exactly what *is* happening - the question of 'where did the photon pass through' is almost a 'forbidden' question here, in the sense that trying to answer it generally only brings us inconsistencies. This has given birth to many different quantum mechanical interpretations, and many of them exists 'till today - though we are not concerned here about the details of existing interpretations, but with the properties held by quantum interference phenomena and confirmed by experiments even within the context of seemingly illogical physical effects of self-interference of single photons. We continue then, in the following sections, to explore these properties and try to gain some intuition about the behavior of particles in the quantum regime.

2.2 Matter Waves and the Complementarity Principle

Surprisingly, we are able to get interference patterns in a double-slit interferometer for light *even* in the single photons regime, and those patterns are formed at our screen following the *exact same* mathematical rules as for high intensity light beams. Although this is true, a very different story can be told about these two (mathematically identical) situations that put them widely apart when it comes down to our interpretations and concepts about the physical world. While the latter can be completely and satisfactorily explained by use of electromagnetic fields following the wave equation, we seem to lose our ground when trying to grasp the reality of the first. It still seems illogical that physical indivisible objects could 'interfere with themselves' to produce visible, real interference fringes. Wave and particle properties and concepts seem to be intertwined in a single, strange physical being. As was mentioned in the introduction to this chapter, what brought the discussion back about what could be the real nature of light, even years before the double-slit interferometer experiment was ever performed in the quantum regime, was the paper published by Max Planck in 1900 where he introduced to the scientific world the mathematical concept of energy divided in packs, the later named *photons*. In this paper it was showed how the paradoxes surrounding the black body radiation curve could be solved by the quantization the energy exchange between light and matter - a concept that, as we now know, followed by Einstein's quantization of radiation energy, came to be very fruitful and escalated to the development of the modern quantum theory. The so introduced Planck's indivisible packs of energy followed the simple mathematical relation:

$$W = hv, \tag{2.8}$$

where W is the total energy of the *photon*, v is the frequency, and h a mathematical constant known as the Planck's constant. The first noticeable thing about this relation is that at first sight it seems to present us with some kind of inconsistency. Through it an indivisible photon can be identified with a *frequency*, knowingly a wave property. What is the kind of periodicity that can be intrinsically attributed to a single, indivisible object? From this early relation, it seemed to be clear that a theory that guides the photon's behavior could not be a purely corpuscular, nor a purely wave one.

So, even though light was found to be composed by groups of indivisible separated photons, it could still be associated with different *frequencies*. In times following Planck's paper, physicist Louis de Broglie was intrigued by the fact that small known particles were at times demonstrating to posses behavior properties not normally attributed to indivisible corpuscles. Borh's theory for the atom, for example, included quantized orbits for the electrons around the nucleus - so that the atoms could be stable, the energy levels of those electrons had too to be *quantized* [20]. It was in this context and encouraged by these apparent inconsistencies around the behavior of both photons and matter that de Broglie proposed for the first time a sort of parallelism, and shook the scientific world with a strange idea [21]: *just as light demonstrated to have both particle-like and wave-like properties, so should all matter present this duality and possess in themselves both properties of wave and particles.* This parallelism is well expressed in de Broglie's own words:

> '(...)Firstly the light-quantum theory cannot be regarded as satisfactory since it defines the energy of a light corpuscle by the relation $W = hv$ which contains a frequency v. Now a purely corpuscular theory does not contain any element permitting the definition of a frequency. This reason alone renders it necessary in the case of light to introduce *simultaneously* the corpuscle concept and the concept of periodicity. On the other hand the determination of the stable motions of the electrons in the atom involves whole numbers, and so far the only phenomena in which whole numbers were involved in physics were those of interference and of eigenvibrations. That suggested the idea to me that electrons themselves

> could not be represented as simple corpuscles either, but that a periodicity had also to be assigned to them too. I thus arrived at the following overall concept which guided my studies: for both matter and radiation, light in particular, *it is necessary to introduce the corpuscle concept and the wave concept at the same time.* In other words the existence of corpuscles accompanied by waves has to be assumed in all cases.' [22]

In his doctoral thesis, and making use of relativistic principles we will not dive into, de Broglie showed how any moving piece of matter can be associated with a wavelength λ following the relation:

$$p = h\lambda = \hbar|\vec{K}|, \tag{2.9}$$

where p is the total momentum of the particle's center-of-mass, $\vec{K} = 2\pi/\lambda$ is called the *wave vector* and $\hbar = h/2\pi$. Both relations (2.8) and (2.9) were now considered applicable for all physical objects, light or matter, in the exact same fashion.

The wave nature of electrons was first demonstrated in an experiment performed by Davisson and Germer just a few years after de Broglie's proposal [23]. Atoms in a crystal act as a tridimensional arrange of diffraction centers for the 'electron waves', strongly scattering the electrons in various characteristic directions, just as had already at the time been demonstrated to occur for the case of X rays. The results of this experiment could only be explained as being a result of the *constructive interference* of waves scattered by the periodic array of atoms in the planes of the crystal, in complete analogy with the already known *'bragg reflections'* for light. The form of the diffraction patterns obtained by this method experimentally confirmed the validity of the de Broglie relations for the case of electrons.

It is in this manner and in this sense that both light and matter were found to hold in themselves two apparently confronting natures, depending on when or how they were observed. Strangely, that is indeed the common sense for things existing on a quantum scale - they are unlike anything our classical minds can have any direct experience of. Electrons were first introduced to our knowledge as very small particles constituting an important part of the atomic structure of our universe, yet as we now know they can be demonstrated to behave as something rather stranger. Electrons are not only particles and they are not only waves - they can behave like both and, therefore, overall they really behave like *neither*. They are neither. However, physicist Richard Feynman pointed out a lucky break: *electrons* *behave just like light. The quantum behavior of atomic objects (electrons, protons, neutrons, photons, and so on) is the same for all, they are all "particle waves", or whatever you want to call them* [3]. All objects in the quantum world posses strange, extremely counterintuitive behaviors, but they all act strangely in the same manner. Therefore, all of the essential results of quantum theory are valid for all these small physical objects, including the results surrounding the double-slit interferometer experiment that was discussed in Sec. 1. It is possible, today, to perform a double slit interferometry experiment using single electrons, and we shall deeply explore this idea in the last part of this dissertation.

One such experiment was performed by the Hitachi Group in 1989 [4]. Instead of a screen with two apertures for the passage of the electrons, in their experiment an electron biprism was used to spatially separate the two possible paths of the interferometer. This biprism consists of two parallel plates with a thin positive charged filament placed at the center. A sketch of the used experimental apparatus is depicted at Fig 2.5. Electrons emitted by a source can pass on either side of the filament when passing through the electron biprism, and the interference of the amplitudes associated with each of these two paths is captured by an specially modified detecting screen that accuses each electron's arrival by a light emission. At first the electrons seem to arrive at random positions at the detecting screen, but enough exposition time reveal the formed interference fringes (See Fig 2.6). In this experiment the electrons were accelerated to reach 40 percent of the speed of light and were emitted at time intervals such as that no more than one electron traveled inside the interferometer at the same time.

In 2002, science historian Robert Crease asked the readers of the *Physical World* magazine to submit candidates for the 'most beautiful experiment in physics' [24]. The leading result of a list published in the September edition was the Young's double slit interferometer experiment applied to the case of single electrons. What is it that makes the single electrons interference pattern so astoundingly beautiful, when by the time it was first performed so many strange quantum results had already been experimentally tested? Quoting Mark P. Silverman, maybe "*the unambiguous directness of the observable results, despite being expected, have the capacity to shock the intellect into realizing, like no mathematical proof is capable of achieving, that the formalism of quantum mechanics reveals a strange and disturbing reality*" [25]. In the closing remarks of his report, Crease wrote:

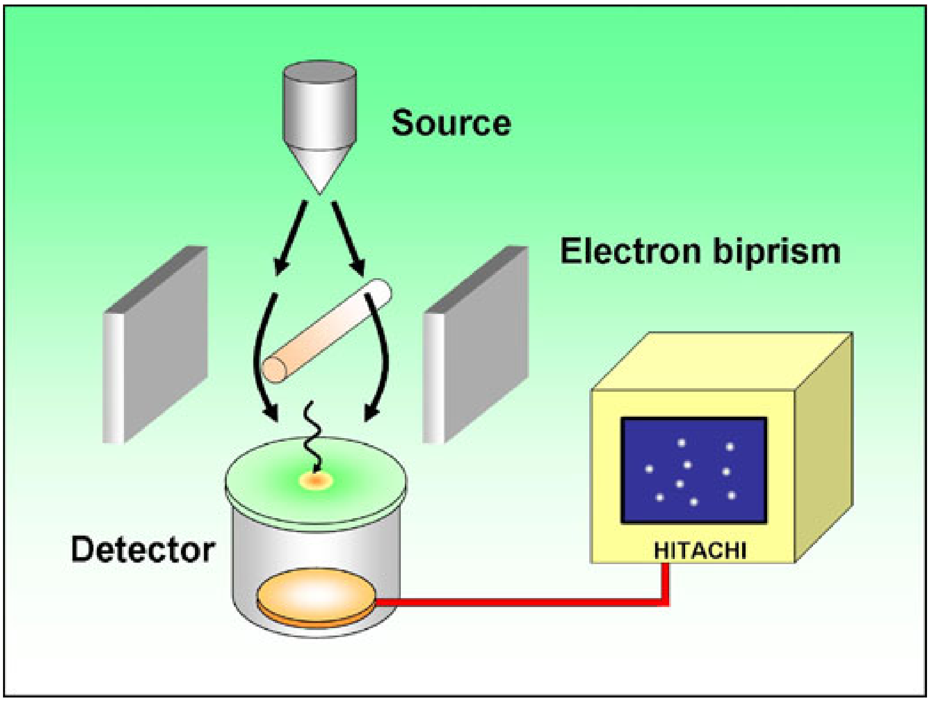

Figure 2.5: Experimental apparatus of the HITACHI double-slit interference experiment with single electrons. The path division is accomplished by a thin filament positioned inside an elelctron biprism. *Image extracted from ref. [4].*

> It is natural to call beautiful those [experiments] that captivate and transform our thinking, that make the result stand out clearly [. . .] in a materially embodied way, and that reveal that we are actively engaging with something beyond us.

It is not just electrons that were observed to have a wave nature. Another experiment that well illustrates the wave behavior of matter, this time presented by atoms and molecules, is an interferometric experiment performed in the year of 1995 by Michael S. Chapman *et. al.* [5]. In this experiment the center-of-mass of atomic and molecular sodium particles could be coherently manipulated and their wave properties could so be visualized and demonstrated. Nanofabricated diffraction gratings were used to measure the properties of the object's diffraction. Also, for this experiment a pure molecular beam was created so that the wave properties of the Na_2 molecules could be solely analyzed. This was accomplished by use of resonant light pressure forces acting solely on the atomic specimens to deflect them sideways from a previously created mixed beam containing both Na and Na_2 specimens. This situation is depicted in Fig 2.7. The deflecting laser beam was produced with a laser tuned to the $F = 2 \rightarrow F' = 3$ transition of the D2 line in Na (589.0 nm). The

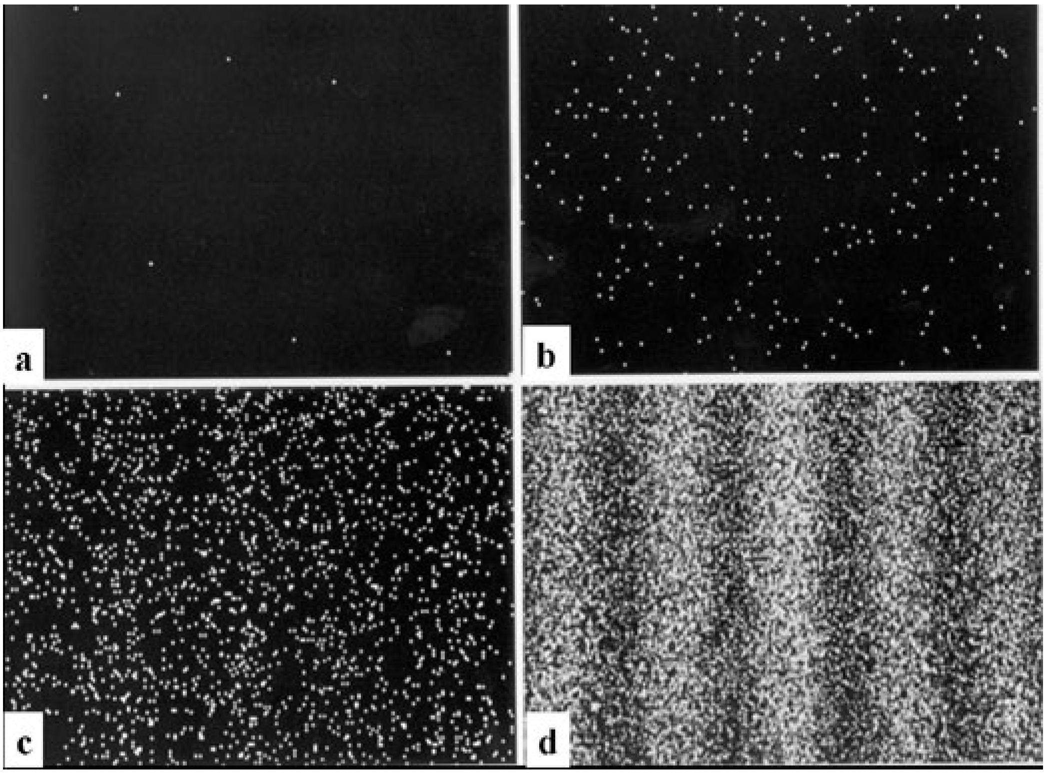

Figure 2.6: **Figure 4.** The arrival pattern for single electrons in a double slit interference experiment for increasing exposition times. Each image correspond to: (a) 8 electrons; (b) 270 electrons; (c) 2000 electrons; and (d) 160 000 electrons. The total exposure time to form the final image (d) was of 20min. *Image extracted from ref. [4].*

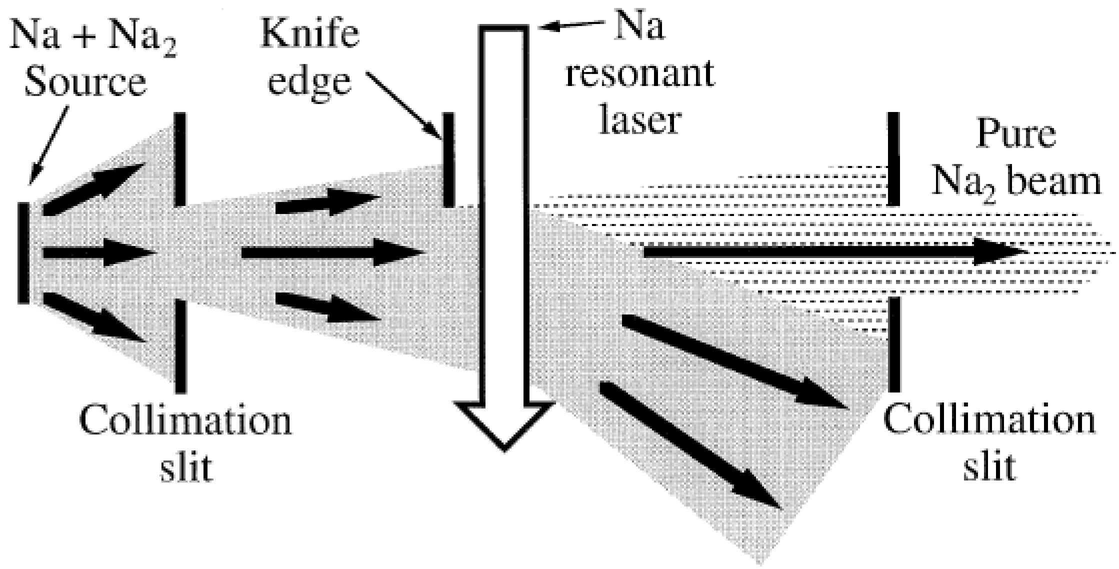

Figure 2.7: **Figure 5.** Sodium atoms are removed from a mixed beam containing both Na and Na_2. The deflecting lased gives transverse momentum to the atomic specimens, thus deflecting them away from the final collimation slit. A knife edge blocks the sodium atoms that could escape the deflecting process. *Image extracted from ref. [5].*

Na_2 molecules are not resonant with this deflecting laser and were therefore unaffected by its presence.

Since the atomic and molecular specimens in the previously created mixed beam had nearly the same velocity, their momenta and therefore their de Broglie wavelength differ by a factor of 2 due to their mass difference. Fig. 2.8(a) shows the measured diffraction pattern of the matter beam using a nanofabricated 100nm grating in the case where the deflecting laser was turned off and the beam remained in its mixed form. The diffraction grating can be seen as a *multiple slit interferometer* having a 100nm separation between its various slits, with quantum interference happening due to the superposition of the this time various possible paths for the diffracted physical objects. We see that the diffracted orders of the atomic sodium specimens are well resolved and sufficiently separated so that the intermediate molecular diffraction peaks at half the atomic diffraction angles can be unambiguously identified. When the deflecting laser is turned on, the diffraction pattern for a nearly pure Na_2 molecular beam is resolved out to the fourth diffraction order, as shown in Fig 2.8(b). The use of these nanofabricated diffraction gratings for matter waves constitutes a powerful experimental non-destructive way of analyzing the properties of very weakly bound matter systems, and have been also used for example to produce evidence of the existence of He_2 molecules [26]. The interference patterns arising from matter wave diffraction at material diffraction gratings were experimentally observed even for much larger objects such as C_{60} molecules [27].

Hence, we see that the wave-like and particle-like behaviors of both radiation and matter were, with experimental evidence, undoubtedly established - physicists now accept that they must 'borrow' concepts from *both* models for any complete description of the same physical entities. It is very important to note here, however, that these concepts *cannot* be applicable simultaneously. In fact, the wave-like and particle-like behaviors of physical objects are *complementary* behaviors, in the sense that a single object cannot depict both under any single experimental context. This *complementarity principle* was first introduced and strongly upheld by Niels Bohr in the last century, in an attempt to embrace in it the singularities held by the known quantum phenomena at the time and to clarify peculiar aspects of observational problems within this scientific field [28, 29]. The complementarity principle is an interesting one, and derives from the notion that the account of our knowledge about the physical reality can be achieved only through experimental data, and this data must in turn 'speak our classical language'. In other words, as much as the physical reality of events deviates from those of our classical, intuitive world, any evidence that can be tested in our laboratories must be expressed in our own classical terms. This corresponds to an inseparability between what we can know about the behavior of existing physical objects and the necessary, uncontrollable interaction that these objects have with our classical apparatus. Bohr named it an 'individuality' of typical quantum phenomena that any attempt to subdivide these phenomena to create new observational evidence will demand an exchange of the experimental arrangement, uncontrollably introducing new possibilities of interactions between the central physical objects and our measuring devices that act as to change our whole observational picture. These studied objects cannot, therefore, be comprehended within single pictures, and *only the totality of observational phenomena can 'exhaust the possible physical information about them'*. The contexts where these two seemingly irreconcilable types of behavior, particle and wave, appear, correspond in the context of complementarity to mutually exclusive experimental builds. We choose by each placing or configuration of the experimental apparatus which behavior is it that we are going to observe, and only

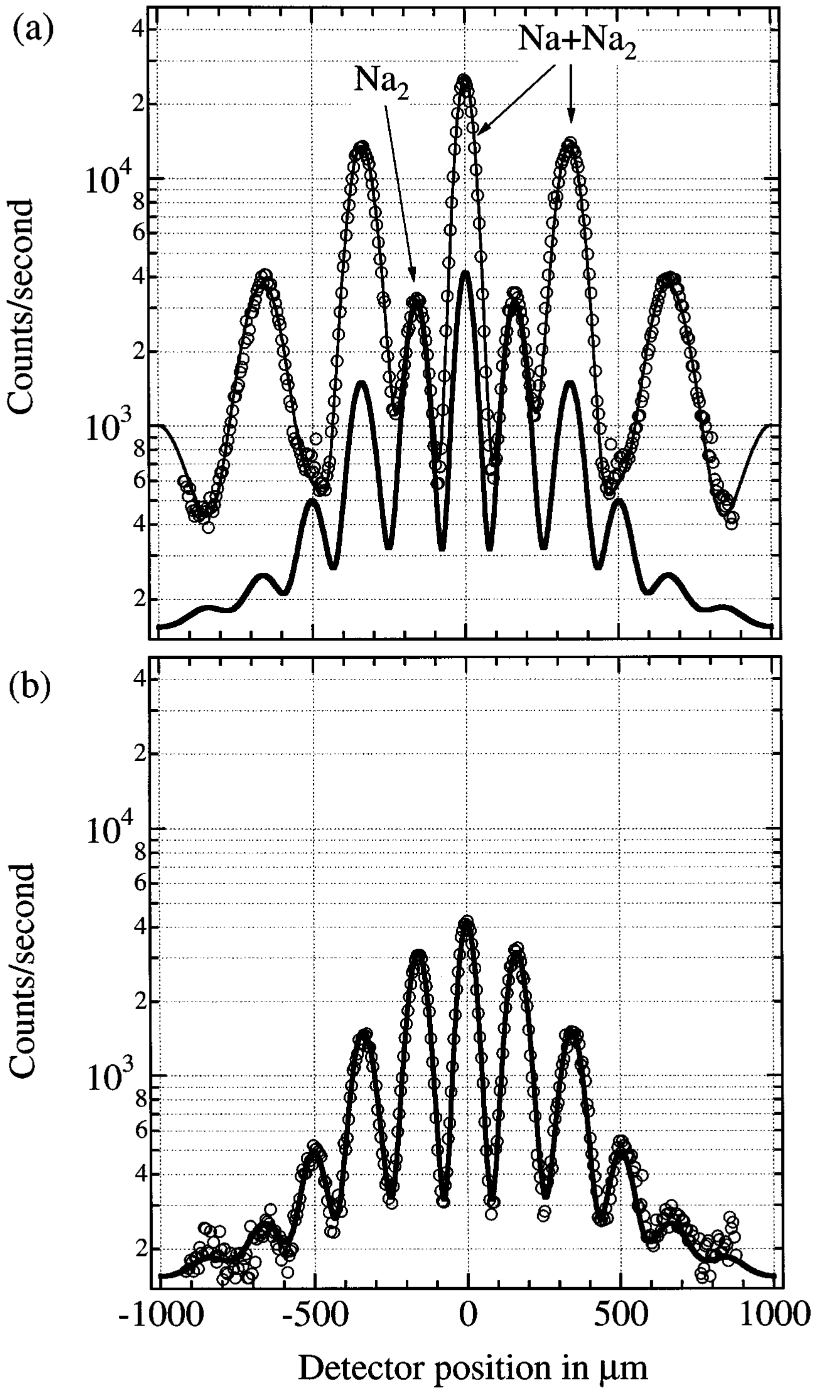

Figure 2.8: **Figure 6.** (a) Diffraction patterns of the mixed atomic/molecular sodium beam when the deflecting laser is turned off and (b) of the molecular sodium beam by a nanofrabricated grating of 100nm period. The thin solid line in (a) is a fit for the diffraction pattern of Na_2 and indicates that 16,5 percent of the detected intensity are from the molecular specimens when the deflecting laser is off. *Image extracted from ref. [5].*

taking account of all of these contexts together can bring us all the information needed to a complete knowledge of these quantum entities.

Concepts contained in Bohr's complementarity principle bring into scene the question about the reality of unobserved physical phenomena. By saying that we can only talk about what has, in fact, been measured, and that the simple act of performing a measurement on a system always includes uncontrollable physical interactions between this system and our measurement devices, the question is open about what was 'really' there before any measurement was made. For example, can we as physicists affirm, after having obtained a measured result about a certain physical quantum system, that this result was true even before our act of measurement had been performed? The answer is, typically, "No". This kind of classical objectivity appears to be simply lost at this point. Even the concept of physical 'realism' becomes, in the context of Bohr's quantum mechanical complementarity, questionable. Such perturbing ideas have historically found resistance in famous physicists such as Einstein, Planck and Ehrenfest. Reffering to those, Heisenberg wrote:

> "... all the opponents of the Copenhagen interpretation do agree on one point. It would, in their view, be desirable to return to the reality concept of classical physics or, to use a more general philosophical term, to the ontology of materialism. They would prefer to come back to the idea of an objective real world whose smallest parts exist objectively in the same sense as stones or trees exist, independently of whether or not we observe them."

The measurement problem in quantum theory was and is an exhaustive theme of research and much can be gained by the studies of its characteristics and implications [30, 31, 32].

The 'self-interference' of particles, the intrinsic wave nature of matter and the complementary principle are all parts of a whole that sometimes we may find difficulty in accepting, but are every bit as scientific as any other seemingly 'less fantastic' theory is. This apparent fantastic or 'mystic' aspect of quantum theory is probably the reason why its name has derived so much into less scientific statements and beliefs of the modern popular imagery. It is clear that there are times when may find necessary to adjust our intuition and question our previously untouchable statements in order to be able to better explore this quantum '*brave new world*'. With this in mind, we continue our discussion of the properties of quantum particles, specially concerning the characteristics and apparent paradoxes of quantum superposition and quantum interference phenomena.

2.3 Wheeler's Delayed Choice Experiment

Perhaps the most unsettling feature of the Young's double-slit interference phenomenon with single photons is the apparent incompatibility between our classical concepts of a spatially distributed wave traveling through two different paths at once and a localized particle that can only take one path at a time. Intrigued by this incompatibility and by the fact that how we choose to perform the experiment seems to define which type of behavior we expect to observe (a good example would be the thought experiment that was briefly described in the first section of this chapter, where we could choose between placing or not the two detectors behind the screen and observe or not the full interference pattern), various thought experiments were proposed around the end of last century to try to answer the question: since the photons can take either a wave-like or a particle-like behavior, but not both at the same time, at what time does the photon 'chooses' how it is going to behave? The question essentially means to test the possibility that the photon could 'sense' what lies ahead of its path and previously adjust its behavior accordingly, or if it remains in a indeterminate form until the time of its detection. These famous thought experiments were proposed by John Archibald Wheeler in his paper named "The "Past" and the "Delayed-Choice" Double-Slit Experiment" [33].

The delayed choice experiment consists in determining the final configuration of the experimental apparatus in a time past the entry of the photon in the interferometer. In that manner, even if the photon could somehow sense this configuration before-time and 'decide' between behaving as a wave by taking both paths or behaving as a particle and taking a single path, it could not have known at which configuration the apparatus would be by the time it left the interferometer. This would bring up an apparent paradox if a last minute change in the configuration indicated that the photon could have decided to behave in an opposite way even after having 'chosen' previously about its paths. As to make clear the implications of this, an ingenious version of the experiment was proposed by Wheeler that consists in considering a giant, cosmic interferometer of single photons [33]. In this cosmic version of the delayed-choice experiment we imagine a photon source on a distant quasar,

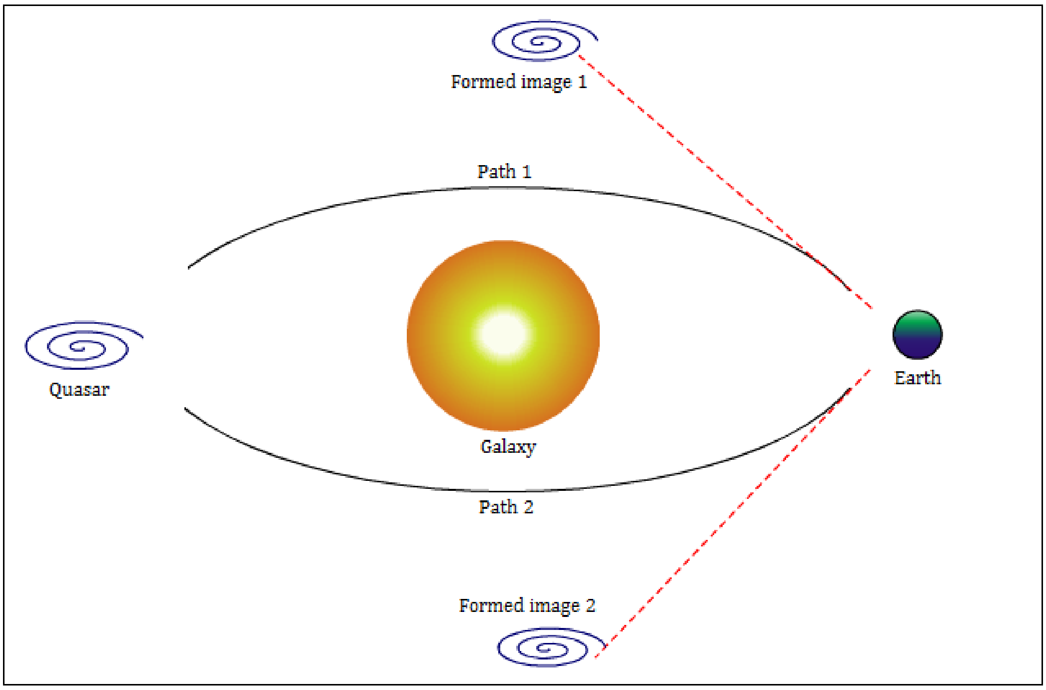

Figure 2.9: Cosmic version of the delayed-choice interferometric thought experiment (not in scale). A photon coming from an emitting distant quasar can reach a point on Earth traveling through two possible paths. The image indicates the two formed images of the quasar if looked directly with a telescope. How an experimenter on Earth decides to measure the incoming photons determines the type of behavior he is going to observe.

billions of light-years away from Earth. Midway across this distance there is a galaxy or cluster of galaxies that act on the photon as a gravitational lens. The distortion in space-time in the vicinity of this galaxy would alter the path of the photon as to send it directly towards some point on Earth, however this photon could reach this point either by passing by one side of the galaxy or the other. A physicist on Earth could then make a choice of how he wishes to observe the incoming photons. He could either point his detectors - lets say telescopes - directly at the two formed images of the quasar, and by it infer that light has traveled billions of years as a particle, or make the more complicated choice of combining the output of the two telescopes in a single beam-splitter device to form interference fringes and by it infer that light has traveled billions of years as a wave. Fig 2.9 represents a sketch of this thought experiment.

Fortunately there are simpler ways where we could test this assumptions and analyze the complete behavior of the photons in a delayed-choice type of experiment in the laboratory.

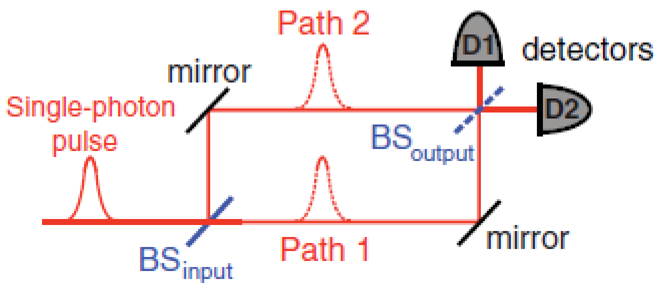

Figure 2.10: Mach Zehnder interferometer for single photons. The presence of the output beam splitter BS_{output} represents the closed configuration of the interferometer. When BS_{output} is absent, the arrival of the photons at each one of the final detectors D_1 and D_2 correspond to a determined path inside the interferometer and the interference effect is lost. *Image extracted from ref. [6].*

For this consider a Mach-Zehnder interferometer of single-photons sketched in Fig 2.10. This represents a closed configuration of our interferometer, where the first beam-splitter BS_{input} gives the photon an equal probability of being transmitted or reflected, and thus separates spatially the two possible paths for the photon. The photon is thus in a superposition of amplitude components associated with the two arms of the interferometer. If we denote the states corresponding to each of the separated path directions as the state vectors $|I\rangle$and $|II\rangle$, then the total state of the photon just after having passed through beam-splitter BS_{input} can be written in the form of a quantum superposition as $|\Psi\rangle = (|I\rangle + i|II\rangle)/\sqrt{2}$, where i represents the phase shift due to a reflection on the beam-splitter. The paths are then recombined and made to interfere at the second beam-splitter BS_{output}. By altering the length of one of the arms we could vary the phase difference Φ between the components, and then get the superposition before BS_{output}, writing it as $|\Psi'\rangle = (|I\rangle + i\exp(i\Phi)|II\rangle)/\sqrt{2}$.

We analyze how beam-splitter BS_{output} acts on this superposition. We know that, in the simple case of a photon arriving at a beam-splitter in a given direction, it has an equal chance of being transmitted or reflected. A phase i is introduced to the state every time the photon is reflected. So, if the photon arrives in the state $|I\rangle$, it will have a fifty percent probability of leaving in a state $|I\rangle$ (transmitted) and a fifty percent probability of leaving in a state $i|II\rangle$ (reflected). The same thing is valid for the inverse case when where the arrival direction is the state $|II\rangle$, only now the transmitted and reflected states are, respectively, $|II\rangle$ and $i|I\rangle$. The states denoting the two different directions $|I\rangle$ and $|II\rangle$ are *orthogonal* and *normalized*, so that $\langle I|I\rangle = \langle II|II\rangle = 1$ and $\langle I|II\rangle = \langle II|I\rangle = 0$. With this, we can construct an operator U_{BS} that represents the action of a beam-splitter on an arbitrary superposition of states $|I\rangle$ and $|II\rangle$:

$$U_{BS} = 1/\sqrt{2}[|I\rangle\langle I| + |II\rangle\langle II| + i(|I\rangle\langle II| + |II\rangle\langle I|)],$$

where the first two terms are associated with transmissions and the terms containing the phase shift i are associated with reflections on the beam-splitter.

We are now able to get the detection probabilities of the output ports D_1 and D_2 as the square of the amplitudes:

$$\begin{aligned} P_{D1} &= |\langle I|U_{BS}|\Psi'\rangle|^2 \\ &= |1/2(\langle I| + i\langle II|)(|I\rangle + i\exp i\Phi|II\rangle)|^2 = \frac{1}{2}(1-\cos\Phi) = (\sin(\Phi/2))^2, \quad (2.10) \\ P_{D2} &= |\langle II|U_{BS}|\Psi'\rangle|^2 \\ &= |1/2(\langle II| + i\langle I|)(|I\rangle + i\exp i\Phi|II\rangle)|^2 = \frac{1}{2}(1+\cos\Phi) = (\cos(\Phi/2))^2. \quad (2.11) \end{aligned}$$

These probabilities depend on the phase shift between the arms of the interferometer and represent the interference between the components associated to the two paths. Of course, we have $P_{D1} + P_{D2} = 1$ for all Φ. In this case, the existence of an interference pattern is associated with a wave-like behavior of the photon.

The open configuration consists in removing BS_{output} so that detections at each output port D_1 and D_2 are now uniquely associated with a given path inside the interferometer - as we choose not to combine the amplitudes in a second beam-splitter, we could say that a photon arriving at D_1 came through arm I and a photon arriving at D_2 came through arm II. The probabilities are the square of the projections:

$$\begin{aligned} P_{D1} &= |\langle I|\Psi'\rangle|^2 = 1/2, \quad (2.12) \\ P_{D2} &= |\langle II|\Psi'\rangle|^2 = 1/2, \quad (2.13) \end{aligned}$$

which do not vary with the phase shift Φ. In the case where the detectors are associated with unique paths, we do not get interference, and the detection probabilities are constants. Thus the photons have a corpuscular behavior in the absence of the output beam-splitter.

Here, the delayed-choice experiment consists in deciding between these two configurations in a time past the photon has passed the input beam-splitter BS_{input}. An experiment like described was performed in 2007 by Jacques *et al* [6]. This experiment was performed in a highly single photon regime and with a guaranteed relativistic space-time separation between the choice of the configuration and the entry of the photon inside the interferometer. This is important so that no information about the choice of the configuration could reach the photon before it passes BS_{input}. The choice of the presence or not of beam-splitter BS_{output} in each run was made using a quantum random number generator (QRNG), which functions based on an intrinsic random quantum processes, so that its choice cannot be in any way predicted. In this way, even if the photon had somehow all knowledge about the details of the state of the generator, it would not be able to predict the final configuration. Finally, for each run of the experiment, a different phase shift Φ is set between the arms of the interferometer. For each realization, the configuration of the interferometer, the detection events, and the set phase difference Φ were recorded.

After many experimental realizations, the collected data is sorted for the times where the output beam-splitter was absent and for the times it was present. Plotting the so sorted data as a function of the phase shift Φ between the arms gives us the statistics for the photon for each configuration of the interferometer. When this is done, the plotted data clearly indicates the existence of a interference pattern between the interferometer arms as a function of Φ at both detectors for the cases where the output beam-splitter was present, and no sign of interference can be seen in the cases where it was absent (See Fig 2.11). With this we are led to the conclusion that, even if the choice of the apparatus configuration is made at a time when the photon is already inside the interferometer, we can still choose to observe a wave-like or a particle-like behavior by choosing to place or not a beam-splitter at the end of the photon's path. Mathematically, this means choosing at which basis to project the photon's state after its entry: we can either project it at basis $|I\rangle, |II\rangle$, or at the alternative rotated basis $|I'\rangle = U_{BS}^{\dagger}|I\rangle = (|I\rangle - i|II\rangle)/\sqrt{2}$, $|II''\rangle = U_{BS}^{\dagger}|II\rangle = (|I\rangle + i|II\rangle)/\sqrt{2}$, where $U_{BS}^{\dagger}$ represents the hermitian conjugate of our constructed beam-splitter operator U_{BS}. This result can be directly derived by an inspection of Eq. (2.11). So, to project the photon's states at the detectors at the end of the experimental apparatus means projecting them at different basis sets according to which configuration the apparatus is on. This whole picture is in total accord to Borh's complementarity principle.

But if our choice of placing or not the second beam-splitter is made after the photon

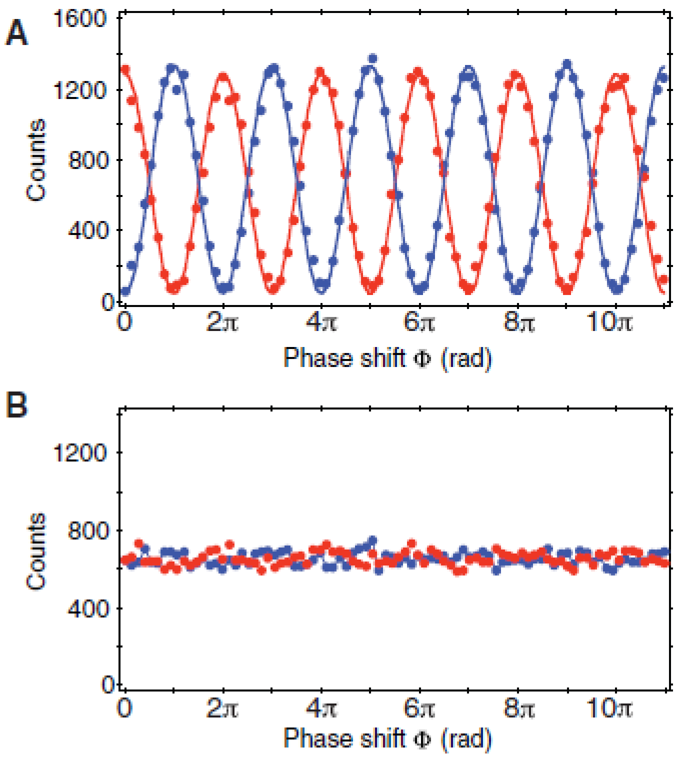

Figure 2.11: Counts of photon detection in a delayed choice interferometric experiment for both detectors D_1 (blue points) and D_2(red points) of the Mach Zehnder interferometer as a function of the varying phase shift Φ between the arms of the interferometer. According to the authors of the experiment, each point was recorded with an exposition time of 1.9s and corresponds to the detection of about 2600 photons. **A** represents the detection counts for the closed configuration of the interferometer, when the output beam splitter was present, while **B** represents the counts for the open configuration. The counts of photon arrival in the closed configuration on the detectors shows an interference pattern with phase shift Φ of 94 percent visibility. In the open configuration, no interference is observed and equal detection probabilities of (0.50 ± 0.01) were observed for both detectors, corresponding to the full knowledge of the photons paths. *Image extracted from ref. [6].*

is surely already inside the interferometer, how can we explain this outcome? Again, as in the case of the cosmic interferometer, at first it may seem that our late choice of the configuration has influenced the photon's past behavior at the slits, somehow creating an effect of reverse causality. In Wheeler's own words, "(...)*we have a strange inversion of the normal order of time. We, now, by moving the mirror in or out, have an unavoidable effect on what we have a right to say about the already past history of the photon*" [34]. This paradox creates a tension with Einstein's theory of relativity, indicating that we could be twisting the arrow of time, causing the future to influence the past.

However, relativity theory and causality can remain untouched by the strange however plausible conclusion that the photon is, in fact, in a still indeterminate form *until the time it reaches the detectors* - that is, until the time any real measurement is made. As was already previously discussed, it is an idea strongly supported by Bohr that as physicists we are only able to talk about what has in fact been measured, and therefore to make an affirmation about the photon's unmeasured past, i. e. to affirm that it has passed through only one or both slits at the beginning of our experiment, is a common fallacy. Even in a mathematical point of view, the projection of the photon's state occurs only upon the arrival at the detectors - *until then*, the photon remains in a evolving superposition of states, and nothing can really be said about the physical nature of its behavior. We make a pause here to recall the example presented in Sec. 1, where the detectors D_1 and D_2 were placed in the vicinity of the two apertures of a double-slit interferometer in an attempt to mark the photons paths. In the case where we have set $b = 0$ and the 'wrong' detector could not be triggered by any passing photon, we had then affirmed that a click in detector D_1 meant that the photon had "passed through aperture 1". We are now able to understand that this conclusion is in fact essentially *incorrect*. Before the click of the detector, the photon is still in the superposition of states represented by $(\varphi_1 + \varphi 2)/\sqrt{2}$, and not yet projected at state φ_1, which would actually mean that 'it had passed through aperture 1'. The projection at one of the photon's eigenstates only takes place upon the time the photon's state reaches the detectors, and we have indeed no right to say anything about its behavior in earlier times. To make such affirmations would inevitably result in creating a type of retro causality, in the sense that removing detectors D_1 and D_2 after the photon had passed through the first screen could alter what we could say about its past behavior at the apertures. But in reality, by removing the detectors, we only leave the superposition unperturbed and free to evolve until the final screen is reached. At the end, it is not a case of *path marking*, but more precisely it is about our *detector's placement*. And with this we can conclude that the choice of apparatus configuration does not, as in Wheeler's words, have an effect on what we have a right to say about the past history of the photon, therefore creating a time paradox - either the case, what it seems most is that we as physicists never get to say anything about this past history at all.

2.4 Erasure of Information: The Quantum Eraser

In the first section of this chapter, we have discussed how the interference pattern in a double-slit interference experiment with single photons is intrinsically dependent on what we have called the 'which-way' information of each photon, and how this dependence comes about very naturally by means of the quantum mechanical formalism - we have concluded that, if we can with this information completely determine the photon's trajectory inside the interferometer, then the interference pattern must disappear. A subtle question however may arise when confronting this facts: what if we could, by some means, erase the path information of the photons? What would happen with the interference then? In 1982, this very question was asked by physicists Marlan O. Scully and Kai Drühl [35], who first proposed the concept of quantum erasure in a theoretical standing. A few years later, Marlan O. Scully, B.G. Englert and H. Walther [7] proposed an experiment to bring this new concept of quantum erasure about: in their paper, they proposed a double-slit type experiment where the interfering objects were atoms with electrons excited to very high energy levels. Behind each aperture of the dividing screen of their interferometer there is a cavity which purpose is to capture the photons emitted by the excited atoms as they decay to lower energy levels. The idea behind the experiment is quite simple: while there is no connection between the two cavities, the atom's paths are completely marked by the presence or not of the photons inside them, and thus no interference pattern should appear at the final screen. But if a connection was created so that the photons could freely travel between the cavities, then there would be no way of knowing exactly behind which aperture the photon was emitted and this 'erasure' of the path marking would allow us to fully recover the interference pattern. The details of this proposed experiment are as follows.

First, we take a closer look at the theoretical 'which-way' detector device, showed in the sketch of the proposed experimental apparatus presented in Fig 2.12. As is shown, a series of wider slits is first used as the collimators to define the two atomic beams that then arrive at the two apertures screen of our standard double-slit interferometer. If we disregard for a moment the presence of both the laser and the cavities, this experiment is then just reduced to the double-slit interference experiment of Sec. 2.1 now applied to atoms instead of photons, and we expect, just as then, to see an interference pattern formed at the final screen. However, for the present quantum erasure experiment, both the laser and the cavities are introduced as to function as the so-called 'path markers' for the atoms in the beam. The idea then is as follows: first, the laser beam is introduced as to prepare for the interferometric experiment a beam of atoms that are in an *excited internal state*. After the interaction with this laser, the atoms in this beam will then proceed go through one of the two placed cavities, each associated with a single aperture in the double-slit interferometer's dividing screen. The cavities are created so that whenever one of the excited atoms of the atomic beam travels through it, it decays to a lower internal energy level by emission of a microwave photon. If we suppose that there were no photons present at the cavities before the experiment, then the presence of a photon in the cavity stores information about the path taken by the atom and thus the interference pattern should be destroyed. We note here that the process of photon emission by the excited atoms in the cavity does not affect the spatial state of the traveling atoms - it is possible to show that the interaction of the atoms with the cavity *does not* disturb their center-of-mass motion [7], so that the net momentum transfer to the atoms due to the this interaction is approximately *zero*. This is important because it presents in itself an example where the interference pattern is lost to path information without the existence of any real disturbances in the motion of the atoms.

After the atom has passed through one of the so placed cavities and made a transition from an excited state to a lower energy level, which we denote here by $|a\rangle \rightarrow |b\rangle$, the total joint state of the atoms spatial and internal degrees of freedom and the cavities is:

$$|\Psi_T\rangle = \frac{1}{\sqrt{2}}[|\psi_1\rangle|\phi_1\rangle + |\psi_2\rangle|\phi_2\rangle]|b\rangle, \tag{2.14}$$

where $|\psi_1\rangle$ and $|\psi_2\rangle$ are the spatial state vectors of the atom associated respectively with apertures 1 and 2 of the first screen of the interferometer and $|\phi_1\rangle = |1_1 0_2\rangle$ and $|\phi_2\rangle = |0_1 1_2\rangle$ are the states of the cavities representing respectively the cases where cavity 1 has a photon

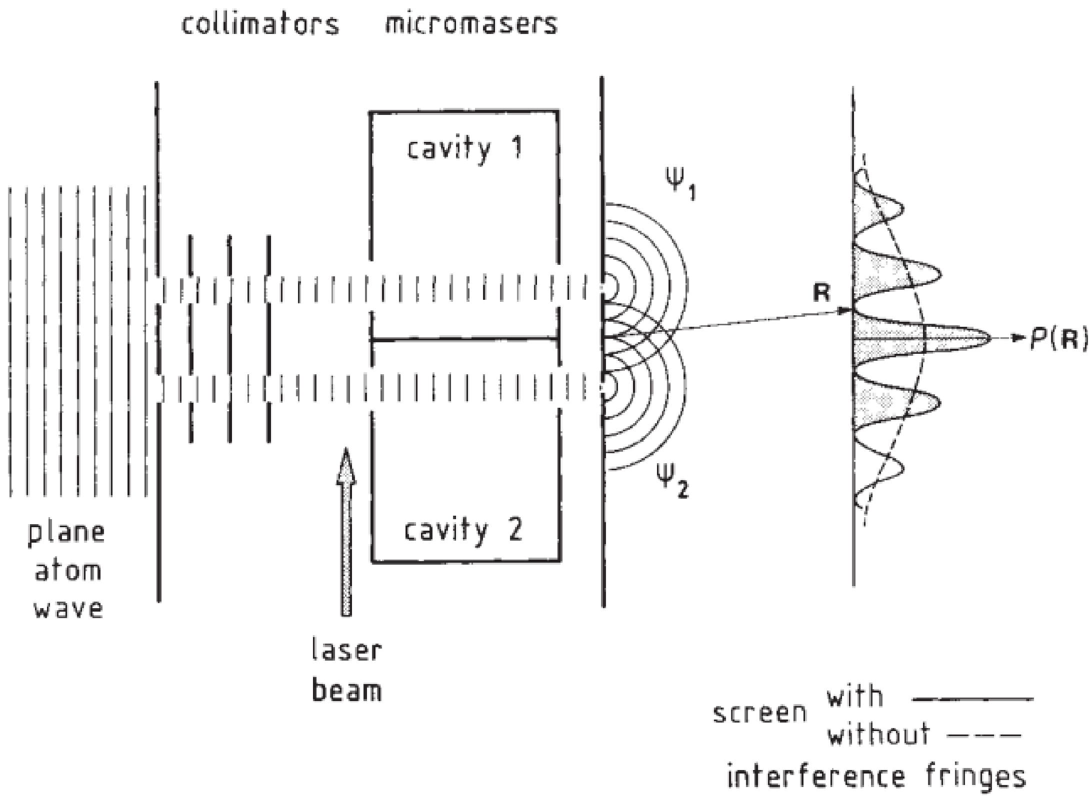

Figure 2.12: The double-cavity 'which-way' detector device coupled to a double-slit interferometry experiment using atoms in excited internal states, as proposed in [7]. The existence of a photon in one of the two placed cavities indicates the passage of an atom through a given cavity, therefore storing information about the path taken by the atoms in the experiment and eradicating the phenomenon of interference. *Image extracted from ref. [7].*

(and cavity 2 has none) or cavity 2 has a photon (and cavity 1 has none). The total state of the system is then as usual a superposition of the possibilities for the atom and the cavities.

The arrival probability curve for the atom at a point x at the final screen with this setting of the apparatus is then $|\langle x|\Psi_T\rangle|^2$:

$$P(x) = \frac{1}{2}[|\psi_1|^2 + |\psi_2|^2 + \psi_1 * \psi_2\langle\phi_1|\phi_2\rangle + \psi_2 * \psi_1\langle\phi_2|\phi_1\rangle]\langle b|b\rangle \tag{2.15}$$

where $\psi_1 = \langle x|\psi_1\rangle$ and $\psi_2 = \langle x|\psi_2\rangle$ are the wave functions in coordinate representation associated with apertures 1 and 2 of the first screen. Because $|\phi_1\rangle$ and $|\phi_2\rangle$ are orthogonal, their inner product vanishes and the arrival probability is then reduced to

$$P(x) = \frac{1}{2}[|\psi_1|^2 + |\psi_2|^2], \tag{2.16}$$

and as expected no interference can be seen at the final screen.

The important question now is: is there a way to retrieve the interference terms in the arrival probability curve by erasing the path information of the atom that is stored at the cavities? Theoretically, as is shown with detail in ref. [35], the answer is 'yes', and the proposed way of doing so in this present experiment is sketched in Fig 2.13. If we imagine that the cavities are now separated by a shutter-detector combination, then, if the shutters are set open, the photon existing at either one of the cavities will be allowed to interact with a centered photo-detection wall. Photon detection is a destructive phenomenon and, if the photon turns out to be absorbed by the wall in this manner, its 'memory of passage' can be said to have been *completely erased*. If we now expand the total state of the system after the passage of the atom through the cavities to include the state of the introduced detection wall when the shutters are closed, we will have:

$$|\Psi_T\rangle = \frac{1}{\sqrt{2}}[|\psi_1\rangle|\phi_1\rangle + |\psi_2\rangle|\phi_2\rangle]|b\rangle|d\rangle, \tag{2.17}$$

where $|d\rangle$ is the vector state of the detection wall ground state (no detected photons). When the shutters are set open, the detector can then make a transition $|d\rangle \to |e\rangle$ to an excited state $|e\rangle$ (representing photon detection).

Before we continue, it is convenient to introduce here an alternative vector basis consisting of the symmetric and antisymmetric states, denoted by:

$$|\chi_\pm\rangle = \frac{1}{\sqrt{2}}[|\chi_1\rangle \pm |\chi_2\rangle], \tag{2.18}$$

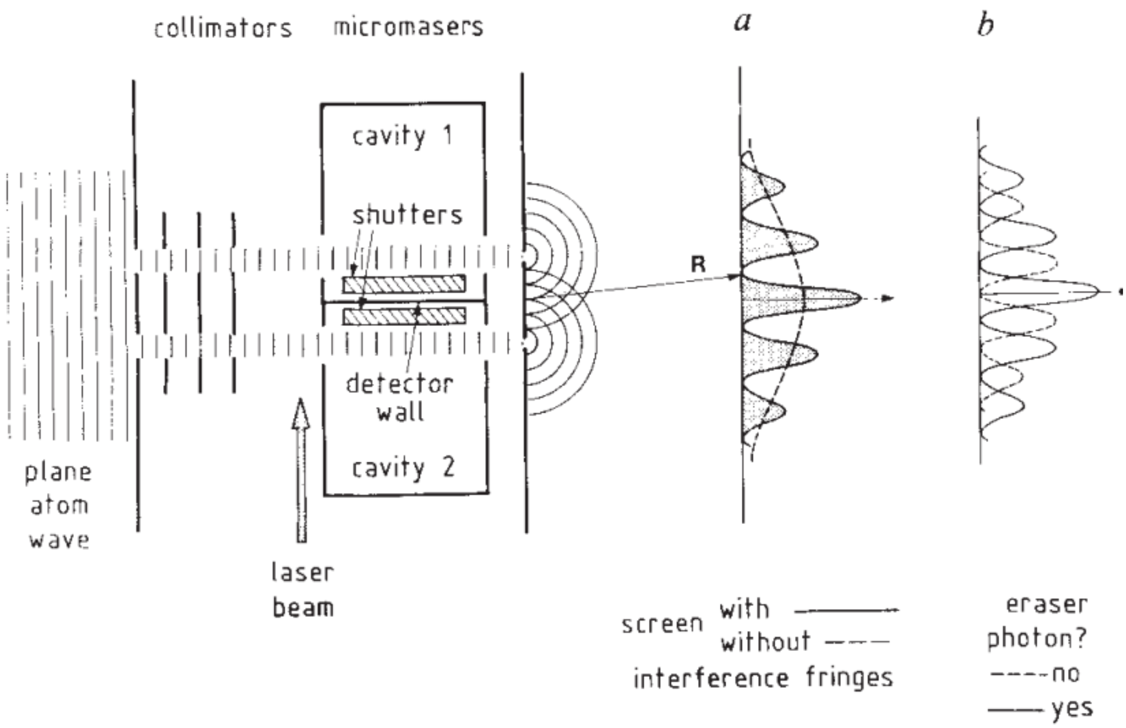

Figure 2.13: The implemented shutter-detection device allowing the photons in the cavities to reach a photo-detection wall is indicated in the space between the cavities. As photon detection is a destructive physical phenomenon and no information is left about the origins of the so absorbed photons, this process culminates in a 'erasure' of our previous path information and the recovery of interference *Image extracted from ref. [7].*

where, in our discussion, χ can be replaced by either ψ or ϕ. The total state vector of the system in Eq. 2.17 written on this alternative basis set for the degrees of freedom of ψ and ϕ is then:

$$|\Psi_T\rangle = \frac{1}{\sqrt{2}}[|\psi_+\rangle|\phi_+\rangle + |\psi_-\rangle|\phi_-\rangle]|b\rangle|d\rangle. \tag{2.19}$$

We consider the interaction between the radiation in the cavity and the photodetector, which we consider as having two possible states, $|d\rangle$ and the excited state $|e\rangle$, in the likes of a two energy leveled atom. The interaction Hamiltonian for this case between the radiation and the detector is so that it will depend on the symmetric combination of the state variables, in a way that only the symmetric combination for the photon in the cavity could be 'detected' (and the antisymmetric combination remains unchanged). With this in mind, the total state is then turned into:

$$|\Psi_T\rangle = \frac{1}{\sqrt{2}}[|\psi_+\rangle|0_1 0_2\rangle|e\rangle + |\psi_-\rangle|\phi_-\rangle|d\rangle|b\rangle], \tag{2.20}$$

where $|0_1 0_2\rangle$ means no photons present at either one of the cavities.

It is easy to see that, as long as the final state of the photodetector is unknown, we remain observing no interference pattern at our final screen, as we get an arrival probability curve for this final state in the form of Eq. 2.16. But something seemingly unusual happens when we ask the question of what is the probability $P_e(x)$ of atom arrival at the screen and *in the same event a count at the centered photodetector*. For this cases, we have an arrival probability:

$$P_e(x) = |\langle x|\psi_+\rangle|^2 = \frac{1}{2}(|\psi_1|^2 + |\psi_2|^2 + Re(\psi_1 * \psi_2)), \tag{2.21}$$

and we have, here, surprisingly *regained the interference term*. For the complementary cases when the photodetector does not trigger any counts (corresponding to the antisymmetric state of the photon, that is not 'detected'), we have a similar arrival probability distribution:

$$P_d(x) = |\langle x|\psi_-\rangle|^2 = \frac{1}{2}(|\psi_1|^2 + |\psi_2|^2 - Re(\psi_1 * \psi_2)), \tag{2.22}$$

where the sign of the interference term is changed, indicating the existence of the called *antifringes* at our screen, an 'inverted' interference pattern. Thus, when we lose the path information, interference is regained. The case of no interference will correspond to half the sum of the probability curves $P_e(x)$ and $P_d(x)$.

Although the idea contained in this experiment is a simple one, a quantum eraser experiment has not been performed following directly this original proposal, since there are much simpler, equivalent ways to perform it in the laboratory. Here, to again visualize what is happening in a quantum erasure type of experiment, let us once more consider a double-slit interferometer of single photons. To analyze the quantum erasure process in this context we will for the first time make use of an internal property of the photons, namely their polarization states. We proceed as follows: we prepare our photons so that each photon arrives at the first screen with linear vertical polarization, which we denote as the state $|V\rangle$. Behind only one of the two apertures, say aperture 1, we place a half wave plate to rotate this polarization into a horizontal polarization state $|H\rangle$. A half wave plate is an optical device used to 'rotate' the direction of polarization of linear polarized light by altering the phase shift between orthogonal components - here we use them to rotate the direction of the light's polarization from an angle θ to a new angle $\theta + \pi/2$. This should erase our interference pattern, since now measuring the polarization of the photons that have passed the first screen gives us information about through which aperture it has passed in the beginning of our experiment - the photons that passed through aperture 1 will have horizontal polarizations, while the photons that passed through aperture 2 will remain with the prepared vertical polarizations. This situation is represented by the total final state:

$$|\psi\rangle = \frac{1}{\sqrt{2}}\left(|\psi_1\rangle|H\rangle + |\psi_2\rangle|V\rangle\right), \tag{2.23}$$

in which the vector states associated with the passing through each aperture have a one-to-one correspondence with the photon's polarization states. To calculate the arrival probability of the photons at the final screen as a function of x in this case, we project this state at the the position basis and then take the square of the absolute value:

$$\begin{aligned} P(x) &= |\langle x|\psi\rangle|^2 \\ &= 1/2(|\psi_1|^2\langle H|H\rangle + |\psi_2|^2\langle V|V\rangle + \psi_1 * \psi_2\langle H|V\rangle + \psi_1\psi_2 * \langle V|H\rangle) \\ &= 1/2(|\psi_1|^2 + |\psi_2|^2), \end{aligned} \tag{2.24}$$

where ψ_1 and ψ_2 are both functions of x. Here, since the polarization states $|H\rangle$ and $|V\rangle$ are orthonormal with respect to each other, we have that $\langle H|H\rangle = \langle V|V\rangle = 1$ and $\langle H|V\rangle = \langle V|H\rangle = 0$. Thus we see that, as expected, we get no interference pattern at the screen.

In a quantum erasure scenario, however, is not enough that we can mark the way of the photon - it is also necessary that we can erase the information about its path so we are able to get the quantum interference pattern back. We can accomplish this in our simpler version of the quantum erasure interferometric experiment by directing the photons to a optic polarizer oriented at an angle of $\pi/4$ with respect to the basis (H, V) in a time before they can reach the final screen. Mathematically, we project the basis (H, V) in a new rotated basis (D, A), $|D\rangle = 1/\sqrt{2}(|V\rangle + |H\rangle)$ and $|A\rangle = 1/\sqrt{2}(|V\rangle - |H\rangle)$. The letters D and A used to define this new basis set derives from the words 'diagonal' and 'anti-diagonal'. The rotated final state will then be written as:

$$\begin{aligned} |\psi\rangle &= 1/\sqrt{2}\big(|\psi_1\rangle|H\rangle + |\psi_2\rangle|V\rangle\big) \\ &= \frac{1}{\sqrt{2}}\left[|\psi_1\rangle 1/\sqrt{2}(|D\rangle - |A\rangle) + |\psi_2\rangle\frac{1}{\sqrt{2}}(|D\rangle + |A\rangle)\right] \\ &= 1/2[(|\psi_1\rangle + |\psi_2\rangle)|D\rangle - (|\psi_1\rangle - |\psi_2\rangle)|A\rangle]. \end{aligned} \tag{2.25}$$

Taking a look at this expression we can see what happens to the state when the photon passes through the polarizer in the two cases where this polarizer is oriented along the directions D or A. If we choose to orient the polarizer along the direction D, we project the photon's state in the expression (2.25) at the polarization vector $|D\rangle$ and thus get a final state in the form of the familiar superposition $|\psi_1\rangle + |\psi_2\rangle$, leading to quantum interference and the existence of dark and light fringes in our final screen. This is just what we would get in the case where the half wave plate and the polarizer were both absent. In the case where the polarizer is oriented along A, the projection is made at the polarization vector $|A\rangle$ and we get a final state in the form $|\psi_1\rangle - |\psi_2\rangle$. Here, the rotation of the vector state has introduced a phase difference of π between the two partial amplitudes in the superposition, leading to the existence of *anti-fringes* in our final screen (dark and light areas are now exchanged). Still, what we get is an interference pattern. The probability distribution leading to fringes and anti fringes at the screen are complementary, in the sense that *their addition leads to (twice) the probability distribution we would get in the case of no interference.*

So inserting a half wave plate to rotate the polarization of any photon that passes through aperture 1, and thus differentiating it to any photon that has passed through aperture 2, have blurred our interference pattern, but projecting all photons in our experiment at a common polarization vector has brought it back. First, we must note that the uncertainty principle have no say here, since *polarization and position are not conjugate quantities.* So the uncertainty principle invoked by Bohr in his discussions with Einstein must really not be what ultimately enforces the complementarity between wave-like and particle-like behaviors. What is, then, that is enforcing this complementarity? The answer here is *entanglement*. Without the presence of the polarizer between the screens, the final total state represents an entanglement between the position and polarization states of the photon. The presence of the polarizer will 'mix' the state vectors that previously made up for the total state superposition by rotating the vector state basis and in this process entanglement is lost - we lose our previous one-to-one correspondence between the aperture through which the photon has passed and its polarization. Thus, we can recover the interference pattern. Secondly, we see here how it gets even harder to associate the vector states to any physical reality in any time before some real measurement is made. What we choose to measure determines the type of behavior we are going to observe, and as we have concluded we have really no say in what was the behavior of the photon in any time before this measurement.

An experiment similar to the one described was performed by S. P. Walborn, M. O. Terra Cunha, S. Padua and C. H. Monken in 2002 [36, 8], where they have used circular polarization instead of linear polarization states for the photons that have passed the dividing screen. The idea presented was the same and the results analogous - the presence or not of a filter before the photons reached the final screen determined the presence or not of interference patterns. Erasing the 'which-way' information of each photon have brought back the quantum interference phenomenon.

However, in addition to this version of the quantum erasure experiment, another experiment was performed to dramatize even more the results obtained by our simplistic method that makes use of entanglement in a even less intuitive way [8]. The main idea was asking the question: what if we only erased the which-path information of the photons in a time past they have already been irreversibly detected? This idea follows the line of Wheeler's delayed choice experiment and has been called a 'delayed choice quantum erasure experiment'.

In their delayed choice quantum erasure, they prepare twin photons with entangled polarization states. The photons are labeled photons a and b. This can be achieved by a nonlinear optical process, named 'spontaneous parametric down-conversion' [37]. The twin photons are prepared so that every time photon a is found to have vertical polarization, photon b will have horizontal polarization, and vice-versa. This situation can be represented by the total state vector

$$|\psi\rangle = \frac{1}{\sqrt{2}}(|H\rangle_a|V\rangle_b - |V\rangle_a|H\rangle_b), \tag{2.26}$$

where the states corresponding to each photon are marked with the respective subscripts. The photons are separated from each other and directed so that photon a is sent through a double-slit interferometer containing quarter wave plates behind each aperture at the first screen. In their version of the experiment, the quarter wave plates rotate the photons polarization states so that a photon that passes through aperture 1 would end up with a right-circular polarization state and a photon that passes through aperture 2 would end up with a left-circular polarization state, and thus, again, the plates create which-path information for the photons. The fact that they used circular polarizations instead of linear polarizations as path markers does not change the experiment's final outcome. Finally, photon b is redirected directly to a separated polarizer P. This process is schemed in Fig. 2.14.

The idea behind sending photon b to a separated polarizer is that, as the photons are entangled with each other, every measure we make in photon's b state will determine the state of its twin. That said, we can regard photon b as our quantum erasure 'controller' - by sending it to the separate polarizer P, we can choose whether we want to measure its polarization in a way that preserves the previously created path information of photon a or whether we want to destroy this information and recover interference. This is done exactly as described in the first part of this section - if we measure photon b in the (H, V) basis, we preserve the which-way information of photon a and thus get no interference, but if we measure photon b in the rotated basis (D, A) we are able to destroy the information and thus recover the interference pattern in our screen, whether in the form of fringes or anti fringes. The way we measure photon b determines the observed behavior of photon a. The striking feature about this version of the quantum eraser experiment is that *the outcome does not depend on the order in which photons a and b are detected in* - so the choice of the measurement basis for b can be made in a time long after photon a has *already been irreversibly detected*. Again, we get an odd sort of situation where it may seem like the future influences the past and common causality is lost. Even more so, as the photons are spatially separated during this experiment, it seems to be possible for two separated parties to communicate supraluminally using this sort of experimental apparatus.

But again, this is not so. Quantum mechanics remains true to relativity theory and does

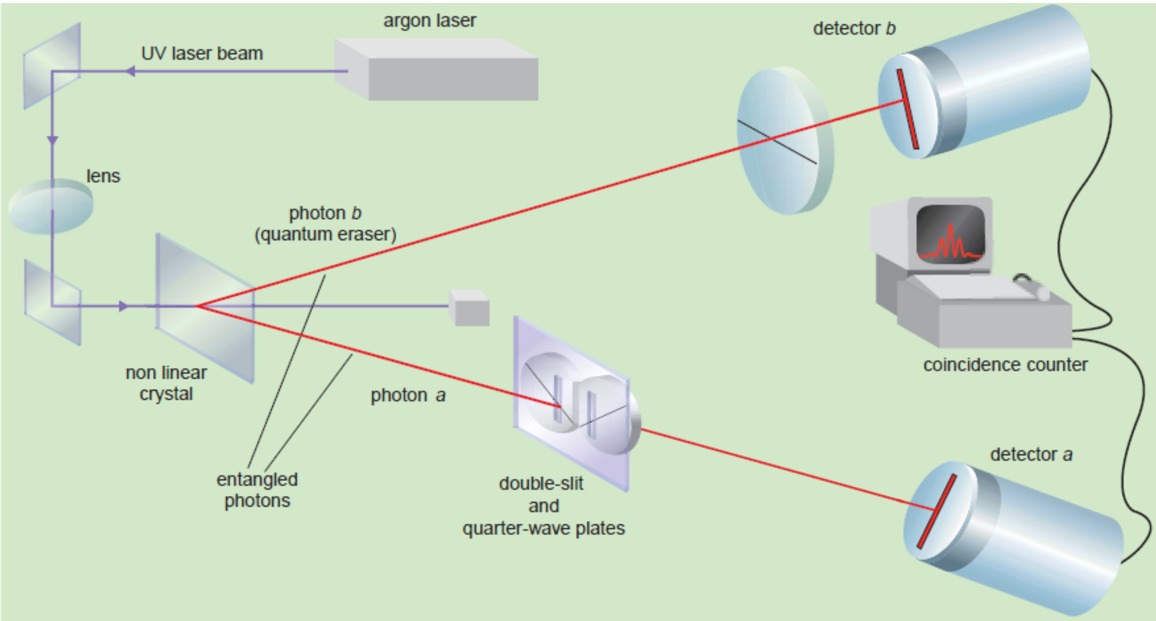

Figure 2.14: Scheme of the quantum erasure experiment involving twin photons. The twin, or entangled photons are produced as a result of a parametric down conversion process in a non linear crystal, and behave such as that any measurement of the polarization of b immediately determines the polarization of a . After their production, the photons are separated from each other and sent through two different measuring apparatus: photon a is sent to a double-slit interferometer containing quarter wave plates behind each slit, while photon b is sent directly through a polarizer. Even after photon a has been detected, the polarization of b is entangled with its 'which path' informaton. *Image extracted from ref. [8].*

not permit such things. What is really happening then? To try to shed some light on this subject, we present the following fictional situation. Lets say a physicist named Charlie creates various pairs of polarization entangled photons using spontaneous parametric down-conversion, but does not tell anyone that these photons are entangled. He proceeds by sending the twin photons with labels a and b to two separated parties, physicists Alice and Bob, along with instructions of which experiment each one should perform with their photons. Following instructions brought to her in this manner, physicist Alice sends her photons a through a double-slit interferometer with the described quarter wave plates, and what she observes is that *nothing unusual happens*. Her results are *exactly what she would get using any other group of photons*, and that being, she gets no interference at the final screen. During her experiment, Alice records the data for the arrival for each of her photons. Far away, physicist Bob too follow his instructions and sends each of his photons through a polarizer, and each time he does so he chooses along each vector of basis (H, V) or (D, A) to orient this polarizer. Again nothing unusual happens, and he gets results following exactly the predicted quantum probabilities followed by any ordinary group of photons. Bob also record the data of his experiment, always including the measurement results along with the chosen orientation of the polarizer. It is an ordinary day on both their laboratories.

Both Alice and Bob have thus no way of knowing that their photons have entangled twins. Where lies the mystery then? The fundamental aspect we are concerned with here appears only in the form of *quantum correlations* between the outcomes of Alice's and Bob's measurements. It is only when Charlie brings the two physicists together to interchange their data that they can see something rather 'unusual' has happened. Charlie asks Alice to plot the pattern created by the arrival of her photons only in the cases where Bob projected his photons states at polarization vector $|D\rangle$, and, surprisingly, what Alice gets on her computer by doing so are actual interference fringes! Following this line, if Alice now chooses to plot the pattern created by her photons in the cases where Bob projected his at $|A\rangle$, she gets anti fringes. But for the cases where Bob used the unrotated (H, V) measurement basis, still there is no interference pattern to be seen. In their 2003 paper [8], the authors of this experiment compared this situation to correlated tosses of two quantum coins. If we look at the coins when they are separated, we get heads or tails with fifty percent probability on both coins, but the fact is that every time Coin 1 lands on heads (tails), so does Coin 2, and vice-versa. Here, every time Bob's measurement basis is (H, V) there is no interference, and every time the measurement basis is (D, A), the quantum interference phenomenon is brought back. The entangled photons behave thus like correlated, strange quantum coins.

Chapter 3

Paper: 'The classical limit of quantum optics: not what it seems at first sight'

3.0.1 Introduction

In our previous chapter, we brought attention to the wide difference that exists between our concepts about the reality of the physical world when analyzed in the classical or quantum regimes - a difference that stands itself out even in the cases where both theories demonstrated to bring up the same results, as was the case of our double-slit interference experiments with high intensity light beams or single photons. While we have no difficulty accepting one, the other seems to us rather counterintuitive. This brings up the question of what would be the transition between these two regimes and how would this transition work. In fact, the classical limit of the quantum theory is not nearly a well understood matter and constitutes an area of scientific research till this day [38, 39, 40, 41]. Still, much can be gained by exercising our intuition about both reality in quantum context and quantum logic. It was with this in mind that a paper was published in 2013 by Yakir Aharonov, Alonso Botero, Shmuel Nussinov, Sandu Popescu, Jeff Tollaksen and Lev Vaidman, named "The classical limit of quantum optics: not what it seems at first sight" [1], a paper that inspired both the work presented in this dissertation and our overview on quantum interference phenomena. In this paper, the authors introduce a light interferometry experiment where our understanding about the involved physical processes differ drastically between the two regimes, classical and quantum, even when both theories give us exactly the same mathematical expected result. In their proposed thought experiment with light it is shown that, in the quantum context, it seems to be possible for the combination of the two possibilities of pushing a mirror outwards or leaving it still to result in a inward pull in that mirror. How could this be possible is extremely counterintuitive and is, in fact, as we shall see, a direct result of a quantum superposition and quantum interference phenomenon.

3.0.2 The Momentum Transfer from Light to a Mirror

We begin our discussion with a brief overview on how can light change the momentum of a mirror. We do so by considering both contexts, classical and quantum, in the cases where light is considered whether as a traveling electromagnetic wave in space-time or a traveling group of individual and indivisible photons.

Classically, light is described as an electromagnetic disturbance in space-time traveling with fixed velocity c. According to standard electromagnetism theory and Maxwell's equations, such electromagnetic disturbances carry linear momentum, and this momentum is stocked in the electromagnetic fields constituting the wave. The density of linear momentum of an electromagnetic field is given by the vector $\mathbf{S}/c^2 = (\mathbf{E} \times \mathbf{H})/c^2$, where $\mathbf{S}$ is the so called Poynting Vector and $\mathbf{E}$ and $\mathbf{H}$ are the electric and magnetic field vectors [17]. The Poynting vector characterizes the electromagnetic wave's energy flux. For an electromagnetic monochromatic plane wave traveling in the $\hat{z}$ direction, we write:

$$\mathbf{E} = [E_0 \cos(kz - wt + \delta)]\hat{x}, \tag{3.1}$$

$$\mathbf{H} = [E_0 \cos(kz - wt + \delta)/(c\mu_0)]\hat{y}, \tag{3.2}$$

$$\begin{aligned} \mathbf{S} &= [E_0^2 \cos^2(kz - wt + \delta)/(c\mu_0)]\hat{z}, \\ &= [E_0^2 c\epsilon_0 \cos^2(kz - wt + \delta)]\hat{z}, \end{aligned} \tag{3.3}$$

where k is the absolute value of the wave vector $k = 2\pi/\lambda$, w the wave's angular frequency and δ an arbitrary wave phase. The electric and magnetic field vectors oscillate in directions that are orthogonal to the direction of the wave propagation, which we have taken to be $\hat{z}$. We note that the absolute value of the Poynting vector $\mathbf{S}$ varies in time along this direction of propagation of the wave, and as a result so does the momentum density. In this context we usually work with the temporal averages of the carried physical quantities. The mean value of $\mathbf{S}$ is taken as the average over the wave's period $T = \pi/\lambda$, so that the averages values of energy flux and momentum density are:

$$\langle \mathbf{S} \rangle = (E_0^2 c\epsilon_0)\hat{z}/2, \tag{3.4}$$

$$\langle \mathbf{p} \rangle = (E_0^2 \epsilon_0)\hat{z}/2c. \tag{3.5}$$

As stated, the mean magnitude of the Poynting vector $\langle \mathbf{S} \rangle$ represents the average value of the electromagnetic wave's energy flux, and is in Electromagnetism used to formally define the wave's *intensity*, $\langle \mathbf{S} \rangle \equiv I$. In this manner, finally, we arrive at the conclusion that an electromagnetic monochromatic plane wave carries linear momentum along the direction of its propagation and that the carried momentum's magnitude is proportional to the wave's total intensity I, in the form:

$$\langle \mathbf{p} \rangle = I/c^2. \tag{3.6}$$

Thus, when the incident pulsed almost-monochromatic wave described above hits a material surface and is reflected, it exerts a pressure on this surface and this pressure results on a transferred total linear momentum that depends only on the intensity of the incoming wave. The pressure exerted due to electromagnetic waves in this manner is called *radiation pressure*, and is by definition a force acting per unit area per unit time on the material surface. In the case where the almost-monochromatic wave front makes an angle of α with a perfectly reflecting mirror, as sketched in Fig. 3.1, and we take the mirror to have unit area

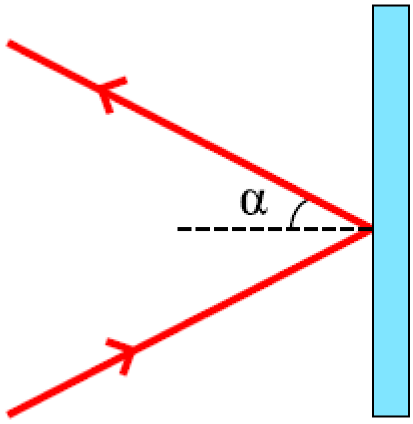

Figure 3.1: **Figure 10.** Light reflecting on a mirror. [*From "The classical limit of quantum optics: not what it seems at first sight", Yakir Aharonov et. al., NJP. 2013.*]

and the experiment to last a unit time, then the total linear momentum transferred by the wave to the mirror is proportional to twice the component of the wave's momentum normal to the mirror:

$$\Delta p_M = 2I\cos\alpha/c^2. \tag{3.7}$$

Quantum mechanically, the story is quite different. Energy is now quantized and light consists of indivisible, independent energy packs - or photons - each carrying momentum $p = \hbar w$. This is a result that can be deduced with a first-principles treatment for a photon reflection by a quantum mirror M [42]. In this case we understand the transfer of momentum as being due to separated mechanical collisions of individual photons with the material surface. Thus, when each photon hits a perfectly reflecting mirror and is reflected, it transfers to it a total momentum equal to twice its moment component normal to the mirror. The sum of the momentum transferred by a number of $\bar{n}$ photons impinging on the mirror in the same manner is then:

$$\Delta p_M = 2\bar{n}\hbar w\cos\alpha. \tag{3.8}$$

Thus, if we take the intensity I of the light beam hitting this same mirror (in the same case where we have taken the mirror to have unit area and the experiment to last a minute time) to be numerically equal to $\bar{n}\hbar w/c$, both theories give the exact same mathematical result for the momentum transferred to the mirror by the reflection process. It seems, then, tempting to assume that the transition between these theories happens smoothly in this context. As the authors show in their paper [1], and we shall analyze in detail in the following discussion, strangely it does not happen so.

3.0.3 Aharonov's Interferometer

We proceed by considering the light interferometer depicted in Fig. 3.2. All three mirrors contained in this experimental apparatus are taken to be perfectly reflecting, with mirror M being silvered on both sides. This interferometer is a varied version of a standard Mach-Zehnder interferometer for light, with the only difference that light emerging from the second beam-splitter towards D_1 does not go directly into it, but instead is previously redirected to an external reflection on mirror M. In this way, light traveling through the interferometer can be reflected by this mirror in two different, separated occasions - one of them from the inside the interferometer, in which it makes an angle α with the mirror, and one from the outside, making an angle β with it. We are free to design the experimental apparatus so that the relation between this two reflection angles can be chosen. To the purpose of this proposed thought experiment, we take $\cos\beta = \cos\alpha/2$. Thus, during our experiment, mirror M can receive momentum kicks in the two opposite directions as a result of the reflections of light hitting on it from both sides. The total momentum gained in this manner by the so positioned mirror M inside the interferometer is the focus of our attention in this interferometric thought experiment and is to be analyzed in the following.

Suppose we project the interferometer to have two identical beam-splitters BS_1 and BS_2, with reflectivity r and transmissivity t so that $r^2+t^2 = 1$ and $|r| > |t|$. This unbalance results in the most part of light impinging on each of the the beam-splitters to be reflected rather than transmitted, for a reason that will become clear later. Thus, the first beam-splitter BS_1 divides the light's incoming state into a superposition of states corresponding to the two different spatially separated arms inside our interferometer. If the states corresponding to each of these separated arms are denoted by the state vectors $|A\rangle$ and $|B\rangle$, we have that, just as before, the total state of a photon after having passed through beam-splitter BS_1 can be written as the superposition:

$$|\psi\rangle = ir|A\rangle + t|B\rangle. \tag{3.9}$$

Here we recall that, when describing the delayed choice interferometer experiment with single photons in Sec. 2.3 , we have concluded that the presence of the output beam-splitter

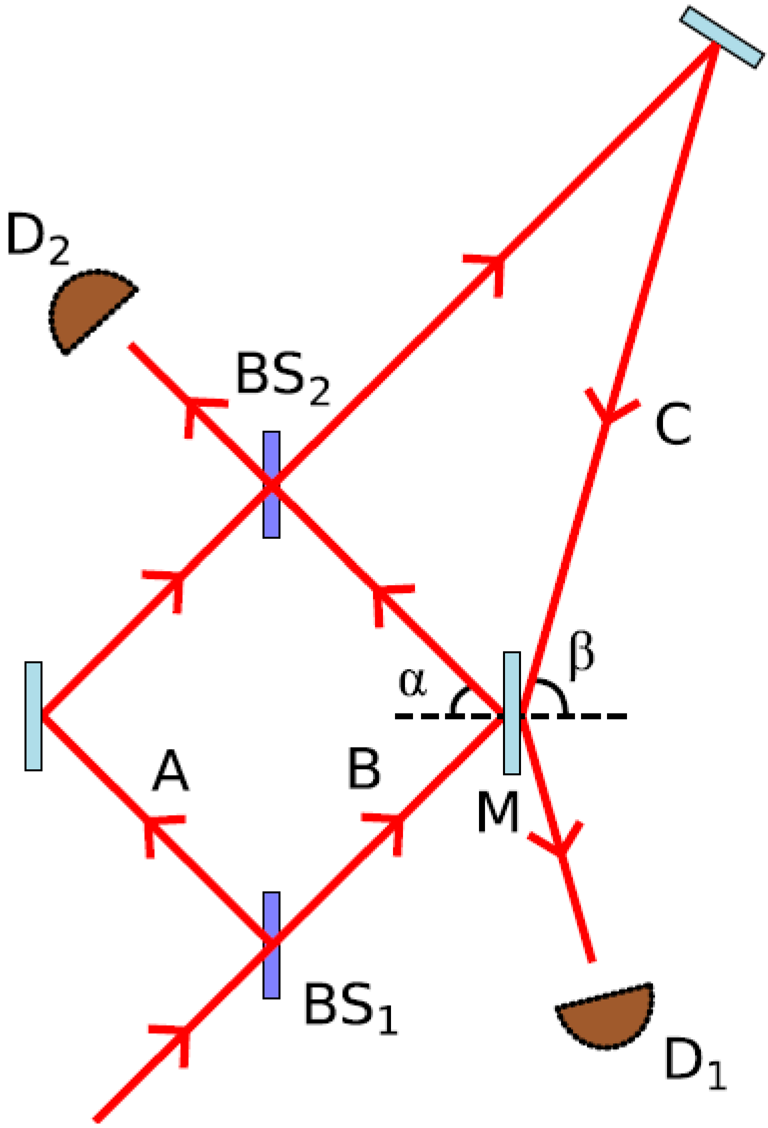

Figure 3.2: Modified version of a Mach Zehnder interferometer for light where one of the output beams is reflected back onto the exterior side of the two-faced mirror M. *Image extracted from ref. [1].*

in the interferometer mathematically meant that to project the photon's state at the final detectors mathematically meant to project this state at an alternative rotated basis, there denoted by the vectors $|I'\rangle$ and $|II'\rangle$. This also meant that a photon that is in a state represented by $|I'\rangle$ and $|II'\rangle$ when inside the interferometer will end up arriving at detectors D_1 and D_2, respectively, with probability 1. A generalization of the state vectors $|I'\rangle$ and $|II'\rangle$ in the more general present case of unspecified values for r and t gives us the basis vectors $|I'\rangle \rightarrow |A'\rangle$ and $|II'\rangle \rightarrow |B'\rangle$ in the form:

$$|A'\rangle = t|A\rangle - ir|B\rangle, \tag{3.10}$$

$$|B'\rangle = -ir|A\rangle + t|B\rangle, \tag{3.11}$$

as can be readily checked.

So, in our present interferometer, projecting the photon's state $|\psi\rangle$ at the vector states forming the rotated basis (A', B') means projecting the photon's state at the final detectors D_1 and D_2. The probability amplitudes that the photon will trigger detectors $D_1$and D_2 are then, respectively, $\langle A'|\psi\rangle$ and $\langle B'|\psi\rangle$. In this manner we are able to calculate the full detection probabilities at both detectors:

$$\begin{aligned} P_{D1} &= |\langle A'|\psi\rangle|^2 = 4r^2t^2, & (3.12)\\ P_{D2} &= |\langle B'|\psi\rangle|^2 = (r^2 - t^2)^2 = 1 - 4r^2t^2. & (3.13) \end{aligned}$$

What if, instead of single photons, we sent a classical light beam of intensity I towards this interferometer? In the same manner, given the above setting of the apparatus the intensity of the light beam traveling in arms A and B are respectively $I_A = r^2 I$ and $I_B = t^2 I$, and equally the arriving intensities at the detectors are $I_{D1} = 4r^2t^2 I$ and $I_{D2} = (1 - 4r^2t^2)I$.

It is in this context trivial to calculate the total momentum gained by mirror M during the interferometric experiment. If we take for simplicity the light beam to have an unit cross-section area and the experiment to last an unit time, the momentum given to M by the beam inside the interferometer is $2I_B \cos\alpha/c^2 = 2t^2 I \cos\alpha/c^2$. In the same manner, the momentum given to M by the beam on the outside of the interferometer is $2I_{D1}\cos\beta/c^2 = 8r^2t^2 I \cos\beta/c^2$. Using the previously fixed constraint that $\cos\beta = \cos\alpha/2$, we obtain the net momentum transferred to the mirror:

$$\begin{aligned}\Delta p_M &= \frac{2t^2 I}{c^2}(\cos\alpha - 4r^2\cos\beta) \\ &= \frac{2t^2 I}{c^2}(1-2r^2)\cos\alpha = -2t^2 I(r^2-t^2)\cos\alpha. \end{aligned} \tag{3.14}$$

Thus, in the case where we previously fixed the values of r and t so that we have $|r| > |t|$, the net momentum gained by mirror M has an overall negative sign that indicates that it has received a push towards the inside of the interferometer. This result was calculated classically, but we already have concluded that a quantum approach to this same question of momentum transfer yields equivalent mathematical results.

Our focus, however, is not in the question of mathematical equivalency concerning the numerical results, but rather it is in the story each theory has to tell. The story told by classical optics is a simple one - during the interferometric experiment, light hits mirror M from both sides. Although the light beam coming from the external side of the interferometer hits the mirror at a shallower angle of incidence, its intensity is higher than the intensity of the beam hitting M from the inside, so that the total momentum transferred by it to the mirror is larger and as a result M gains a net momentum towards the interior of the interferometer. Here, we note that the role played by the external reflection on mirror M is central to the process, in the sense that the negative contribution for the transferred momentum in this context its totally attributed to the existence of this reflection, as in fact our intuition tells us it must be.

Remarkably, although we may feel tempted to assume that the same logic must be true in all correct descriptions for this process of momentum transfer, as usual our intuition fails when trying to make an understanding of the quantum world. The assumption that the photons constituting the external light beam are the responsible ones for the inward push in mirror M is false, as we shall here demonstrate. For that purpose we analyze in detail, using a quantum description, the momentum transferred to M by the photons that end up reaching detectors D_1 and D_2.

3.0.4 The Negative Radiation Pressure

First it must be noted that, to maintain the quantum interference effect, the path of the photons cannot be marked. This adds a limitation on the process of reflection of the photons on mirror M, in the sense that the momentum δ transferred to it by each individual photon on the interferometer must be small if compared to the quantum uncertainty Δ of the mirror's momentum. This guarantees that there will be no essential change in the total momentum of the mirror. In any other way the photons would become entangled with the mirror, the coherence of the photons inside the interferometer would be destroyed and interference would be lost. This asks for a quantum description of the mirror M. While a photon coming through arm A produces no momentum kick on M, a photon coming through arm B transfer to it a momentum δ. If the quantum state of mirror M in momentum representation is previously denoted by $\phi(p)$, then after the entry of the photon inside the interferometer and possible reflection on M the total state of the system becomes:

$$|\Psi\rangle\phi(p) = \big(ir|A\rangle + t|B\rangle\big)\phi(p) \rightarrow ir|A\rangle\phi(p) + t|B\rangle\phi(p-\delta), \tag{3.15}$$

where the mirror states $\phi(p)$ and $\phi(p-\delta)$ must *not* be orthogonal, as to prevent the path marking. We take the simple case where the mirror's state in momentum representation has a form of minimum momentum uncertainty. This state is represented by the Gaussian function $\phi(p) = \exp\left[\frac{-p^2}{2\Delta^2}\right]$. In the case of a single photon impinging on M from inside the interferometer, and given that $\delta = 2\hbar w \cos\alpha << \Delta$, we can approximate the function $\phi(p)$ to the fist two terms of its Taylor series expansion. Thus we rewrite the joint state of the photon and mirror system just before the photon reaches BS_2 as:

$$\begin{aligned} |\psi\rangle\phi(p) &\approx ir|A\rangle\phi(p) + t|B\rangle\left(\phi(p) - \frac{d\phi(p)}{dp}\delta\right) \\ &= |\psi\rangle\phi(p) - t|B\rangle\frac{d\phi(p)}{dp}\delta. \end{aligned} \tag{3.16}$$

In the case where the photon ends up reaching the first detector D_1, the state of the mirror is obtained up to normalization by projecting the joint state represented by Eq. (3.16) at the vector state $|A'\rangle$ of Eq. (3.10), that represents the case where the photon is directed towards D_1. The projection yields:

$$\begin{aligned} \langle A'|\left(|\psi\rangle\phi(p) - t|B\rangle\frac{d\phi(p)}{dp}\delta\right) &= \langle A'|\psi\rangle\left(\phi(p) - \frac{t\langle A'|B\rangle}{\langle A'|\psi\rangle}\frac{d\phi(p)}{dp}\delta\right) \\ &= \langle A'|\psi\rangle\phi(p - P_B^w\delta) \end{aligned} \tag{3.17}$$

where $P_B^w = \frac{t\langle A'|B\rangle}{\langle A'|\psi\rangle}$. To calculate the numeric value of P_B^w in our interferometer is straightforward by use of Eq. (3.10) and (3.11):

$$\begin{aligned} P^w_B &= \frac{t\langle A'|B\rangle}{\langle A'|\psi\rangle} \\ &= rt/(rt+rt) = 1/2. \end{aligned} \tag{3.18}$$

With this we are led to the conclusion that, after the photon directed towards D_1 has entered the interferometer through the first beam-splitter BS_1, but just before it reaches BS_2, the state of the mirror M in momentum representation is represented by the function $\phi(p - \frac{1}{2}\delta)$ ($\phi(p)$ being a Gaussian wave packet in momentum). That is the same as to say that a photon that ends up reaching the detector D_1 changes the momentum of the mirror M by an amount of $\frac{1}{2}\delta = \hbar w \cos\alpha$ when still inside the interferometer, a momentum transfer which is just the mean value we would get for the two situations where the mirror gains a momentum kick of δ or no kick at all. These situations correspond to the propagation of the photon through the two possible arms inside the interferometer.

When the photon directed towards D_1 leaves the interferometer through the output beam-splitter BS_2, it produces another momentum kick on mirror M, this time from the outside, which produces a momentum transfer in the opposite direction. This second momentum transfer is straightforwardly calculated as $2\hbar w \cos\beta$. By using the previously fixed angle relation $\cos\beta = \cos\alpha/2$, we are able to calculate the *total* momentum transferred to mirror M by a photon that ends up reaching detector D_1 after going through the interferometer:

$$\Delta p_M = \hbar w \cos\alpha - 2\hbar w \cos\beta = 0. \tag{3.19}$$

And with this we arrive at a crucial point of our discussion. Since we are in a context of linear quantum optics, although this result was reached by analyzing the behavior of the system for a single photon going through the interferometer and reaching detector D_1, this same conclusion is valid for any number of photons that goes through the so constructed interferometer and eventually emerges towards D_1: *none of those photons produce a net change on the momentum of the mirror M*. The contribution to the net momentum transfer to M of the photons that arrive at D_1 is *null*. At the same time, we have already previously concluded that, during our interferometric experiment, M gains a non zero net momentum of $2t^2\bar{n}\hbar w(r^2 - t^2)$, in the direction of the interior of the interferometer. Where does this momentum come from? Rather strangely, the answer is that this net momentum appears due to *the photons that emerge towards the detector D_2*. A calculation similar to our previous one, but interchanging the projection vector $|A'\rangle$ for $|B'\rangle$, leads to the final state of the mirror in the cases where the photons end up arriving at the second detector D_2

$$\begin{aligned}\langle B'| \left(|\psi\rangle\phi(p) - t|B\rangle \frac{d\phi(p)}{dp}\delta \right) \\ = \langle B'|\psi\rangle(p - P_B'^w\delta),\end{aligned} \tag{3.20}$$

with $P_B'^w$ being the quantity

$$\begin{aligned} P_B^w &= \frac{t\langle B'|B\rangle}{\langle B'|\psi\rangle} \\ &= -t^2/(r^2 - t^2), \end{aligned} \tag{3.21}$$

and the momentum kick received by mirror M from a single photon arriving at detector D_2 is:

$$\Delta p_M = P_B^w\delta = -(t^2)\frac{2\hbar w}{c}\cos(\alpha)/(r^2 - t^2). \tag{3.22}$$

At the end of our experiment, the total momentum transferred to the mirror M by the totality of the photons that emerge towards the second detector D_2 is equal to the momentum due to the collision of each of these photons with the mirror multiplied by the number of photons in this beam. Since the probability for a photon to end up in the beam directed towards the detector D_2 after emerging from BS_2 is given by $(r^2 - t^2)^2$, we obtain for the net momentum transferred to M:

$$\Delta p_M = \bar{n}(r^2 - t^2)^2[(-t^2)/(r^2 - t^2)]2\hbar w\cos\alpha = -2t^2\bar{n}\hbar w(r^2 - t^2)\cos\alpha, \tag{3.23}$$

a result identical to our previously classically calculated result in (3.14).

We bring our attention to how different the stories told by the two theories are in the present context. We have seen that, classically, the light beam that reaches D_1 is the beam responsible for the negative momentum given to the mirror M. In fact, our intuition tells us that it is the *only light beam* that could transfer any momentum to M in that direction, since light traveling inside the interferometer can only push the mirror outwards (beam B) or leave it still (beam A) - the classical case is, therefore, closed. Quantum Mechanically though, and against all intuition, we find that the photons constituting this beam have no overall effect on the net momentum change of the mirror M - the two momentum kicks given by these photons to the mirror cancel out and their sum is found to be *strictly zero*. All the momentum change of the mirror must come from the photons that reach D_2 and therefore *are never reflected outwards by M.* How can this be? Although the only reflection suffered by these photons on the mirror M is from the inside the interferometer, still somehow they manage to pull it inwards! This is a result that is achieved by the quantum superposition of transferring to the mirror positive momentum or no momentum at all - and this superposition here is somehow equivalent to transferring to the mirror M a negative net momentum. The mathematical form of such a superposition can be visualized by projecting the total joint state 3.15 of the photon and the mirror M at the vector state representing only those photons that will end up reaching D_2 (represented throughout this discussion by the vector $|B'\rangle$):

$$\langle B'|\big(ir|A\rangle\phi(p) + t|B\rangle\phi(p-\delta)\big) = -r^2\phi(p) + t^2\phi(p-\delta), \tag{3.24}$$

where we have again used Eq. (3.11). With this we are able to make clear the existence of the superposition of the two Gaussian functions of momentum, one centered in zero (no momentum transfer) and the other displaced by an amount of δ (momentum transfer of δ). The coefficients of this superposition are, respectively, $-r^2$ and t^2.

It is in this scenario striking to visualize how our every day logic does not apply to the happenings in the quantum world and how these happenings can be, for our classical way of thinking, quite nonsensical. Niels Bohr is said to have remarked that anyone who did not feel dizzy when thinking about quantum theory must not have really understood it. Even so, it is hard to stress enough the extraordinary success that quantum theory has in predicting the observed behavior of physical systems. Quantum theory results have now been tested in various diverse ways, and never found wanting - to the point we can tell, its results seem to be strictly correct. Even when dealing with larger scale systems, these results seems to loose their random, probabilistic aspect and are now found in various ways to agree with the results of classical mechanics. The inverse situation is, however, not true. Confronted by this apparent universal and very much successful applicability, we are led to the conclusion that we must accept quantum theory, even when its results and predictions seem too odd for us. As in Robert Gilmore's words, 'however nonsensical quantum mechanics may at times appear to us, that seems to be the way nature wants it - and so we have to play along' [43]. And sometimes, playing along means stressing our imagination far and trying our hardest to forge new intuition about the very unusual, and even disturbingly odd scenario that is that where quantum phenomena takes place.

Chapter 4

Quantum Interference of Force

In Chapters 2 and 3 of this dissertation we were introduced to the concept and implications of the quantum superposition phenomena, using nothing more than basic quantum formalism most advanced undergraduate students are already familiar with. In this manner, we have seen how quantum states consisting of superposing different possibilities for the physical objects existing in the quantum regime are able to generate quite counter intuitive physical results, even in the most simple cases where we do not have to dive too deep into the theory to reach them. There is something special about keeping the discussion simple on a mathematical level, for it allows us to focus more on the fundamental characteristics of the quantum behavior and on the essentials of the quantum theory that could be otherwise lost between the lines of exhaustive mathematical calculations. And yet, as much as we reach further into the depths of the theory, still the most basic results keep their ability to surprise us. In special, in the previous chapter, we have seen how the quantum superposition of states corresponding to the two possibilities of using light to push a mirror M in a certain direction or leaving this same mirror completely still can in a certain situation result in giving the mirror a pull in an opposite direction [1]. To achieve this rather surprising, seemingly nonsensical result, the quantum formalism was used in order to describe the behavior of the mirror

M. Sadly, due to technical limitations and although a great effort is currently being made in order to change this scenario, we have until now found no way of building and working with mirrors so light that the change in it's position must be treated quantum mechanically and so that we could generate the discussed results in the laboratory while working in the single photons regime [44]. So the results presented by the paper we have thoroughly discussed in the previous chapter, though being achieved by application of only basic quantum formalism that have already showed itself successful by many other means, have yet no way of being actually tested. In this chapter we present a similar physical situation where no quantum mirror is needed to observe the almost analogous results. The formalism used is similar and therefore the discussion is kept mathematically simple, although at some points there are some non-introduced bits of formalism that the reader is expected to have previously studied. We note here that, even if we already believe in and accept the fundamentals of the quantum theory and formalism used to derive our results, still there is much to gain by exercising our intuition and our knowledge about the essential, though very counterintuitive behaviors of physical objects existing in the quantum world. We would also like to make a note about the intents of the here presented work. While *Aharonov et. al.* wanted to discuss the difference between the classical and quantum descriptions of physical radiation pressure, our objective here is to describe the effect of 'interferometric anomalous forces' as a genuine quantum phenomenon, which does not have a classical analogous, extending the limit in which the phenomenon can be observed and in a way that could also be observed in the laboratory.

In the present chapter, we introduce for the noted purposes a Mach Zehnder type of interferometer that could be used to interfere the amplitudes associated to the different possible paths *taken by massive charged objects in the quantum regime.* In particular, we develop our present discussion for the specific case of a *single electrons Mach Zehnder interferometer*, an apparatus which is fully sketched in Fig 4.1. The general effect of this interferometer on the traveling electron's wave function is the same that which have already been discussed in the previous chapters for similar interferometric situations: firstly, the incoming electron's state is coherently divided into a superposition of amplitudes by a first beam-splitting device, which we have labeled here as BS_1. These two amplitudes, which are associated to the two different path possibilities A and B inside the interferometer, evolve during the electron's travel inside the apparatus and are finally mixed together and made to interfere in a second beam-splitting device BS_2. The redirection of the electron's paths is accomplished with the help of two correctly positioned 'electron mirrors'. As is shown in Fig 4.1, an electron going through this apparatus emerge from the interferometer in one of two possible final distinguishable directions of propagation. Although Mach Zehnder interferometers of this kind were first introduced as interferometric devices used to interfere the path amplitudes of light beams or single photons, in the following discussion we will show how a single electrons Mach Zehnder interferometer following this same topology can be built using diffraction gratings as both the beam splitting devices and the redirecting 'electron mirrors' [9].

Here, for the purposes of the experiment in discussion, we imagine that the electrons going through the described interferometric apparatus will interact with a controlled electromagnetic force field when - and only when - traveling through the upper arm of our Mach Zehnder interferometer, which we have labeled as path A. We imagine thus that we could build the experimental apparatus so that a certain length of this arm passes right between the two charged plates of a capacitor CAP, which generates a controlled electric field $\vec{E}$ in the $-\hat{y}$ direction in it's interior, as is also shown schematically in Fig.4.1. The other possible path for the electron inside the interferometer is thought as being free of the influence of this electric field as well as of any other possible external disturbance. As we shall see, when this force field region is introduced at only one of the two possible paths for our electrons, we are able in specific situations to generate the quantum counterintuitive results of seemingly 'unusual' momentum gains in our physical system.

For simplicity, in this discussion we take the initial wave function of the incoming electrons to be a Gaussian function of momentum centered in zero in momentum representation in the two spatial directions orthogonal to their propagation. We expect the momentum representation to be simpler than the usual coordinate representation whenever a physical system is invariant under space displacements, as is the case of the electron's free propagation and it's propagation in uniform force fields, which are the two situations we deal with in the interior of our interferometer. While the electrons travel inside the interferometer, we want two things to happen to it's quantum state: (1) we do not want any big spread of the electron's wave function during it's motion and (2) we want the interaction with the electromagnetic force field $\vec{E}$ in the arm A of the interferometer to keep the electron's wave function

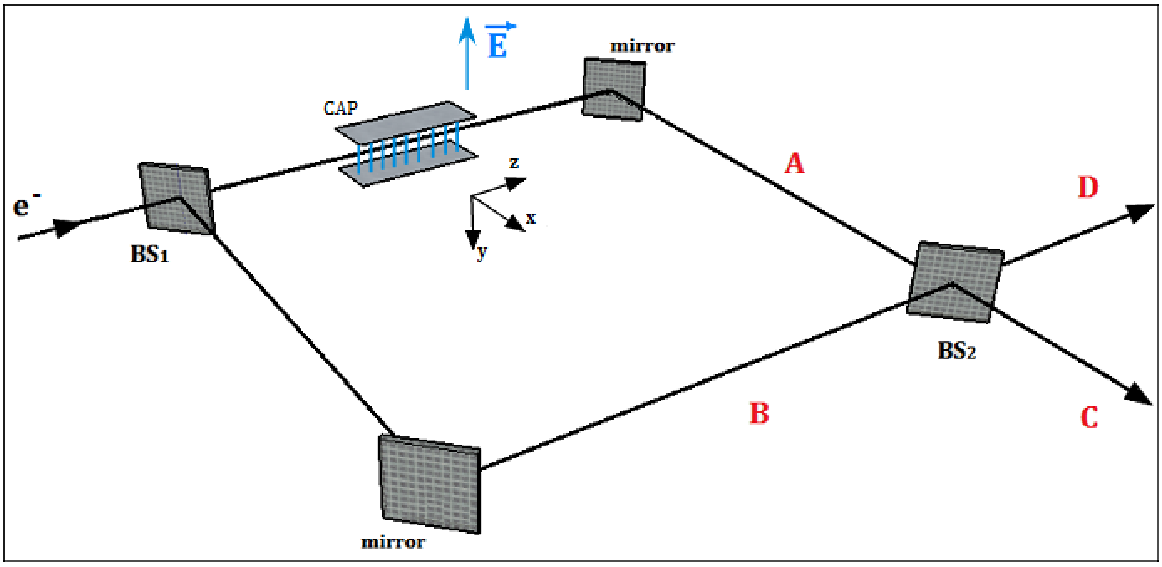

Figure 4.1: A simplified sketch of a single electrons Mach Zehnder interferometer of two exit channels. A capacitor CAP is placed in one of the interferometer's arms, as to create a disturbing electric field in one of the electron's possible paths.

in a Gaussian form. We then start the discussion of this chapter by considering these aspects of the electron's state propagation in our experimental apparatus, while considering that the third direction, the direction of propagation of the electron inside the interferometer, can be treated classically throughout our discussion.

4.1 Free propagation

Firstly, we consider the motion of a free massive particle in an one dimensional space. In momentum representation, the Schrodinger equation is written as:

$$\frac{p^2}{2m}\Phi(p,t) = i\hbar\frac{\partial\Phi(p,t)}{\partial t}, \tag{4.1}$$

since in momentum space the momentum operator is diagonal so that we can take $\hat{p} = p$, m on the equation Eq. (4.1) being the particle's mass. We see that by working in momentum space we have reduced the problem of solving a second order partial differential equation, which would be the Schrodinger equation in coordinate space, to the problem of solving a simpler first order differential equation. Eq. (4.1) has a trivial solution:

$$\Phi(p,t) = \exp\left(\frac{-itp^2}{2\hbar m}\right)\Phi(p,0), \tag{4.2}$$

where $\Phi(p,0)$ is just the initial form of the particle's wave function in momentum space. The exponential term represents the time dependent complex phase of the wave function. Here we take the initial wave function of the particle in momentum space to be a Gaussian distribution of momentum centered in zero, in the form

$$\exp\left(-\frac{p^2}{2\delta^2}\right) \tag{4.3}$$

and we then have that, in a subsequent time t,

$$\Phi(p,t) = \left(\frac{1}{\pi\delta^2}\right)^{-\frac{1}{4}} \exp\left(-\frac{p^2}{2\delta^2}\right) \exp\left(\frac{-itp^2}{2\hbar m}\right). \tag{4.4}$$

Since only the phase of the wave is time dependent and this phase has no real effect on the wave form, we see that the particle's wave function in momentum space remains in the form of a Gaussian centered in zero at all times if it's not under the influence of any external force fields. The constant coefficient was introduced to normalize the wave function so that we have $\int dp|\Phi(p,t)|^2 = 1$.

We can obtain the particle's wave function in coordinate representation by use of a Fourier transform:

$$\begin{aligned}\Psi(x,t) &= (2\pi)^{-\frac{1}{2}} \int dp \exp\left(ipx - \frac{itp^2}{2\hbar m}\right)\Phi(p,0) \\ &= \left(\frac{1}{2\pi^3\delta^2}\right)^{-\frac{1}{4}} \int dp \exp\left[ipx - \left(\frac{1}{2\hbar\delta^2} + \frac{i\hbar t}{2m}\right)p^2\right],\end{aligned} \tag{4.5}$$

where the last integral can be performed in a standard way by completing the squares in the exponential argument. The time dependent wave function of the particle in standard coordinate space is then found to be:

$$\Psi(x,t) = (2\pi)^{-\frac{1}{4}} \left[-\frac{1}{\sqrt{2}\delta}\left(1 + \frac{i\hbar\delta^2 t}{m}\right)\right]^{\frac{1}{2}} \exp\left(\frac{-x^2}{4\alpha^2}\right), \tag{4.6}$$

where $\alpha^2 = \frac{1}{2\delta^2}\left(1 + \frac{i\hbar\delta^2 t}{m}\right)$ is a parameter that characterizes the *width* of the Gaussian function. We notice that the parameter α increases in time, so while the wave function of the particle is also in a Gaussian form in coordinate space, we here have that the form of the Gaussian is time dependent and that the wave function of the particle in coordinate space will spread in time. We can rewrite the wave function of Eq. (4.6) in a way that shows explicitly it's amplitude and phase, so that this behavior is made clearer. This is accomplished in ref. [45]. If we define the real functions W, ψ and R as:

$$W(t) = \frac{\sqrt{2}}{\delta}\left[1 + \left(\frac{2pt\delta^2}{m}\right)^2\right]^{\frac{1}{2}}, \tag{4.7}$$

$$\cos(\psi(t)) = \frac{\frac{\sqrt{2}}{\delta}}{W(t)}, \tag{4.8}$$

$$R(t) = \frac{pt}{m}\left[1 + \left(\frac{m}{2pt\delta^2}\right)^2\right], \tag{4.9}$$

then the particle's wave function of Eq. (4.6) can be rewritten in terms of $W(t)$ $\psi(t)$ and $R(t)$ as:

$$\Psi(x,t) = \frac{\sqrt{\delta}}{\pi^{\frac{1}{4}}}\left[\frac{\frac{\sqrt{2}}{\delta}}{W(t)}\right]\exp\left(\frac{-x^2}{W^2(t)}\right)\exp i\left(\frac{x^2}{2R(t)} + \psi(t)\right), \tag{4.10}$$

and the behavior of the quantities W, ψ and R is illustrated in Fig. 4.2.

We briefly examine the implications of the expression given by Eq. (4.10). Firstly, we note that the function $W(t)$ can now be associated strictly with the Gaussian wave's width as a function of time. We see by looking at the first graphic shown in Fig. 4.2 that this width will steadily increase as time passes, *meaning that the quantum uncertainty associated to the particles position, being represented by this wave function, and that is associated with width given by $W(t)$ is also growing steadily in time.* Here, the value taken by the time function $W(t)$ will directly affect the form taken by the probability distribution of finding the particle in a certain point x in the considered one-dimensional space. Secondly, we briefly discuss the final coordinate wave function's *total phase*, that is strictly given by the argument:

$$\left(\frac{x^2}{2R(t)} + \psi(t)\right) \tag{4.11}$$

in the wave represented by Eq. (4.10). The first term in this expression, $\frac{x^2}{2R(t)}$, have a geometrical interpretation. If we consider a particle traveling in the z axis direction in a two dimensional space containing both the x and z axis, and make the classical association $t = \frac{z}{v}$, v being the particle's velocity, then the phase $\frac{x^2}{2R(t)}$ will represent the distance between a spherical surface of radius $R(t)$ and the z-plane at a height x from the z-axis (See Fig. 4.3). This spherical surface will be centered at a certain point $d(t)$ (not derived here) in the $z < 0$ region. The geometrical meanings of $W(t)$, $R(t)$ and the phase $\frac{x^2}{2R(t)}$ in this situation are schematized in Fig. 4.3. It is shown in the second graphic of Fig. 4.2 that the value of $R(t)/t$ will tend to unity. The second phase term in Eq. (4.10) is given solely by $\psi(t)$, and represents an additional phase shift which is associated to the so-called *phase anomaly near focus* [46]. As shown in Fig. 4.2, this quantity tends to a constant, nominally $-\pi/2$, as the wave packet evolves.

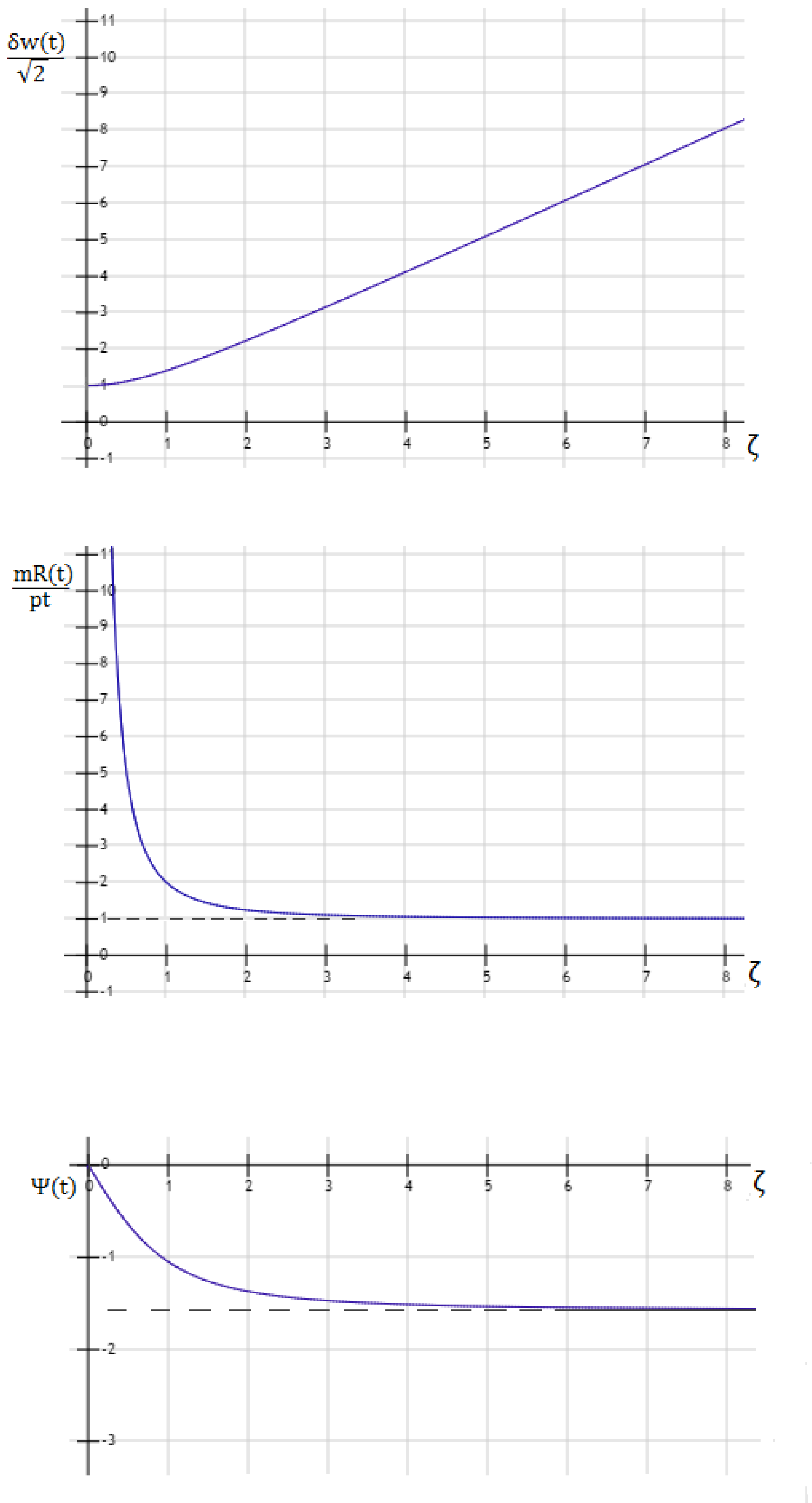

Figure 4.2: Plotted behavior of the quantities $W(t)$, $\psi(t)$ and $R(t)$ defined by Eqs. (4.7), (4.8) and (4.9) associated to a normalized Gaussian wave function as a function of the variable $\zeta = \frac{2pt\delta^2}{m}$.

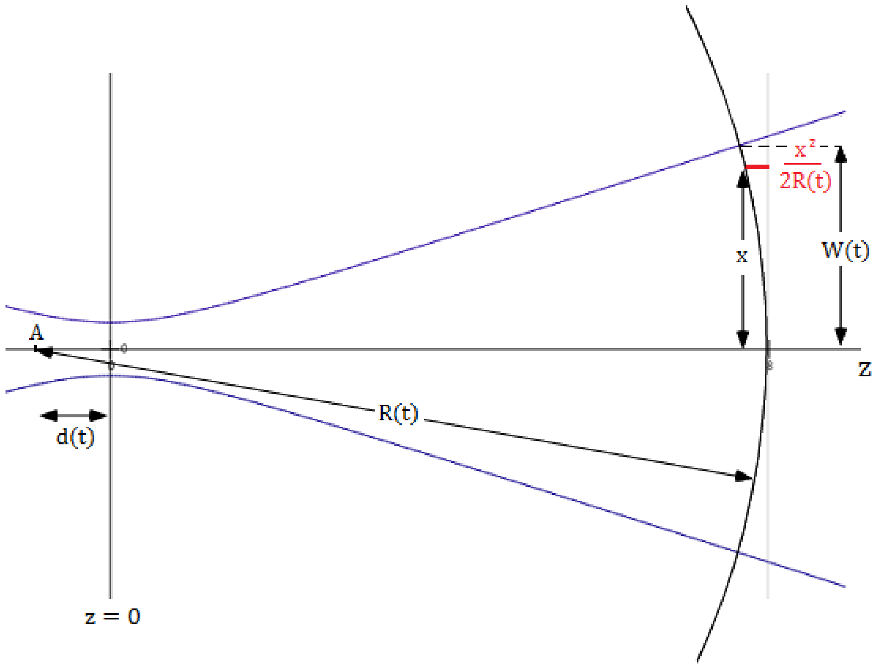

Figure 4.3: Simplified illustration of the geometrical significance of the parameters $W(t)$, $R(t)$ and $\frac{x^2}{2R(t)}$ used to describe the behavior of a Gaussian wave function evolving in the standard coordinate space.

It is important to notice that these additional phases do not affect the probability distribution of the particles detection as a function of x, and as a result the existence and value of these wave phases won't affect the discussion in the development of this chapter, and were only introduced together with the width function $W(t)$ for the sake of completeness.

4.2 Propagation in an Uniform Force Field

During the experiment in discussion, the interfering charged particle also propagates through region disturbed by an uniform electromagnetic force field. The particle is taken to be an electron traveling through a constant electric field $\vec{E} = -E\hat{y}$, generated by a capacitor CAP, that acts on a limited length of the electron's path, as shown in detail in Fig 4.4. Any effect of the capacitor's borders will be neglected. When under the influence of the electric field $\vec{E}$, the one dimensional Hamiltonian of the electron becomes $\hat{H} = \hat{p}^2/2m - F\hat{y}$, where Fy is the absolute value of the electrical potential energy at a position y, p the momentum of the electron in that direction, and F corresponds to the absolute value of the force felt by the electron when under the influence of the field. As only the motion of the electron in the

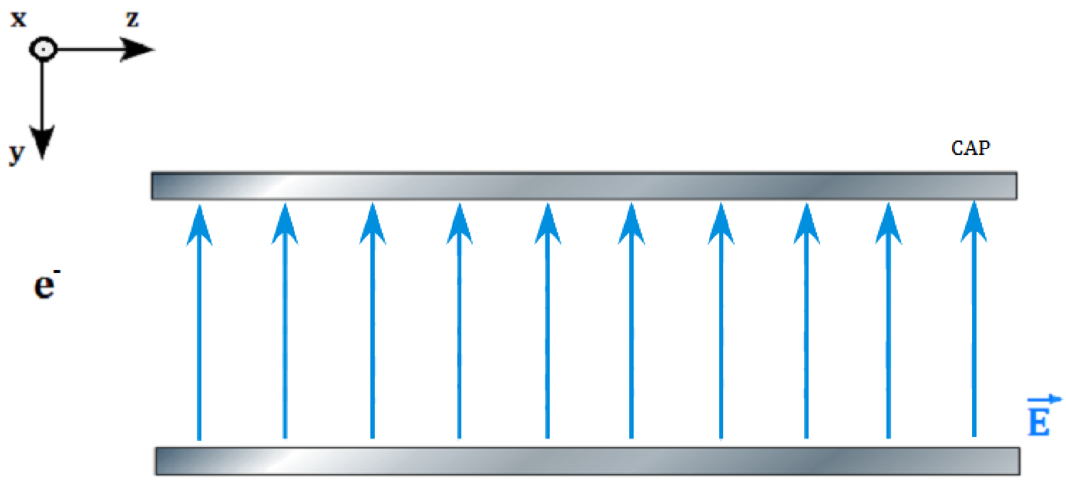

Figure 4.4: Electron traveling though the region containing the disturbing electric field $\vec{E}$ between the capacitor plates.

y direction will be affected by the presence of the disturbing electric field, again we have a problem that is essentially one dimensional. The solution for the Schrodinger equation in momentum space for this case remains simple [47], but some mathematical complications may arise when taking the Fourier transform to find the complete form of wave function in coordinate space. Since the exact form of the electron's wave function in the standard coordinate space will not be important for our following discussion, here we will treat the case of the propagation in an uniform force field in a more qualitative manner.

For this, dropping the hats to ease the notation, we write the equations of motion of the momentum and position operators in this dimension for the electron in the Heisenberg representation (in which the quantum operators evolve with time) as:

$$\frac{dy(t)}{dt} = -\frac{i}{\hbar}[y, H] = \frac{p(t)}{m}, \tag{4.12}$$

$$\frac{dp(t)}{dt} = -\frac{i}{\hbar}[p, H] = F. \tag{4.13}$$

By solving the second of these equations and using the result in the first, we are able to determine the time dependence of the two operators in this particular case. Taking the mean values of the so achieved results will then yield:

$$\langle y \rangle = \frac{\langle p \rangle_0}{m} + \frac{Ft^2}{2m}, \tag{4.14}$$

$$\langle p \rangle = \langle p \rangle_0 + Ft, \tag{4.15}$$

where the subscript 0 indicates that the associated term corresponds to the initial form of each of the operators, taken in a certain chosen origin for the time component.

We notice by Eqs. (4.14) and (4.15) that the mean values of the position and momentum operators for the electrons traveling through a region disturbed by an uniform electromagnetic force field are exactly the same as those of the classical evolution for the corresponding physical dynamical variables. In that manner we can say that the *means here behave classically*. But what about the uncertainty associated to the momentum operator during the electron's motion? If we take $\Delta p_t^2 = \langle p^2 \rangle_t - \langle p \rangle_t^2$ to be a measurement of this uncertainty, we will have that:

$$\begin{aligned}\Delta p^2(t) &= \langle p^2 \rangle - \langle p \rangle^2 \\ &= \langle (p + Ft)^2 \rangle - (\langle p \rangle_0 + Ft)^2 \\ &= \langle p^2 \rangle_0 + 2Ft\langle p \rangle_0 + F^2 t^2 - (\langle p \rangle_0 + Ft)^2 \\ &= \langle p^2 \rangle_0 - \langle p \rangle_0^2 = (\Delta p)_0^2. \end{aligned} \tag{4.16}$$

As we see, the quantity Δp^2, which we have associated with the uncertainty of the momentum operator of the electron, does not change during the electron's motion in the region disturbed by the electric field. This quantity can be directly associated with the width of our Gaussian function (in the case that the motion indeed does not alter the form of the electron's wave function, so that it remains a Gaussian), so that again the width of our Gaussian distribution for the momentum of the electron remains unchanged. The same, however, again does not hold for the analog quantity associated with the position operator, and similar calculations will lead to the result that $\Delta y^2(t) = \Delta y_0^2 + \frac{\Delta p_0^2 t^2}{m^2} + \frac{[\langle yp+py \rangle_0 - 2\langle y \rangle_0 \langle p \rangle_0]t}{m}$, which varies explicitly with time. So in the motion of the electron in the electric field $\vec{E}$, again we have a spread in position, but not a spread in momentum.

We have in this manner seen how the mean values of the position and momentum operators of the electron and the uncertainties associated with them behave during the motion in the uniform electric field, but we have yet to see if the assumption that the wave function in the momentum representation remains in a Gaussian form after the interaction can be taken as valid. For this, we will assume that the electric field acts briefly on the electrons and that during it's action the electrical potential energy exceeds the kinetic energy so that the first term of the electron's Hamiltonian can be ignored during this time (which would mean applying a electric field $\vec{E}$ of a big enough magnitude). We write the initial electron's state as the infinite sum:

$$|\psi_0\rangle = \int dp\psi_0(p)|p\rangle,$$

where $|p\rangle$ are the eigenvectors of the momentum operator with eigenvalues p. The evolved state from a time t_0 to a future time t can be obtained from the initial state with help of the standard quantum evolution operator $U(t-t_0) = \exp\left[\frac{-i}{h}(\hat{H})(t-t_0)\right] = \exp\left[\frac{-i}{h}(t-t_0)\left(\frac{\hat{p}_y^2}{2m} - F\hat{y}\right)\right]$. The evolution operator acts on each one of the vectors in the state decomposition separately, so that:

$$|\psi(t)\rangle = \int dp\psi_0(p)U(t-t_0)|p\rangle$$

$$= \int dp\psi_0(p)\exp\left[\frac{-i}{h}(t-t_0)\left(\frac{\hat{p}_y^2}{2m} - F\hat{y}\right)\right]|p\rangle.$$

If we now make use of the supposition that $\frac{p_y^2}{2m} << Fy$, we get:

$$|\psi(t)\rangle = \int dp\psi_0(p)\exp\left[\frac{-i}{h}(t-t_0)(-F\hat{y})\right]|p\rangle. \tag{4.17}$$

Now the final argument of the exponential function in these equations is $\frac{-i}{h}(t-t_0)(-F\hat{y})$, where $\hat{y}$ here is taken as the position operator associated with the direction y. This exponential argument has become then, according to the quantum mechanical formalism, associated with the *generator of momentum displacement*[47]. This means that the full exponential function of Eq. (4.17) acts on a eigenstate of momentum $|p'\rangle$ by changing it into another momentum eigenstate, now associated with a momentum shifted by a quantity equal to $F(t-t_0) = \Delta p'$. In this manner, Eq. (4.17) becomes:

$$|\psi(t)\rangle = \int dp\psi_0(p)|p + F(t-t_0)\rangle. \tag{4.18}$$

We can rearrange the final expression in Eq.(4.18) by making the simple change of variables $p' = p + F(t-t_0) \rightarrow p = p' - F(t-t_0), dp = dp'$ to show that the shape of the Gaussian function of the electron's state in the y direction does not change, and that the Gaussian distribution will only be dislocated from the origin by a quantity equal to the gain on the electron's momentum in that direction. This result was obtained by assuming that, during the interaction, we can make $Fy = e|E|y >> \frac{p_y^2}{2m}$, which would in turn imply a big enough magnitude for the set (constant) electric field between the capacitor plates. However, we must notice that it is also important that the interaction between a electron traveling between the plates and the electric field $\vec{E}$ in this region doesn't change the electron's momentum in such a significant way as to kill the effect of interference. For the purposes of the experiment in mind, it is necessary that we have that $e|E|\Delta t < \delta$, where Δt is the total time of interaction. Since we need that $|E|$ will be big, we will also need the quantity Δt to be small so that all the suppositions hold and the effect we analyze can be observed.

We have, thus, guaranteed our assumption that, under certain conditions, the interaction with the electrical field $\vec{E}$ keeps the momentum wave function of the electron in a Gaussian form. In this manner, we will only work with dislocated (associated with the interferometer's upper arm A) or non dislocated (associated with the interferometer's lower arm B) Gaussian functions of momentum throughout the following discussion.

4.3 Anomalous Forces in a Mach Zehnder interferometer

While traveling inside the single electrons Mach Zehnder interferometer sketched in Fig 4.1, each electron's wave function is coherently divided into a superposition of terms associated with it's path possibilities and as we expect we are able to observe the phenomenon of interference of the arrival probability amplitudes at the two possible final propagation directions, the 'exit channels' labeled as C and D, as a function of the set phase difference ϕ between the two interferometer's arms. The interferometer we have been referring to, and that is depicted in Fig 4.1, is a simplified version of an actual, experimental Mach Zehnder interferometer built to interfere the path amplitudes of massive charged objects in the laboratory. However, the study of this simplified interferometer of two final exit ports contains in itself all of the important notions needed to understand the quantum physical phenomenon here in discussion. In this manner, during this section and in the following, we discuss the behavior of the interfering electrons while traveling inside a single electrons Mach Zehnder interferometer of two possible exit channels. Following these discussions, we will analyze a more realistic version of a particle Mach Zehnder interferometer.

We note that, during the process of interference, it is very important that the electron's states don't become entangled with the surrounding environment. In other words, during the experiment we can have no physical system acting as the electron's 'path marker', even if the interaction between the electrons and the electric force field $\vec{E}$ generated by the capacitor CAP takes place in arm A of our Mach Zehnder interferometer. For this, we must have that any induced changes on the electron's wave function due to the interaction with this electric field are not bigger than the present *quantum uncertainties* associated with any possibly disturbed quantum observables. In this way, the interference phenomenon can be protected, and we are able to generate the physical results we discuss in the following.

Firstly, we take $\hat{z}$ to be the direction of the electron's propagation at all times and $\hat{x}$ as the direction orthogonal to it in the the plane of the interferometer, as shown in detail in Fig 4.1. The charged plates of the capacitor CAP are positioned so that an electric field $\vec{E}$ is generated inside them and will point in the $\hat{y}$ direction, orthogonal to the plane defined by the arms of the interferometer. As no other external disturbance is present, only the momentum wave function of the electrons associated with the direction of this electric field will be disturbed during the electron's motion through our apparatus, and in this discussion we are only interested in what happens to the wave function associated with this space component (y). *So from here on we will only take into account the wave functions of momentum p associated with direction $\hat{y}$.* We take the initial form of the momentum wave function of each electron sent through the interferometer in direction y just before it reaches the first beam-splitting device BS_1 to be a Gaussian distribution of momentum centered in zero, in the form:

$$\Phi_0(p) = \frac{1}{\sqrt{\delta^2\sqrt{\pi}}} \exp\left[\frac{-(p^2)}{2\delta^2}\right], \tag{4.19}$$

which is in the same form of Eq. (4.3), but normalized so that $\int dp|\Phi_0(p)|^2 = 1$.

In accord with what has been previously discussed throughout our chapters, we are able to derive what will be the total final wave function of each electron going through the interferometer as it arrives at either one of the two final propagation directions, or exit channels C or D, after having left our interferometric apparatus. Let us denote the electron's state vectors associated with the corresponding momentum wavefunctions while inside the interferometer as the vectors $|\Phi_0\rangle$ and $|\Phi'\rangle$ defined so that:

$$\Phi_0(p) = \langle p|\Phi_0\rangle \tag{4.20}$$

and

$$\Phi'(p) \equiv \Phi_0(p - p_0) = \langle p|\Phi'\rangle, \tag{4.21}$$

$p_0 = e|E|\Delta t$ being the total momentum gain of an electron of electric charge $-e$ after having interacted with the electric field $\vec{E} = -|E|\hat{y}$ during a time Δt. Then an electron's momentum wave function just *after* it has passed through the first beam-splitting device BS_1 can be written as:

$$|\Phi_T(p)\rangle = ir_1|\Phi_0, B\rangle + t_1|\Phi_0, A\rangle, \tag{4.22}$$

where r_1 and t_1 are respectively the reflection and transmission coefficients associated to BS_1, satisfying the condition that $r_1^2 + t_1^2 = 1$.

After having passed through BS_1, the electron's state will evolve, each component separately, until it reaches the second and last beam-splitting device BS_2. The electrons total state just *before* it passes through BS_2 and leaves the interferometer can then be written as:

$$|\Phi_T(p)\rangle = ir_1|\Phi_0, B\rangle + t_1 \exp{(i\phi)}|\Phi', A\rangle, \tag{4.23}$$

where ϕ is the total phase shift that represents the possibly different gains in phase between the two arms of the interferometer.

The second beam-splitting device BS_2 will then act individually on each of the components of this state, and the total effect of this device on the electron's state will in turn result in the following components, each associated with the two final propagation directions C and D:

$$\langle p, C|\Phi_T\rangle = \Phi_C(p) = \exp{(i\phi)}\sqrt{1 - r_1^2}\sqrt{1 - r_2^2}\Phi(p - p_0) - r_1 r_2 \Phi(p), \tag{4.24}$$

$$\langle p, D|\Phi_T\rangle = \Phi_D(p) = \exp{(i\phi)}\sqrt{1 - r_1^2}r_2\Phi(p - p_0) + r_1\sqrt{1 - r_2^2}\Phi(p), \tag{4.25}$$

where r_2 and t_2 are respectively the reflection and transmission coefficients associated to BS_2, and where we have written $t_1 = \sqrt{1 - r_1^2}$ and $t_2 = \sqrt{1 - r_2^2}$. The functions Φ in these expressions are quadratic-normalized Gaussian functions of their arguments, in the form of Eq. (4.19). We can check that indeed $\int dp|\Phi_C|^2 + \int dp|\Phi_D|^2 = 1$, as it must be (the complementary probabilities must add to unity). The results of Eqs. (4.24) and (4.25) were obtained considering a phase gain of $\pi/2$ associated with every reflection on the (symmetric) beam-splitting devices.

The main idea upon performing an interferometric experiment with single electrons using the above described interferometric apparatus is to create with it a situation that mimics the results obtained by Aharonov *et. al.* [1] that were described in the previous chapter, where the quantum superposition of terms associated with two different possibilities for a quantum system adds up to a very non-intuitive physical situation in what concerns the exchange of momentum within the studied physical system. For that purpose, and for reasons that shall be made clear in the following, we shall try to create a physical situation with our interferometer where the wave functions of the electron associated with each of the interferometer's paths *interfere destructively* at a chosen one of our final exit channels (and therefore constructively at the other). Destructive interference can be achieved in our two terms superposition when a total phase difference of $\phi = \pi$ is introduced between the wave functions associated with the different interferometer's paths - this is the phase shift that corresponds to a *sign difference* between the two amplitudes associated with the two paths, since we have that $\exp(i\pi) = -1$. We notice, by direct inspection of Eqs. (4.24) and Eq. (4.25), that in our given apparatus this situation can be achieved at the final propagation direction C by setting the controllable phase shift as $\phi = 0 mod 2\pi$ and at the final direction D by setting $\phi = \pi mod 2\pi$.

We now develop our discussion by considering the case where, by adjusting say the length of the interferometer's upper arm A, we choose to set $\phi = 0 mod 2\pi$ to get a destructive quantum interference at the exit port C. We can notice by inspection of the expression in Eq. (4.24) when we set $\phi = 0$ that, even in the cases of destructive interference, the probability amplitude associated with the detection of the electron at the chosen exit C will not vanish entirely, and there will be still (though small) a chance that a traveling electron will actually be detected leaving the interferometer through that exit port.

For our experiment, we assume that we are able to choose to set the value of the reflection coefficient of the second beam-splitting device as the fixed value $r_2 = 1/\sqrt{2}$, so that while leaving the interferometer an electron has an equal chance of being reflected or transmitted by BS_2. With this, we are left with three other variables within our system that we assume we could somewhat freely manipulate, namely, δ, associated with the incoming Gaussian's width, p_0, the momentum gained by the electron in the $\vec{y}$ direction due to the interaction with the electric force field $\vec{E}$ in the upper arm A of the interferometer, and r_1. Fig. 4.5 shows what happens to the curve corresponding to an interfering electron's momentum distribution when, for example, we choose to run the experiment setting $\frac{p_0}{\delta} = 0.5$ and $r_1 = 0.84$ in the context of destructive interference set at the exit port C ($\phi = 0 mod 2\pi$).

We see by the momentum distribution curve of the electrons traveling at C represented in Fig. 4.5 that we have managed to create a physical situation where the expectation value

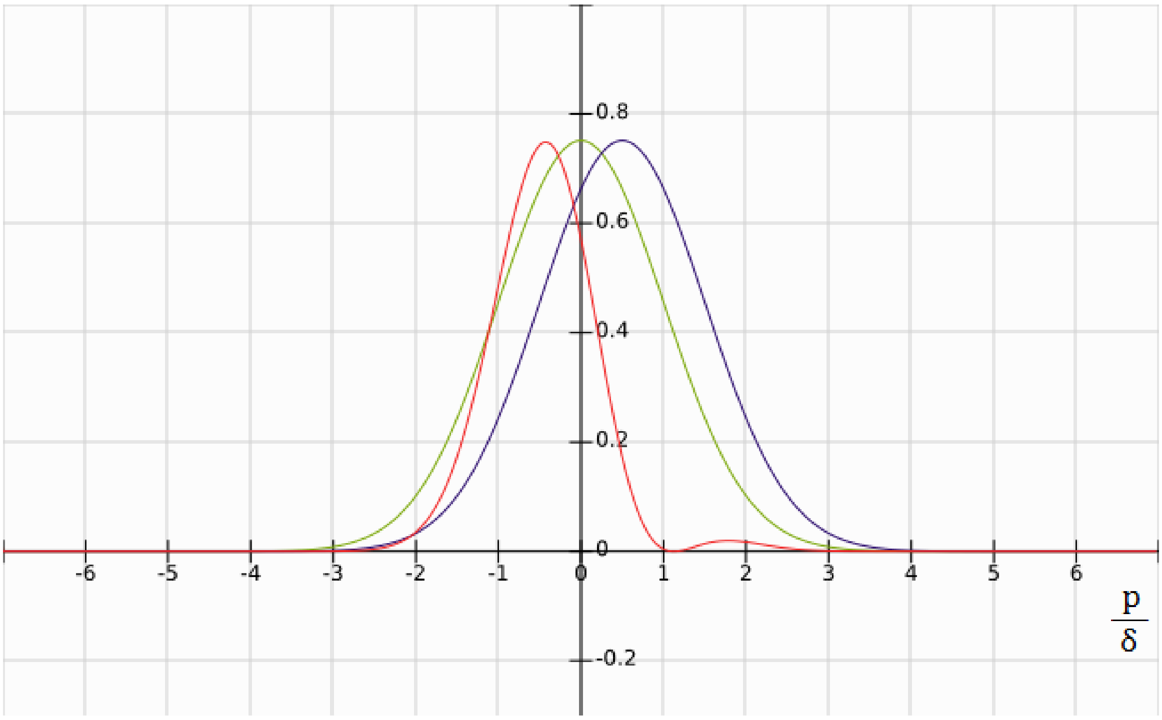

Figure 4.5: The electron's wave functions in momentum representation and associated with the lower path B (green line - no external electric field) and the upper path A (blue line - external electric field $\vec{E}$ acting in a portion of the electron's path) of the single electrons Mach Zehnder interferometer. The (15.5 times augmented) momentum distribution associated with the arrival of the electron at the exit channel C in the case of destructive interference occurring at this exit ($\phi = 0 mod 2\pi$) and when we set $\frac{p_0}{\delta} = 0.5$ and $r_1 = 0.84$ is shown in red. The mean, or expectation value $\langle p \rangle$ for the electron's momentum in this scenario is *negative*.

$\langle p \rangle$ of the electron's momentum at exit channel C is turned *negative*, even though this result derives directly from a superposition of possibility amplitudes where the electron has either gained *positive* momentum during it's accounted interaction with the external electric field or has had no momentum gain at all in any direction. We can explicitly calculate what will be the expectation value $\langle p \rangle$ of the momentum variable of an electron arriving at exit C under the described interferometric conditions of induced destructive interference as a function of the physical and experimental variables concerning our system as:

$$\langle p \rangle_\chi \equiv \frac{\int_{-\infty}^{\infty} p|\Phi_\chi(p)|^2 dp}{\int_{-\infty}^{\infty} |\Phi_\chi(p)|^2 dp}, \tag{4.26}$$

where we need to substitute χ for C to get:

$$\frac{\left(\sqrt{1-r_1^2} - r_1\sqrt{1-r_1^2}\exp(\frac{-p_0^2}{4\delta^2})\right)}{1 - 2r_1\sqrt{1-r_1^2}\exp(\frac{-p_0^2}{4\delta^2})} p_0. \tag{4.27}$$

By analyzing this general result for the value of $\langle p \rangle$ in C we realize that, in fact, for our interferometer, there *exists specific sets of the system variables windows where 'anomalous' events such as the one presented in Fig. 4.5 are expected to happen.*

In Fig. 4.6 we show the graphic behavior of the ratio between the expectation value $\langle p \rangle$ given by Eq. (4.27) and the initial Gaussian width δ for an interfering electron's momentum at exit channel C for $\phi = 0$ as a function of both the ratio $\frac{p_0}{\delta}$, concerning the overall shape of the incoming electron wave function, and r_1. As we can see, for certain values of $\frac{p_0}{\delta}$ there is a range in the highest possible values for the reflecting coefficient of the first beam-splitting device r_1 that makes it so that $\langle p \rangle \leq 0$, meaning that the electrons emerging from the interferometer's exit port C in these prepared situations will have a *negative* mean value for their momentum in the $\hat{y}$ direction. In Fig. 4.7 we show two different cross-sections of the 3D Fig. 4.6 made respectively at the fixed values $\frac{p_0}{\delta} = 0.15$ and $\frac{p_0}{\delta} = 0.5$. A cross-section of Fig. 4.6 with a fixed value for $r_1 = 0.8$ is shown in Fig. 4.8.

As we have noted, the described phenomenon of anomalous momentum gain is directly associated with a situation of destructive interference happening at one of the interferometer's exit channels. In turn, destructive interference is a quantum phenomenon associated with a lower probability of occurrence. In Fig. 4.9 we show the behavior of the electron's probability of arrival at C for $\phi = 0$ and again as a function of both $\frac{p_0}{\delta}$ and r_1. We can notice that the areas of this figure corresponding to the range of the variables where the phenomenon is most apparent coincide with the areas of lower arrival probabilities - although not of **vanishing** arrival probabilities. Quantum mechanics doesn't prevent us from observing the phenomenon, just makes it rarer to spot. The probability distribution of electron arrival at the final direction C can be calculated, following the quantum formalism, as:

$$P_\chi = \int dp|\Phi_\chi|^2 \tag{4.28}$$

where we take $\chi = C$.

How can this be? Considering our experimental apparatus, there is no obvious way that the electron could have gained momentum in the negative y axis direction, and still the interfering superposition of states of the electron shows that in some cases an electron can leave our Mach Zehnder interferometer having somehow gained momentum in this direction with a non vanishing probability. This is an almost analogous situation to the one created for the quantum mirror M in Aharonov's interferometric thought experiment [1], with the difference that here it is the interfering object going through the interferometer (the electron) that suffer this 'anomalous' momentum gain, and not one of the devices building the experimental apparatus. If we make a comparison between the form of the final wave functions associated with our interfering electron and Aharonov's mirror M, given respectively by Eq. (4.24) (with $\phi = 0 mod 2\pi$) and (3.24), we see that they have identical forms. Both represent a superposition of two Gaussian functions of momentum, each one representing either positive or no momentum gain - only the coefficients of the superposition differ. We strain however that in our discussion it is not necessary that we have $p_0 << \delta$. We are able to maximize the effect by choosing p_0 in the same order (but still smaller) than δ.

Here we shall postpone for a brief moment further discussion about the aspects of the interferometer to focus our attention at this strange result by taking a closer look on the form of superpositions of Eq. (4.24) and Eq. (3.24), and try to understand how come this unusual situation is made possible by quantum physics. In a purely mathematical point of view, the question resumes to 'how can the combination of the two Gaussian functions in the expressions for the wave functions in momentum representation of the electron or the mirror M result in a final function that is dislocated in the negative y axis and that in turn results in a negative expectation value for the final momentum of these objects?'. The answer to this question is made clearer in a graphic manner by Fig 4.10. We see by this figure that such a situation can be achieved by a superposition of Gaussian functions in the form $a\phi(p) + b\phi(p - p_0)$ in some of the cases where (1) there is a sign difference between

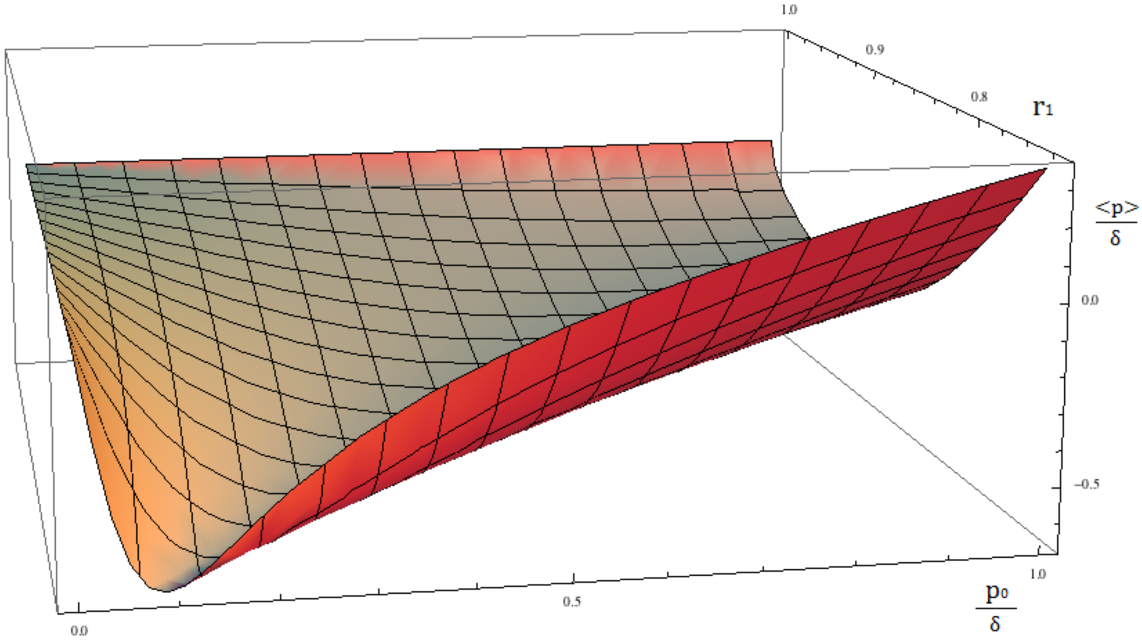

Figure 4.6: The ratio between the expectation value $\langle p \rangle$ for the momentum of an electron leaving the interferometer at the direction marked by C and the initial Gaussian width δ of the electron's momentum wave function in the case of destructive interference occurring at this exit and as a function of $\frac{p_0}{\delta}$ and r_1. We can see clearly that a portion of the graphic indicates a *negative expectation value for the momentum* of an electron leaving the interferometer at exit C under these conditions.

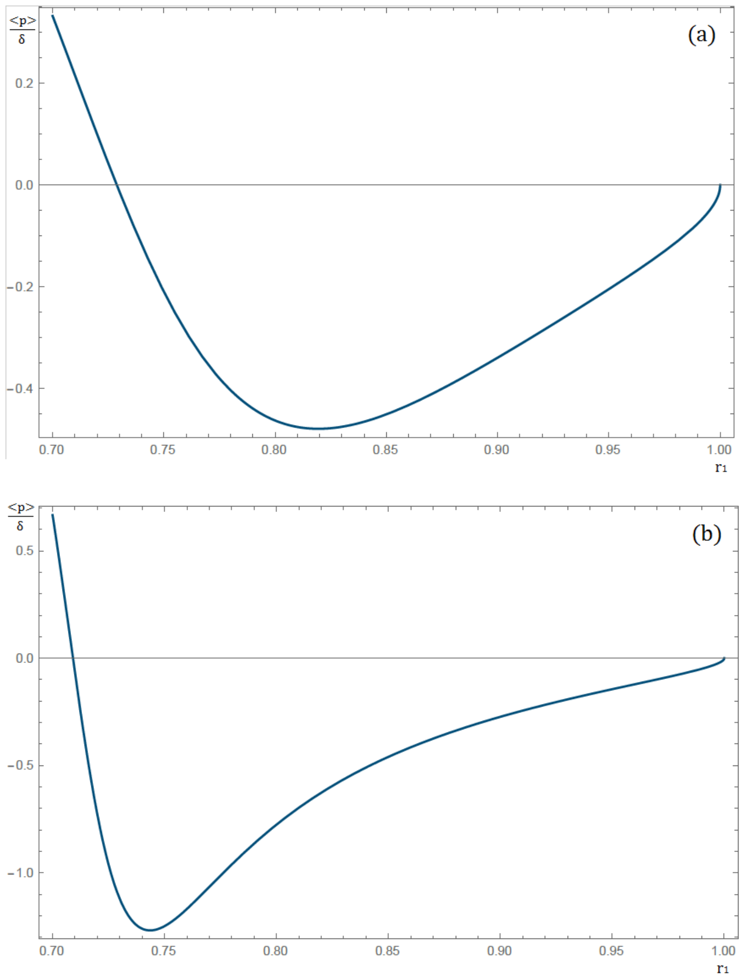

Figure 4.7: Cross sections of Fig. 4.6 where we have fixed the values $\frac{p_0}{\delta} = 0.5$ (a) and $\frac{p_0}{\delta} = 0.15$ (b). The reflection coefficient r_1 varies over it's upper range, where the expectation value $\langle p \rangle$ shows negative values.

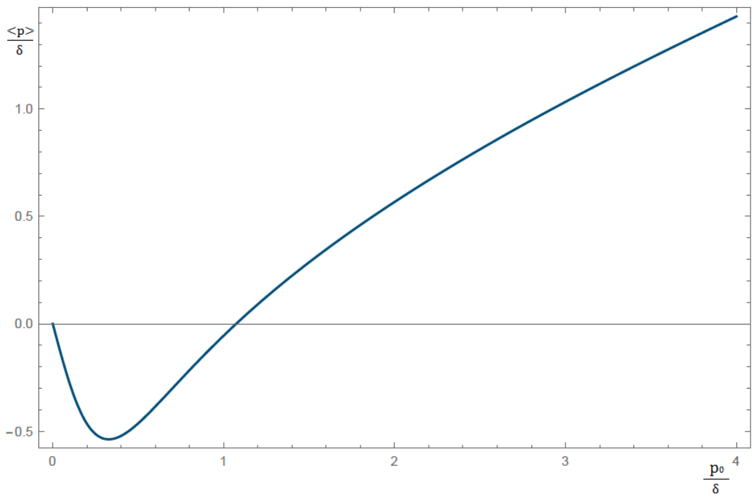

Figure 4.8: Cross section of Fig. 4.6 where we have fixed the value for $r_1 = 0.8$.

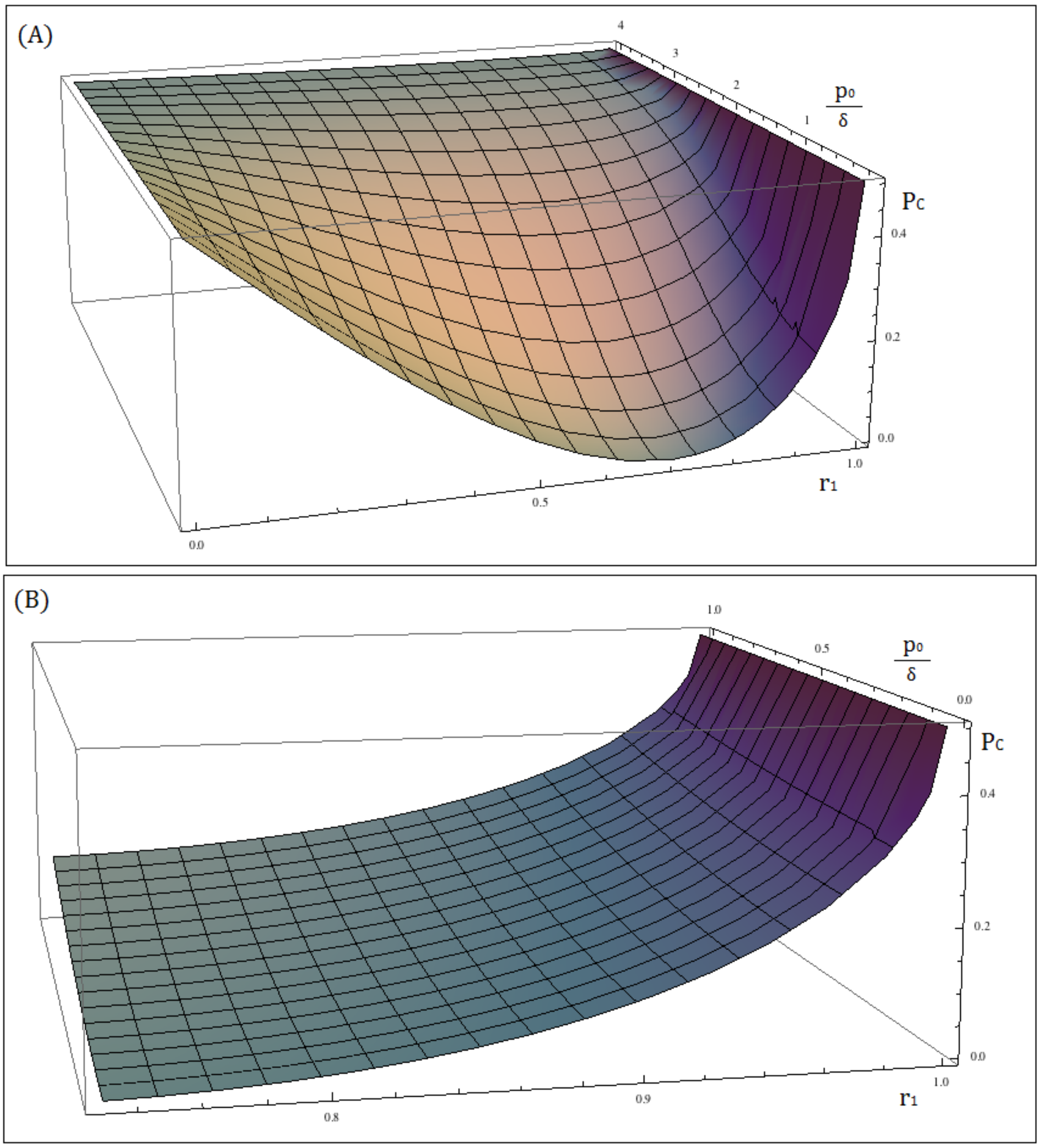

Figure 4.9: (A) Probability distribution of electron detection associated with the case of destructive interference at exit port C as a function of $\frac{p_0}{\delta}$ and r_1. (B) Portion of the above probability curve P_C plotted in the higher range of the variable r_1 and for values of $\frac{p_0}{\delta}$ between 0 and 1. Negative values for the expectation value $\langle p \rangle$ for the momentum of an arriving electron are associated in this figure with smaller, however non vanishing probabilities of detection.

the superposition coefficients (one of the superposing Gaussian functions is turned negative) and that (2) we set $|b| < |a|$. With such settings, we are able to create a 'lump' in the negative y axis while at the same time canceling out the function in a significant part of the positive y axis, creating in this way a total function that appears to be simply dislocated towards the negative part of this axis. This process inevitably culminates in a final wave function that has a lower total amplitude, which in turn is directly associated with a lower total probability of occurrence. This is exactly why we wanted to create a case of destructive interference at the specific detector where we wished to observe the phenomenon.

A destructive interference occurring at one of the final interferometer's exit channels chosen to observe the phenomenon in discussion, where the electron is expected to gain momentum in the 'wrong' direction, implies in turn in a constructive type of interference at the other exit, so that the detection probabilities will add to unity. Fig. 4.11 shows the form of the wave function of the electron leaving the interferometer in the final direction D for the case of destructive interference happening at direction C and for the same values that were previously set for the variables $\frac{p_0}{\delta} = 0.5$ and $r_1 = 0.84$ as in Fig. 4.5. We see that in the case of constructive interference at this propagation direction the final electron's wave function is dislocated in the positive y axis direction, so that the expectation value of the electron's final momentum there is *positive*, as is intuitively expected. Also, as a direct result of a constructive interference, the probability for the electron to leave the interferometer traveling in the D direction is in this situation significantly higher than the probability for it to leave the interferometer in the direction C, where the wave functions interfere destructively. This characterizes an 'inverse version' of the phenomenon occurring at propagation direction C, since the electron leaving the interferometer here ends up gaining momentum now in the positive y axis direction and have a higher probability of arrival - this is, in fact, actually necessary so that the mean value of the electron's momentum is conserved overall. To show that the overall momentum conservation happens in all cases for our single electron Mach Zehnder interferometer with two exit ports, we can calculate the following value:

$$P_C\langle p\rangle_C + P_D\langle p\rangle_D, \tag{4.29}$$

that is, the sum of the expectation values for the electron's momentum at the final directions of propagation C or D weighted by the probabilities of arrival for these electrons at the respective directions. The probabilities of arrival at the final directions of the interferometer

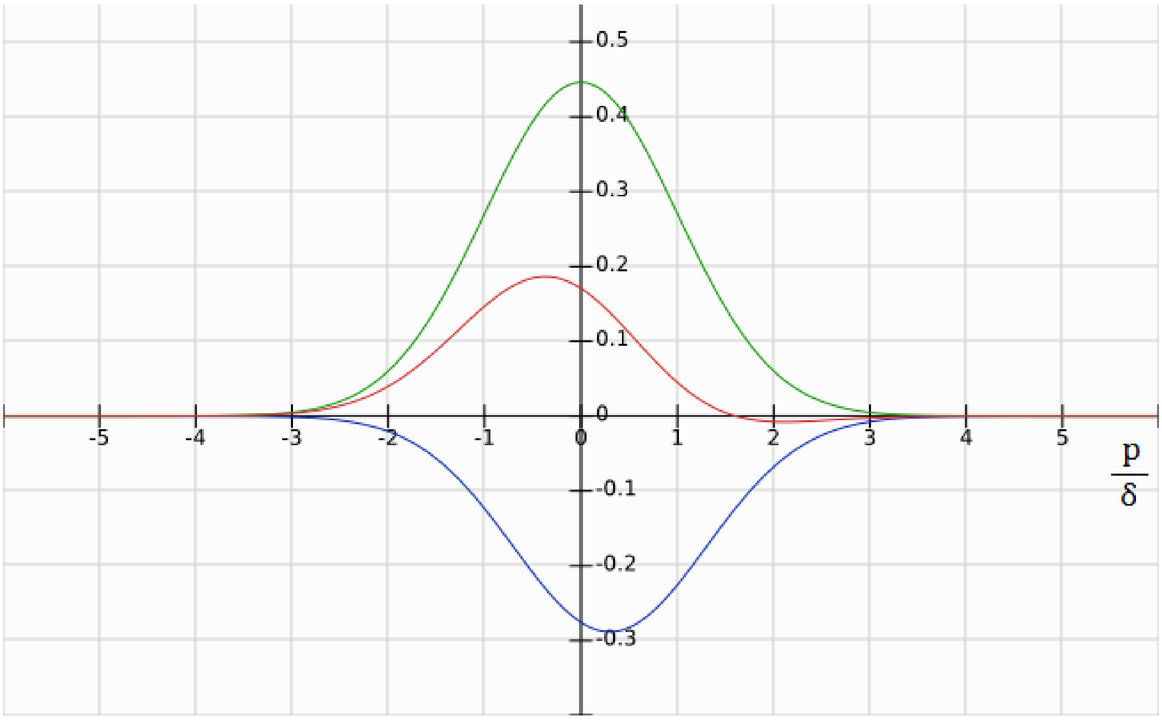

Figure 4.10: To achieve the final wave function in momentum space associated with an electron leaving the interferometer through exit port C for the case of destructive interference at this exit (where we have $\phi = \pi mod 2\pi$), we write a convex combination of the respective two Gaussian functions of momentum, one centered in zero (green line) and the other dislocated in the positive y axis direction (blue line), each associated to one path inside the interferometer, with coefficients given by the physical variables associated to the interferometer, and so that there is sign difference between these coefficients (characterizing the aforementioned destructive interference). One convex combination of this kind, representing a possible final wave function of an electron in this situation and one that leads to a *negative* expectation value for the final electron's linear momentum, is represented in red. This aspect of the red curve is achieved in the case of destructive interference when the coefficient of the convex combination associated to the blue curve (path A) is smaller than the one associated to the green curve (path B).

and the expectation value of the electron's momentum at them are calculated following Eqs. (4.28) and (4.26), where we substitute the variable χ for eitehr C or D. Making use of these results, we will have that:

$$\begin{aligned} P_C\langle p\rangle_C + P_D\langle p\rangle_D &= P_C\frac{\int dp|\Phi_C|^2 p}{P_C} + P_D\frac{\int dp|\Phi_D|^2 p}{P_D} \\ &= \int dp|\Phi_C|^2 p + \int dp|\Phi_D|^2 p = |t_1^2|p_0 \end{aligned} \tag{4.30}$$

as becomes simple to show if we take into account that, for the Gaussian functions, the expectation value of the electron's momentum coincides with the center of the Gaussian lump. We see by this calculation that indeed the mean value $|t_1^2|p_0$ of the electron's momentum, which represents simply the mean value for the cases where it has gained momentum p_0 at one certain direction after being transmitted in the first beam splitter device BS_1 with transmission coefficient t_1, or no momentum at all after being reflected in BS_1, is conserved until the end of the experiment, if we take into account the interference phenomenon happening at both possible exit ports.

What can we make of this physical scenario? Since the initial momentum wave function of an interfering electron is made to be a Gaussian distribution of momentum centered in zero, and therefore having an uncertainty that covers both negative and positive values for the electron's momentum, it is possible to understand the phenomenon of interference happening at both of the interferometer's exit channels described above as an interferometric way of *post-selecting* the momentum variable of an incoming single electron into two different momentum groups: one where the expectation value $\langle p\rangle$ for the electron's momentum will be negative and other where it will be positive. That post-selection would then cover both 'sides' of the initial full Gaussian distribution, where in turn we have that $\langle p\rangle = 0$ overall. We've also seen how, during this process, the total momentum of the system is conserved. This created interferometric post-selection can only be achieved if we assume that p_0, the momentum gain due to the electromagnetic interaction, has an absolute value that is low enough if compared to the initial Gaussian distribution uncertainty , so that in this manner the phenomenon of interference can be maintained and we are able to guarantee our results.

With this we have presented another context where the quantum interference phenomenon have the central part in both bringing forth a new way of understanding how the quantum world works and what can we do with a system possessing quantum properties,

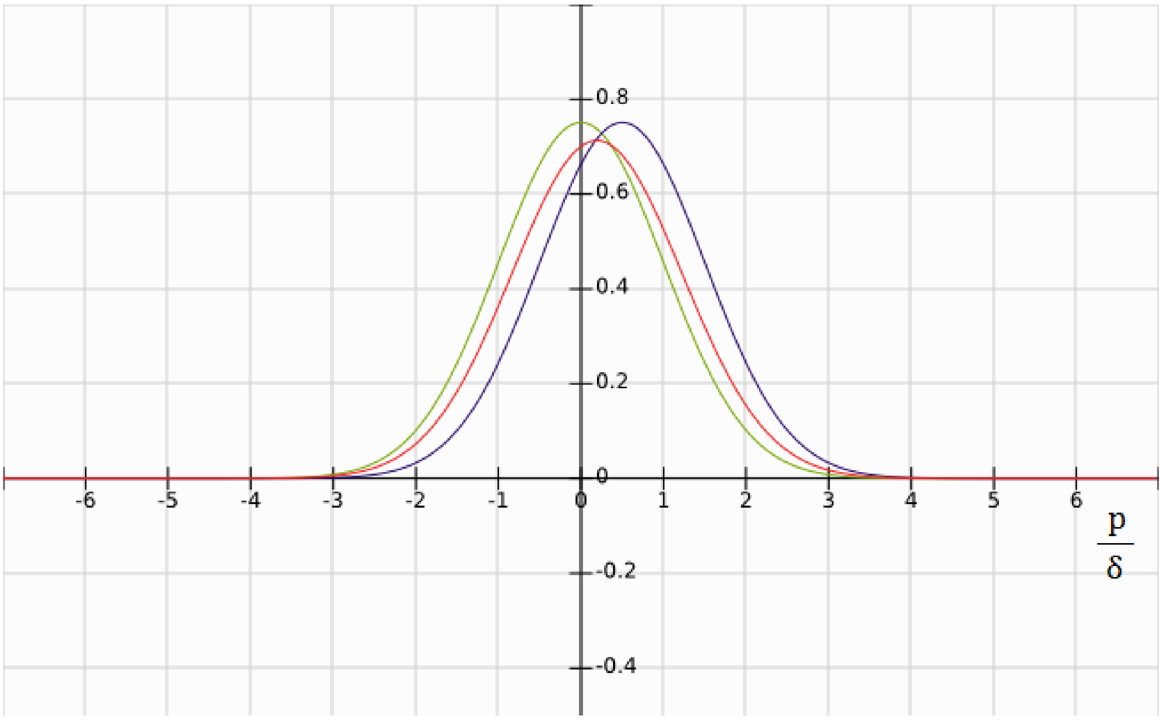

Figure 4.11: The electron's wave functions in momentum representation associated with the lower path B (green line - no external electric field) and the upper path A (blue line - external electric field $\vec{E}$) of the single electrons Mach Zehnder interferometer. The momentum distribution associated with an electron leaving the interferometer at exit channel D in the case of constructive interference occurring at this exit and when we set $\frac{p_0}{\delta} = 0.5$ and $r_2 = 0.84$ is shown in red. The mean, or expectation value $\langle p \rangle$ for the electron's momentum in this scenario is positive, although it's value is small and the curve is less dislocated when comparing to the curve corresponding to the wave function of a electron leaving the interferometer at direction C for the same values of the set variables as in Fig. 4.5. This happens because the sum of the means of the electron's momentum at both exit channels weighted by the arrival probability at these detectors must remain a constant, and here we have a higher arrival probability due to the constructive interference.

while at the same time challenging our intuition about what can or cannot be physically possible. It is important to notice that the experiment of interference with matter here presented cannot have a classic analogous, in the sense that it is not classically possible to separate particles in a group having negative momentum in any classical interferometric experimental realization following our protocol. This happens because the classical and quantum probabilities distributions of particle arrival have intrinsically different properties and are achieved in essential different manners, *with negative probability amplitudes being exclusive to quantum mechanics.* Since the quantum destructive interference is an essential part in our experiment proposal, we conclude that the phenomenon discussed of anomalous momentum gain is intrinsically a quantum phenomenon.

4.3.1 Can two electrons attract each other?

We have seen how in an interferometric experiment and in certain experimental conditions we are able to achieve a situation where we have a non zero probability that a physical object will end up gaining momentum in the 'wrong' direction after having interacted or not with some known physical system while traveling inside a Mach-Zehnder interferometer of two possible exit channels, characterizing what we have called a type of 'anomalous force' in a quantum interferometer. We can stretch this same concept and expand the idea, for example, to the situation where we have an interaction between *two of the interfering objects* while they travel inside the interferometric apparatus. Suppose that instead of having an apparatus consisting of a single electron Mach-Zehnder interferometer and correctly placed charged capacitor plates, we have now a particle Mach-Zehnder interferometer free of the influence of any other external physical system and that we choose to send through it *two electron's at a time.* Each electron on their own will travel through the system taking one of the two possible paths for it with probabilities dictated by the reflection and transmission coefficients of the first beam-splitting device. However, an electromagnetic interaction will take place **between the interfering electrons** in the cases where they happen to take the same path inside the physical apparatus, and, in principle, we can say that the interferometer's arms are far apart and/or shielded from each other so that no interaction exists between them if instead they happen to take different paths. The sum of the quantum amplitudes associated with the different possibilities for this system to evolve is capable of generating physical situations similar to the ones previously studied, where the momentum gain of the involved physical objects behave non intuitively. Throughout this section we discuss the results concerning the momentum gains and the behavior of two electrons sent together through a standard Mach-Zehnder interferometer of two exit channels capable of interfering the path amplitudes for multiple massive charged particles.

We consider the Mach-Zehnder interferometer built to interfere the paths of the electrons in our experiment as depicted in Fig.4.12. This is the exact same apparatus of our previous discussion with the exception that the charged capacitor plates have been removed from the vicinity of the interferometer, so that no external field will now disturb the wave functions of the electrons going though the apparatus, and *only interactions between the electrons* of the experiment are allowed to take place. Again, we suppose that we are able to control the reflection and transmission coefficients of the beam-splitting devices as well as the phase difference associated to the difference in length between the interferometer's two arms. In the same manner, just as was done in the previous discussion, the state vectors $|A\rangle$ and $|B\rangle$ are taken to be the vectors associated with the two distinguishable paths of propagation that are accessible for the electrons during their travel through our system, and the vectors $|C\rangle$ and $|D\rangle$ as the vectors associated to the two possible exit ports of the interferometer.

As has been stated, in this version of the experiment two electrons are sent *at a time* through our matter Mach Zehnder interferometer. We notice that we choose to send the electrons so that they enter the interferometric apparatus from different sides of the first beam splitting device, each one having different directions of propagation prior to their entry inside the interferometer, as is also shown in Fig.4.12. We make that choice so that the only accountable interaction between the electrons occur when they are already inside our system. We label our electrons as e_1 and e_2, which are associated directly with one of the two possible directions of propagation upon their arrival at the first beam-splitting device. Throughout our thought experiment, we suppose that our electrons could still be differentiated from one another by their position in relation to a certain central axis of propagation, as is also sketched in Fig.4.12, where we have marked the expected 'classical path' of the electrons with help of colored dotted lines. With this what we assume is that the wave function's widths in coordinate representation associated to the wave functions of each of the propagating electrons that are given by Eqs. (4.6) and (4.10) can be kept smaller

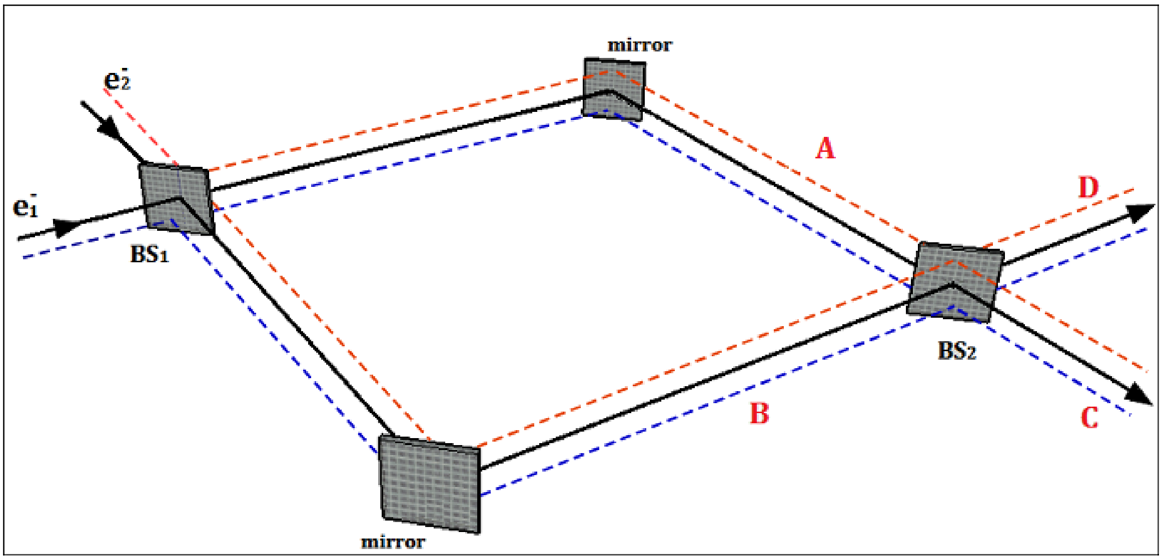

Figure 4.12: Sketch of the two-electrons Mach Zehnder interferometer. The dotted lines represent the classical expected possible 'trajectories' of the electrons e_1 (blue line) and e_2(red line) inside the interferometer. Quantum mechanically, we suppose that we are able differentiate the electrons leaving the interferometer through any specific exit port in what concerns the different regions of detection associated with the different colored lines, and therefore that we are able to associate each electron with their respective initial entry ports after they leave the apparatus.

than the existing separation between them until the end of the experiment. We will also assume that the suppositions made at the beginning of this chapter can still be accounted as valid throughout our following study.

For this version of the experiment, again we denote the electron's state vectors corresponding momentum gains while inside the interferometer as the vectors $|\Phi_0\rangle$ and $|\Phi'\rangle$ of Eq. (4.20) and Eq. (4.21), and introduce the vector $|\Phi''\rangle$ defined so that:

$$\Phi(p)'' \equiv \Phi_0(p + p_0) = \langle p|\Phi''\rangle. \tag{4.31}$$

In this interferometric experiment with two interfering particles, we choose *post select* the events where electron e_1 ends up arriving at exit channel $|D\rangle$ and e_2 at exit $|C\rangle$. This means that all other possible outcomes are excluded from consideration, in the sense that they will not be taken into account in the system's wave functions that we want to consider. As we know, the final joint state of the system composed by the two interfering electrons e_1 and e_2 will consist of a sum over the amplitudes associated with all the possible ways for this system to evolve in time. In our context, where we have thus fixed the exit channels for both the electrons in our experiment, we have *four* possibilities of evolution for our system: two where the electrons take different paths inside the interferometer and therefore do not interact, and two where they happen to take the same path and an electric interaction between them exists. Firstly, we calculate the quantum states associated with the two possibilities of evolution where the electrons take different paths inside our interferometer as:

(1) e_1 goes through $|A\rangle$ and e_2 goes through $|B\rangle$:

$$-r_1^2 t_2^2 \exp{(i\phi)}|\Phi_1, D\rangle_1 |\Phi_2, C\rangle_2, \tag{4.32}$$

(2) e_1 goes through $|B\rangle$ and e_2 goes through $|A\rangle$:

$$-t_1^2 r_2^2 \exp{(i\phi)}|\Phi_1, D\rangle_1 |\Phi_2, C\rangle_2, \tag{4.33}$$

where the states associated to each electron are labeled accordingly.

In turn, the quantum states associated with the two possibilities of system evolution where the electrons take the same path are calculated as:

(3) Both e_1 and e_2 go through $|A\rangle$:

$$-r_1 t_1 r_2 t_2 \exp{[i(2\phi + \alpha)]}|\Phi_1', D\rangle_1 |\Phi_2'', C\rangle_2, \tag{4.34}$$

(4) Both e_1 and e_2 go through $|B\rangle$:

$$-r_1t_1r_2t_2\exp{(i\alpha)}|\Phi_1', D\rangle_1|\Phi_2'', C\rangle_2, \tag{4.35}$$

where α represents the phase gain due to the electromagnetic interaction between the electrons. Here we have already guaranteed that, if electron e_1 gains momentum p_0 due to the electric interaction, then electron e_2 will have a momentum gain of $-p_0$.

If the final *total* joint state of the system formed by the two electrons e_1 and e_2, corresponding to a sum over the joint states associated to each one of *all the possible evolutions for the system* (no post-selections made) is denoted by the vector $|\Phi_T\rangle$, then after the post selection is made we are left with the following global quantum amplitude, calculated for the simpler case where we have taken $r_1 = r_2$ in the above expressions:

$$\langle p_1\langle p_2|\langle D|_1\langle C|_2\Phi_T\rangle = \Phi_{ps}(p_1,p_2) = [\Phi_1(p_1)\Phi_2(p_2)+\exp{(i\alpha)}\cos{(\phi)}\Phi_1(p_1-p_0)\Phi_2(p_2+p_0)]N, \tag{4.36}$$

where N is a normalization constant, p_1 and p_2 are the momentum variables associated respectively with electrons e_1 and e_2, where ϕ again represents the phase shift between the two interferometer's arms. Equation (4.36) is a two dimensional version of the sum of Gaussian amplitudes of the previous equations Eq. (4.24) and Eq. (4.25).

Here, we are able analyze the quantum states associated to *each of the electrons separately* by taking the *partial traces* of the density matrix associated to the quantum state of Eq. (4.36). If we denote $|\Phi_{ps}\rangle$ so that:

$$\langle D|_1\langle C|_2\Phi_T\rangle = \left|\Phi_{ps}\right\rangle = \left[|\Phi_1\rangle|\Phi_2\rangle + \exp{(i\alpha)}\cos{(\phi)}|\Phi_1'\rangle|\Phi_2''\rangle\right]N, \tag{4.37}$$

then the density matrix associated to the state $|\Phi_{ps}\rangle$ can be written, *apart from the normalization constant*, as:

$$\begin{aligned}
\rho_{ps} &\equiv |\Phi_{ps}\rangle\langle\Phi_{ps}| && (4.38)\\
&\propto |\Phi_1,\Phi_2\rangle\langle\Phi_1,\Phi_2| + \exp(-i\alpha)\cos(\phi)|\Phi_1,\Phi_2\rangle\langle\Phi_1',\Phi_2''| + && (4.39)\\
&\quad + \exp(i\alpha)\cos(\phi)|\Phi_1',\Phi_2''\rangle\langle\Phi_1,\Phi_2| + \cos^2(\phi)|\Phi_1',\Phi_2''\rangle\langle\Phi_1',\Phi_2''|. && (4.40)
\end{aligned}$$

The density matrix ρ_1 associated separately to electron e_1 can be obtained by taking the partial trace of ρ_{ps} in Eq. (4.38) with respect to the momentum variable associated with electron e_2, so that we have:

$$\rho_1 = Tr^{(2)}(\rho_{ps}) = \int dp\langle p|_2\rho_{ps}|p\rangle_2, \tag{4.41}$$

$$\rho_1 = |\Phi_1\rangle\langle\Phi_1| + I\exp(-i\alpha)\cos(\phi)|\Phi_1\rangle\langle\Phi_1'| + I\exp(i\alpha)\cos(\phi)|\Phi_1'\rangle\langle\Phi_1| + \cos^2(\phi)|\Phi_1'\rangle\langle\Phi_1'|, \tag{4.42}$$

where we have $I = \int \Phi_2(p)\Phi_2(p+p_0)dp_2 = \exp\left(-\frac{p_0^2}{4\delta^2}\right)$.

In the same manner, the density matrix ρ_2 associated separately to electron e_2 can be obtained as the analogous partial trace:

$$\rho_2 = Tr^{(1)}(\rho_{ps}) = \int dp\langle p|_1\rho_{ps}|p\rangle_1, \tag{4.43}$$

$$\rho_2 = |\Phi_2\rangle\langle\Phi_2| + I\exp(-i\alpha)\cos(\phi)|\Phi_2\rangle\langle\Phi_2''| + I\exp(i\alpha)\cos(\phi)|\Phi_2''\rangle\langle\Phi_2| + \cos^2(\phi)|\Phi_2''\rangle\langle\Phi_2''|, \tag{4.44}$$

with $I = \int \Phi_1(p)\Phi_1(p-p_0)dp_1 = \exp\left(-\frac{p_0^2}{4\delta^2}\right)$ having the same value as for ρ_1.

Both density matrices ρ_1 and ρ_2, which were derived from the entangled pure state of Eq. (4.37), represent *mixed states* for the electrons e_1 and e_2 when looked at separately from each other. This means that the partial states associated to each of the electrons separately will consist of statistical mixtures of pure states, and that they cannot therefore be expressed in standard vector state terms. However, in possession of these partial mixed states, we are still able to obtain the probability distributions $P_1(p_1)$ and $P_2(p_2)$ associated respectively to the momentum observables p_1 and p_2 of both the interfering electrons e_1 and e_2 as:

$$P_1(p_1) = Tr(\rho_1|p\rangle_1\langle p|_1) \tag{4.45}$$

$$P_1(p_1) = \Phi(p_1)^2 + \cos^2(\phi)\Phi^2(p_1-p_0) + 2I\cos(\phi)\cos(\alpha)\Phi(p_1)\Phi(p_1-p_0), \tag{4.46}$$

$$P_2(p_2) = Tr(\rho_2|p\rangle_2\langle p|_2) \tag{4.47}$$

$$P_2(p_2) = \Phi(p_2)^2 + \cos^2(\phi)\Phi^2(p_2+p_0) + 2I\cos(\phi)\cos(\alpha)\Phi(p_2)\Phi(p_2+p_0). \tag{4.48}$$

Both probability distributions have the same form except for a change in sign in p_0.

In Fig.4.13 we have plotted the probability distributions $P(p_1)$ and $P(p_2)$ of the momentum variables associated to the electrons in each run of the experiment for the fixed values $\frac{p_0}{\delta} = 0.3$, and $\phi = 3\pi/4$, and where we have imposed the constraint that the interaction phase follows $\alpha = 0 mod 2\pi$. We are able to observe in the figure that each probability distribution have been dislocated to represent a momentum gain in the 'wrong' direction for each of the electrons in the experiment. The direction in which the curve is dislocated is determined by the sign of the momentum gain due to the electric interaction between the electrons, that are either $\pm p_0$. If the variable p_0 is taken to be positive $\frac{p_0}{\delta} = 0.3$, then the probability distributions represented in the figure makes it so that electron e_1 will leave the interferometer having a *negative* expectation value $\langle p_1 \rangle$ for it's momentum, in spite of having whether gained positive momentum due to a possible electric interaction, or no momentum gain at all. At the same time, electron e_2 will end up leaving the interferometer having a *positive* expectation value $\langle p_2 \rangle$ for it's momentum, in spite of having whether gained negative momentum due to the interaction or no momentum gain at all. We have here that the effect is doubled and each of the electrons going though our apparatus would suffer individually from the phenomenon of 'wrong' momentum gain that was observed for a single electron in our previous version of the experiment, creating the illusion that some sort of *attraction* have happened between them during the evolution of our physical system.

We can calculate the expectation value for the momentum of the electron e_1 leaving the interferometer at the conditions stated above as:

$$\langle p_1 \rangle_{ps} = \frac{\int_{-\infty}^{\infty} dp_1 dp_2 p_1 |\Phi_{ps}|^2}{\int_{-\infty}^{\infty} dp_1 dp_2 |\Phi_{ps}|^2} \tag{4.49}$$

$$= \frac{p_0(\cos^2(\phi) + \cos(\phi)\exp\left(\frac{-p_0^2}{4\delta^2}\right))}{1 + \cos^2(\phi) + 2\cos(\phi)\exp(\frac{-p_0^2}{4\delta^2})}. \tag{4.50}$$

It is straightforward to show that $\langle p_2 \rangle_{ps} = -\langle p_1 \rangle_{ps}$.

In Fig. 4.14 we again show the plotted probability distribution $P(p_1)$ associated with the momentum of electron e_1 for the same set values for the physical variables of the problem (with $\alpha = 0 mod 2\pi$), now together with the terms adding up to this distribution as given by Eq. (4.46). In it we can see the important role of the cross-term in determining the intensity of occurrence of the phenomenon. This term is weighted by the absolute values of both I the set phase ϕ. An equivalent result exists for the analogous distribution $P(p_2)$ associated with electron e_2.

It is interesting to note that in the limit where $I \approx 1$, the partial density matrices ρ_1 and ρ_2 cease to represent statistical mixtures of pure states and become the representation of unique pure states themselves. As the parameter $I = \exp(-\frac{p_0^2}{4\delta^2})$ represents the inner state products $\langle \Phi_1 | \Phi_2^+ \rangle$ and $\langle \Phi_2 | \Phi_1^- \rangle$, this is the limit where the interaction almost doesn't change the electron's initial state, and that can be achieved when $p_0 << \delta$. In this situation the

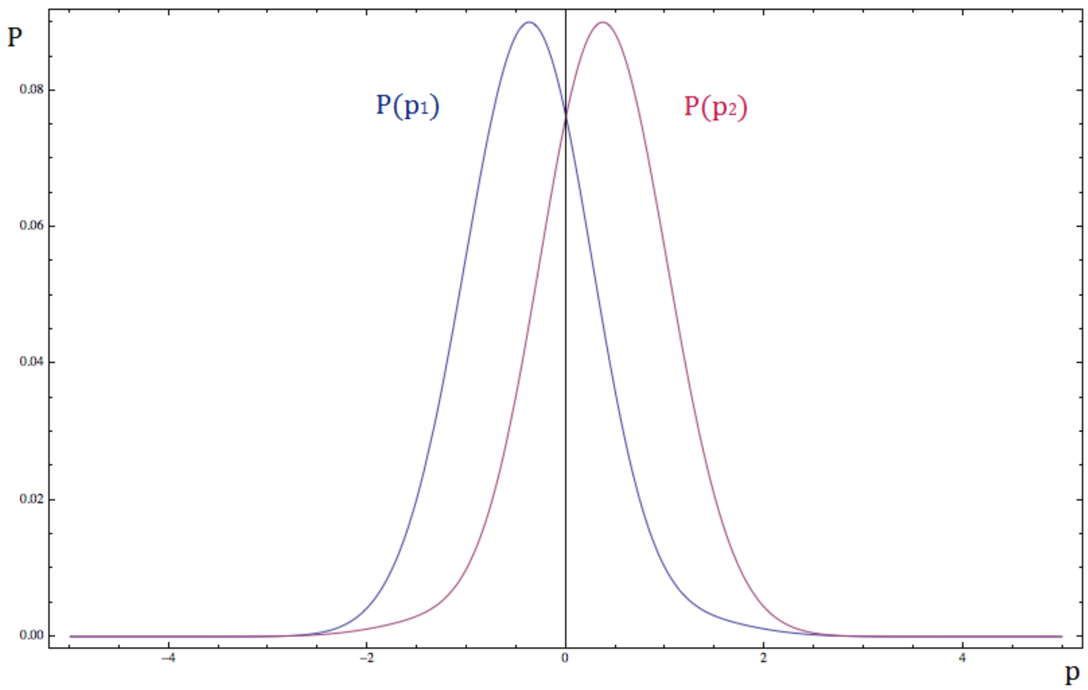

Figure 4.13: The $P(p_1)$ (blue line) and $P(p_2)$ (pink line) distribution curves for fixed values of $\frac{p_0}{\delta} = 0.3$ and $\phi = 3\pi/4$ ($\alpha = 0 mod 2\pi$). Counter intuitively, the expectation value for the linear momentum of the electron e_1 is turned negative, while the expectation value for the linear momentum of the electron e_2 is turned positive. This version of the phenomenon where both particles seem to gain momentum in the 'wrong' direction due to the existence or not of an interaction between them inside the interferometer seem to mimic a type of *physical attraction between the two negative charged particles* in the context of interference.

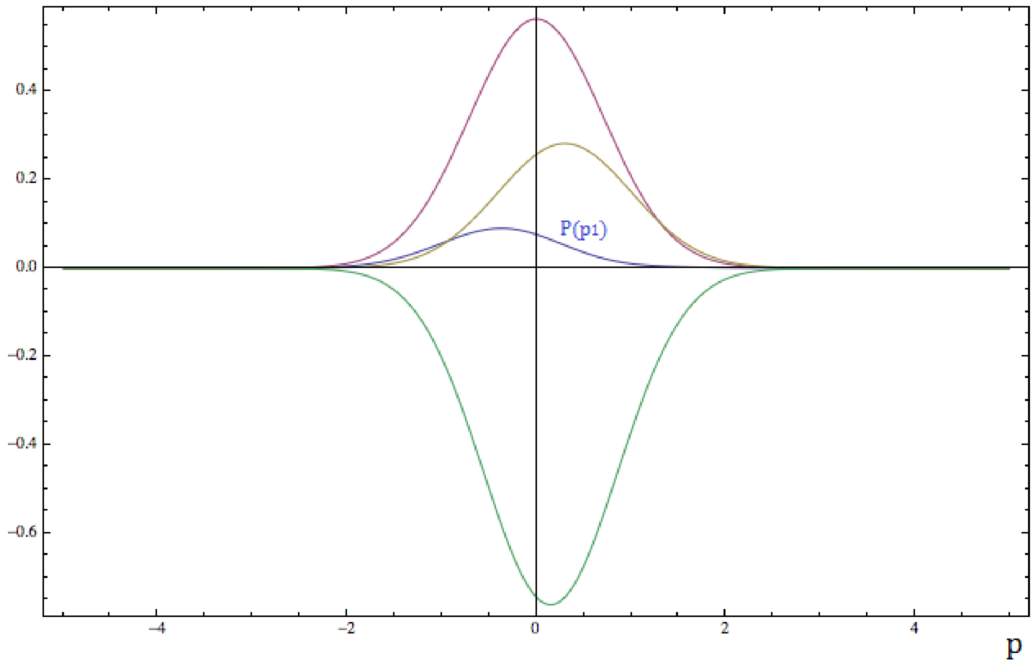

Figure 4.14: Plotted $P(p_1)$ distribution (blue line) together with the it's constituting terms as given by Eq. (4.46) and for the fixed values $p_0/\delta = 0.3$ and $\phi = 3\pi/4$ ($\alpha = 0 mod 2\pi$). In this image, the first term of Eq. (4.46) is represented by the pink line, the second term is represented by a yelowish line and the cross-term is represented by the negative green line.)

electron states can be expressed as the simple state vector sums:

$$|\Phi_1\rangle_{ps} = |\Phi_1\rangle + \cos(\phi)\exp(i\alpha)|\Phi_1^-\rangle \quad (4.51)$$

$$|\Phi_2\rangle_{ps} = |\Phi_2\rangle + \cos(\phi)\exp(i\alpha)|\Phi_2^+\rangle. \quad (4.52)$$

Just as in the previous single electrons version of our interferometric experiment, again the phenomenon of anomalous momentum gains for the interfering particles presented in this section is intrinsically a quantum phenomenon, and cannot therefore be mimicked classically. However, in this particular version, the two electrons in the experiment behave as both the interfering particles *and* the entities generating the required electric disturbance on one another, both being treated quantum mechanically during the process of interference. We can therefore conclude that, purely with the phenomenon of quantum interference, *it is possible to simulate an 'electromagnetic attraction' between two traveling electrons.* This result can easily be extended for any negative charged quantum particles, and an analogous result can be just as easily generated for any positive charged quantum particles.

4.3.2 Particle Mach Zehnder Interferometer with Material Diffraction Gratings

In this section, we study how we can make use of the principles involved in wave diffraction by material diffraction gratings to build experimental Mach-Zehnder interferometers in the context of matter optics, where the action of the beam-splitting devices are accomplished by the selection between the orders of diffraction at these gratings. A more in-depth study concerning this type of wave diffraction is presented in the appendix A.

Suppose we have a physical system composed of three aligned N-slits material diffraction gratings that are sufficiently separated from each other, and send through this system a coherent electron matter beam, as shown in Fig. 4.15. As we have studied, the incoming electron beam will firstly be diffracted into various characteristic directions by the first diffraction grating G_1. Each one of those orders of diffraction will then evolve in time and space until they reach the second diffraction grating G_2, where the process of diffraction will repeat individually for each of the newly formed incoming electron beams. One last step of diffraction will then happen at the third diffraction grating G_3, from where now various different diffracted electron beams will emerge and evolve freely. To create with this system

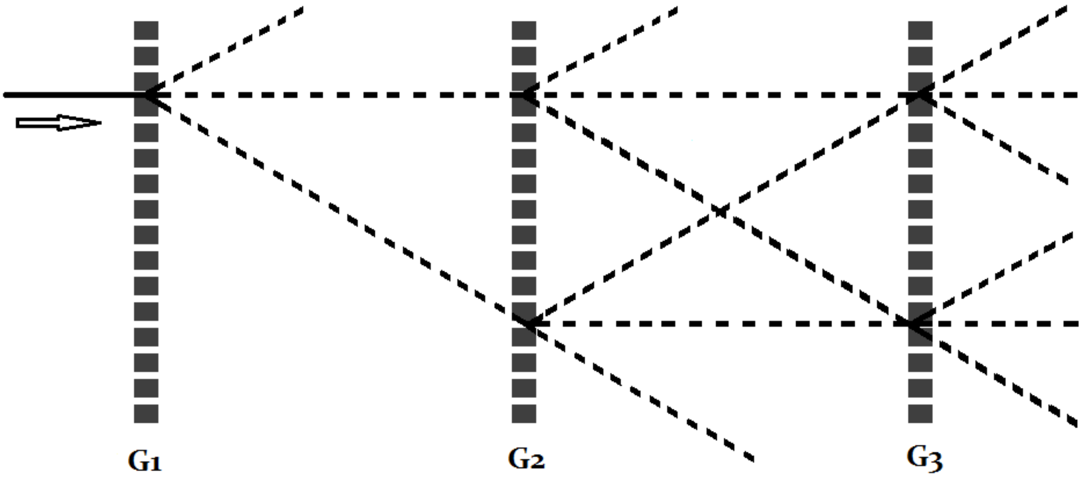

Figure 4.15: Three grating system and progressive diffraction of an incoming beam, represented by the dotted lines. Only the diffraction orders $m = -1, 0$ or 1 are represented for simplification.

an interferometer of the Mach-Zehnder type for matter beams, we *need only to select what orders of diffraction we will take into consideration in our experiment.*

In appendix A we show that the orders of diffraction of an incoming matter Gaussian beam at the N-slits diffraction grating are associated to the angles of diffraction θ' that obey the following relation:

$$\sin\theta' = \frac{2m\pi}{kh} - \sin\theta \tag{4.53}$$

in the limit where N is big, and where θ is the angle of incidence and $m = ... -2, -1, 0, 1, 2...$ characterizes the different existing orders of diffraction. The diffracted orders are also matter Gaussian beams, however with lower beam intensities.

To project our matter Mach Zehnder interferometer with the diffraction gratings forming the described physical system, we first disregard the existence of any order of diffraction with $|m| \geq 2$. With this done, we select the orders of diffraction with m between $-1, 0$, or 1 for each stage of diffraction in our system, in the way shown in Fig.4.16. As we can see, this construct creates in our system two possible 'paths' between the gratings $G1$ and $G3$, which we name as paths A and B, together with two possible exit channels C and D for the matter beam. If we consider that the first two diffraction grating G_1 and G_2 account for the action of a first beam-splitter device BS_1 together with the redirecting mirrors, and that the third diffraction grating G_3 accounts for a second beam-splitting device BS_2, we will

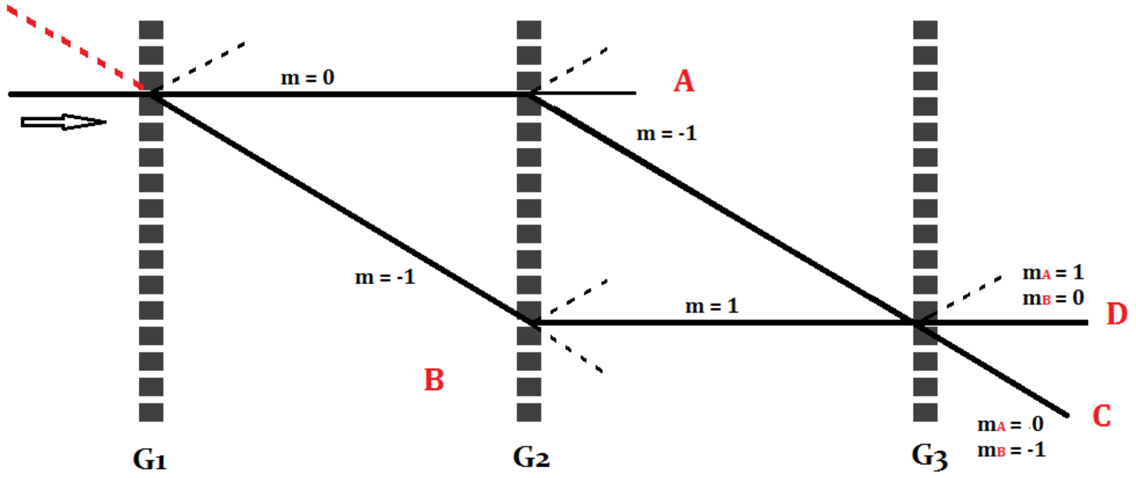

Figure 4.16: A three-grating Mach Zehnder interferometer. An interfering particle enters the interferometer and is diffracted at the first interferometer grating G_1 with diffraction order $m = 0$ or $m = -1$, therefore creating two possible paths inside the apparatus. The particle's wave function taking the upper path suffer a second diffraction at the middle grating G_2 with order $m = -1$ while the lower particle's wave function is diffracted at this grating with $m = 1$. The two beams are then reunited at a final diffraction grating, and two possible output ports for the beams are taken in consideration for the interferometer in discussion.

have that this system have thus the same basic topology of the Mach Zehnder interferometer for matter beams that we have studied throughout our chapter. The relation between the reflection and transmission coefficients associated to the so constructed 'beam-splitters' can be calculated from the theory of Gaussian beam diffraction at the material gratings (studied in the appendix A), being associated directly with the intensity of the matter beam resulting from each order of diffraction m. An alternative entry direction for this interferometer can be considered and is marked in the figure by a red dotted line. As many existing orders of beam diffraction have been disregarded from consideration, it is important to re-normalize the particle's wave functions as to calculate the correct expectation values and probabilities concerning our system, and as to make so that the reflection and transmission coefficients r and t associated to the beam-splitters obey the basic relation $|r|^2 + |t|^2 = 1$.

The first three-grating Mach Zehnder interferometer for atomic beams in the way exposed was built in 1991 by Keith et. al.[48], and an electron beam Mach Zehnder interferometer with three N-slits diffraction gratings have already been built in the past [49, 50, 9], although it is known that the electron-grating interactions can in certain situations give rise to decoherence [51]. Also, electron interferometry has already been applied to many tasks in physics[52, 53, 54]. In 2006, Gronniger et. al.[9] observed electron interference fringes from an electron interferometer using a construct with three nanofabricated diffraction gratings at low energies ranging from 6 to 10KeV. Fig. 4.17 shows the experimental apparatus used in this occasion. A system composed of an electron gun and two collimating slits was used to create the coherent electron beam that was directed at three 100nm periodicity diffraction gratings composing the interferometer. The middle grating was attached to a movable slide which was connected to a device called the piezoelectric transducer (PZT) on one side and fitted with a mirror on the other. The mirror allows the use of a separated optical interferometer fitted with the purpose to measure the movement of the second grating, which is also depicted in the figure. The moving middle grating was used as to controllably change the phase shift between the three-grating interferometer's two arms and better observe the electron interference. The electron detection was accomplished with use of a final slit and an electron channel multiplier. Fig.4.18 shows the so obtained electron interference pattern as a function of the second grating position together with the curves representing the classical and the quantum mechanical theoretical path calculations. The contrast obtained in the experimental data indicates the occurrence of a quantum interference phenomenon, although a better data visibility might be required to observe the results presented in this dissertation.

In 1995, *Ekstrom et. al.* realized a three-grating Mach Zehnder interferometric experiment with sodium atoms where a physical barrier was placed between the two arms of the interferometer, therefore shielding one from another[55]. Much like our proposed interferometric experiment with electron beams, the experiment consisted in exposing the interfering particles to a region containing a disturbing electric potential that only acted on one of the arms of the interferometer. In the occasion, the experimental apparatus permitted the scientists to measure directly the electric polarizability U of the interfering sodium atoms, since the phase shift Φ induced by the interaction is a linear function of this polarizability ($\Phi = U\tau/\hbar$, τ being the time duration of the electric interaction). A simple sketch of the apparatus used is depicted at Fig.4.19. To electrically separate the paths, a thin metal foil was inserted between the two interferometer's arms directly after the second diffraction grating. In this experiment, to observe the atomic interference fringes the third diffraction grating could be moved along it's lenght, which allowed the separated paths to be recom-

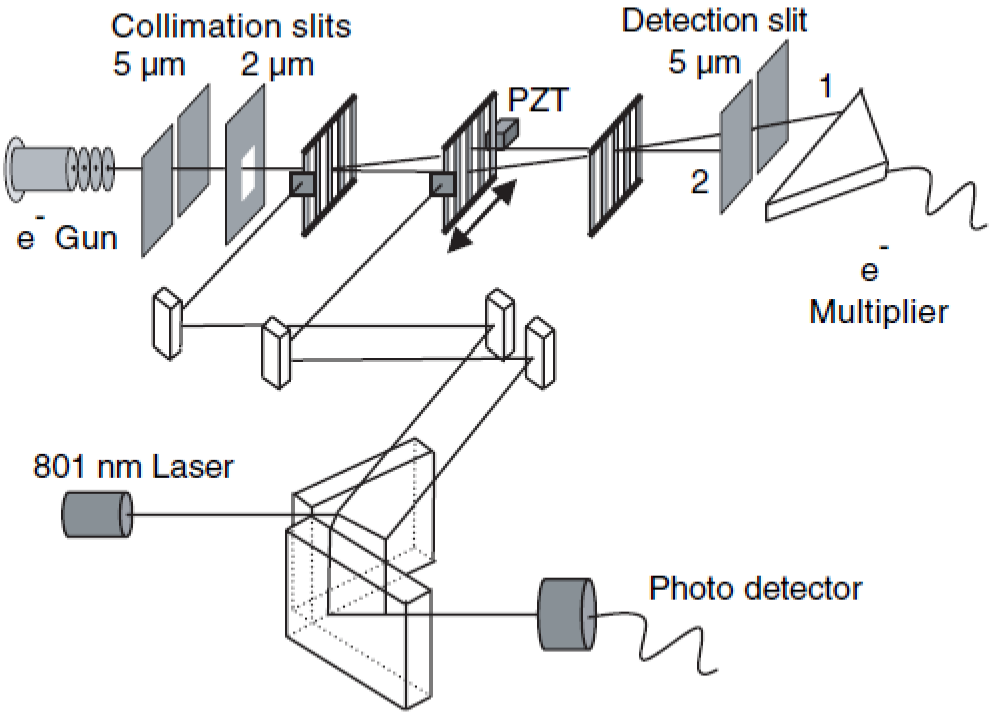

Figure 4.17: The sketch showing the experimental apparatus, including the light interferometer used with purpose to measure the second grating position (not to scale). Two slits are used to collimate the electron beam before it reaches the three-grating (100 nm periodicity) interferometer, and an additional slit is used to select the interferometer output port (output ports 1 and 2 are indicated and 1 is selected in this example). **Image extracted from reference [9].**

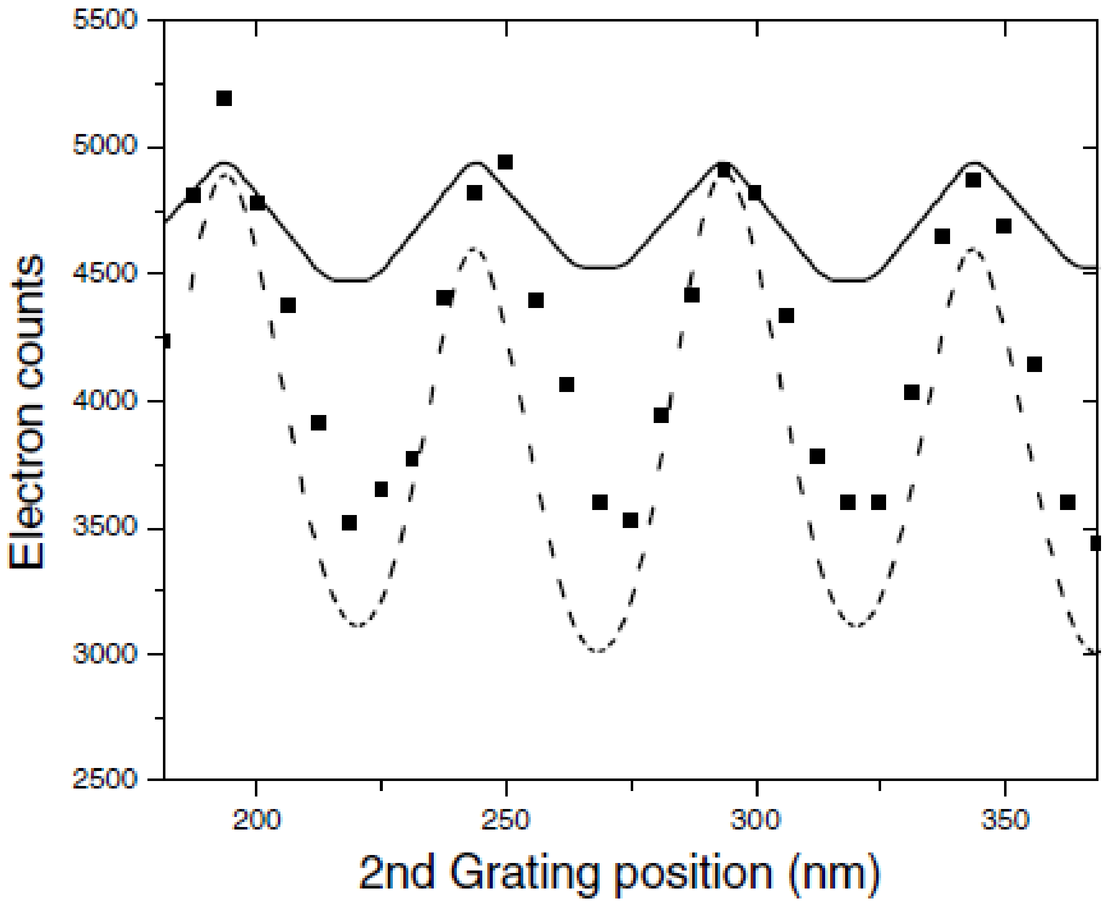

Figure 4.18: Experimental data comparison to theoretical calculations. The result of the classical straight line path calculation is represented by the solid line. The result of the full path integral calculation is represented by the dashed line. Experimental data are represented by square dots. The contrast of the device exceeds the classical contrast by about three times, showing the quantum mechanical nature of the data. *Image extracted from reference [9].*

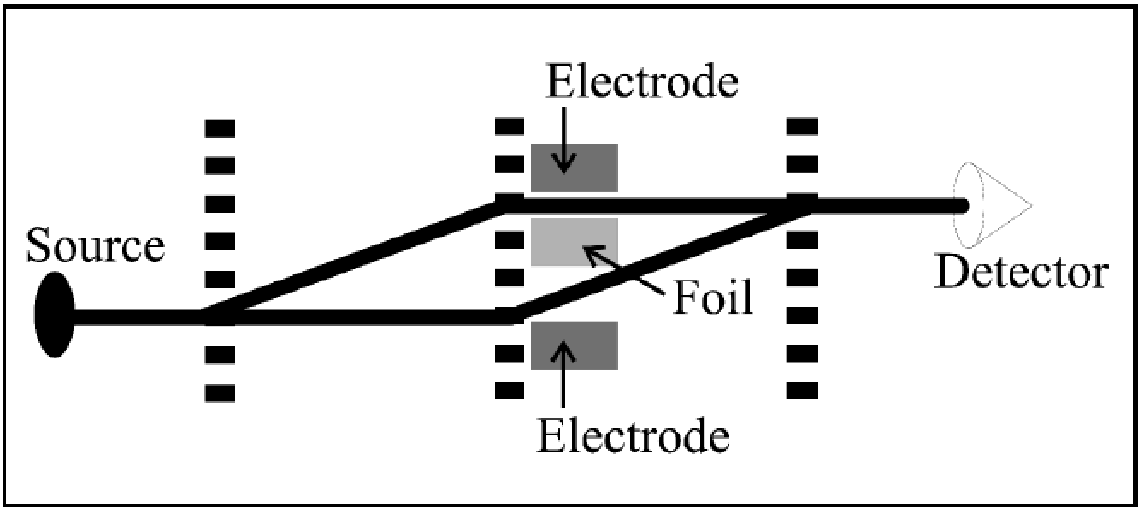

Figure 4.19: The atom Mach Zehnder interferometer at MIT, using nanofabricated diffraction gratings as the beam splitters. The interaction region consists of a metal foil held symmetrically between two side electrodes, allowing an electric field to be applied to one arm only. *Image extracted from reference [10].*

bined having a phase shift which varied according to the grating's position. The results of the measurements in this experiment gave an atomic sodium polarizability with an error of only 0.3 per cent.

In our proposed interferometric experiment, we have treated the interfering electrons in the quantum momentum space. However, to measure the interference pattern and observe the phenomenon here discussed, a measurement in the position of the arriving electrons should take place. As we know, the momentum and position quantum operators of the interfering electrons are closely related to each other, and the wave functions in each of the spaces formed by the eingenvectors of this operators are achieved from one another via Fourier transforms. It is possible to show that, in the far field, after the electrons have traveled away from the interferometer's exit channels, the spatial wave functions of the arriving electrons will fully reproduce their momentum wave functions at the interferometer's exit. In this manner the properties of momentum gain inside the experimental apparatus associated to the interfering electrons can be extracted from the measurements of their later positions. With these measurements we are then able to observe the discussed phenomenon of anomalous momentum gains.

Matter interferometry is a growing area of physics, resulting from the scientific advances in areas such as fundamental quantum mechanics, precision metrology and atomic and molecular physics. We believe that the experimental techniques and scientific advances needed to observe the phenomenon described in this dissertation, with a better and sufficient data visibility and good measurement precision, are well within reach - and finally that the experimental observation of the proposed phenomenon will enrich our experience and understanding of the strange world of quantum mechanics.

A scientific paper containing the original results here presented is in this time under preparation [13].

Chapter 5

Conclusion

In this work we have showed how, in a context of a quantum interference experiment, it becomes possible to create a situation where the expectation value for the linear momentum of an interfering physical object after it has traveled through our apparatus points in an *opposite direction* then what is classically expected for it, creating in this way the illusion that a type of physical 'anomalous' force exists in our apparatus. We have showed however that this is a phenomenon that derives directly from the quantum superposition of the wave functions associated with each one of the 'possible evolutions' for the system inside the interferometer, being therefore a result of the intrinsic characteristics concerning quantum interference. The first version of the here discussed original experiment consisted in coherently sending single electrons through a two-paths Mach Zehnder particle interferometer where one of the arms was exposed to a controlled space-disturbing electric field, while the other remained free from any external disturbance. The resulting wave function of each electron at a chosen exit channel presented then the apparent inconsistency concerning each electron's *momentum expectation value sign*, and the lack of any accounted for physical forces that could have altered the momentum of the electrons giving them momentum in that seemingly 'wrong' direction. We have here argued how this unexpected result is not only consistent within quantum theory, but also that it can in fact only exist and be understood in a quantum physical scenario of interference. A very similar phenomenon of quantum interference was then discussed in a second version of the experiment where now two electrons were coherently sent at a time through the same two-paths Mach-Zehnder particle interferometer, now free from any external influence. We have then discussed how, after a post-selection of each of the electron's exit ports was made, it was possible to observe the same behavior of 'anomalous' momentum gain when the electrons were looked at separately, therefore simulating an *attraction between two negative charged particles* in a quantum context.

The purpose of this dissertation as a whole was to present, together with the aforementioned central counter intuitive results concerning our electron Mach Zehnder interferometer, a brief review about the still strange characteristics of phenomena centrally involving the notion of quantum superposition. This idea was primary nourished in Chapter 2, where we have presented brief accounts concerning quantum double-slit interferometry [14, 3], the wave-particle duality and Bohr's complementarity principle [20, 28, 21, 22, 23, 5], delayed-choice interferometry and it's theoretical implications [6, 34], and the phenomenon of quantum erasure of information and the close relation it posses with the maintenance of quantum interference patterns [35, 7, 8]. The intricacies of quantum theory contained in these examples of behavior of small objects living in the quantum regime are representative of a broader whole of somewhat strange and still seemingly nonsensical behaviors that characterize the rich field that is modern quantum mechanics. A more in-depth example of a classically counter intuitive quantum behavior was then analyzed in Chapter 3, the space that we have dedicated to review the 2013 Aharonov. et. al. paper that inspired this work [1]. This review explored the notion held by the authors in what concerns the wide difference between the possible interpretations of a physical phenomenon whether it is considered in a classical or quantum context, and in our exposure we have argued how the strange results that appeared to exist in the quantum regime version of the phenomenon discussed were a direct result of quantum superposition and quantum interference phenomena, therefore making it an addition to our previous discussion.

Chapter 4 contains the original part of the here presented work. We believe that the presented original discussion is a valid addition to the broader topic of quantum superposition and it's characteristics, forcing us even further in exercising our logic about the world that physics, as a natural science, pursues continually to describe. In addition, we believe that an experimental method of testing our results concerning the ‘anomalous interferometric forces’ and the counter intuitive momentum gain of particles in the single electrons version of our matter Mach-Zehnder interferometry experiment is today within reach, as we have argued throughout examples of accomplished general matter, and specifically electron interferometry experiments with spatially separated beams in the last years.

Appendix A

Gaussian beams in Diffraction Gratings

As we have noted but shall analyze with more depth in our following discussion, one of the main physical devices used to create interferometers of spatially separated beams for interfering massive particles is called a *diffraction grating.* Diffraction gratings are periodic optical components used to scatter an incoming optical beam into several characteristic directions by making use of the physical phenomenon of wave diffraction. A common diffraction grating consists of a material structure containing a periodic array of finite apertures or slits used to scatter an incoming beam, although it is possible to create diffraction gratings for matter beams in alternative manners, where for example the material structure is replaced by laser standing waves [56]. We discuss in this section the scattering of an incoming matter beam through a diffraction grating consisting of a one-dimensional wall containing a number of N slits of size b and with a fixed slit separation of h. This type of material diffraction grating is depicted in Fig.A.1. Firstly, we consider the diffraction of an incoming *plane wave* through this N-slits diffraction grating, and with this extend our results to the case where the incoming wave is in the form of a *Gaussian matter beam.*

We start by introducing a known mathematical result in the field of electromagnetism and optics, named the *Kirchhoff Integral Theorem*, that can be written as:

$$U_P = -\frac{1}{4\pi}\int\int\left(U grad_n \frac{\exp(ikr)}{r} - \frac{\exp(ikr)}{r} grad_n U\right) dA. \tag{A.1}$$

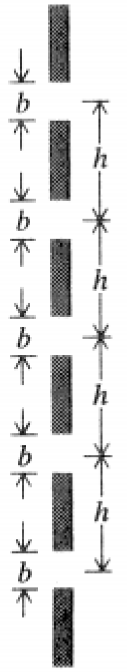

Figure A.1: Multiple slit aperture or diffraction grating, with slit size b and slit separation h. *Image extracted from reference [11].*

This is a theorem that mathematically establishes the relation between the value of any scalar wave function U at any point P *inside* an arbitrary closed surface A, and the value of this same function *at* this surface. In Eq. A.1, $grad_n$ represents the gradient operation in the direction $\vec{n}$ orthogonal to the surface A. This theorem can be derived directly by manipulation of Green's Theorem.

In the application of the above Kirchhoff Integral Theorem in the context of wave diffraction, the function U is known as the calculated 'wave disturbance' at a point P beyond a positioned diffracting object. (The function U is by definition a scalar function of space and time, and therefore it cannot directly represent an electromagnetic vector disturbance. However, the scalar approximation where the square of the absolute value of the function U can be associated with a measurement of the wave disturbance radiance is in great accord with experimental observations). Fig. A.2 shows the standard case where the wave diffraction of an incoming wave happens due to the presence of a wall containing a small aperture. In this figure, S represents the source of the incoming wave, and P is the point where we wish to calculate the wave disturbance resulting from the diffraction on the wall. To reach the wanted results, two simplifying assumptions are made concerning U - first, that both U and

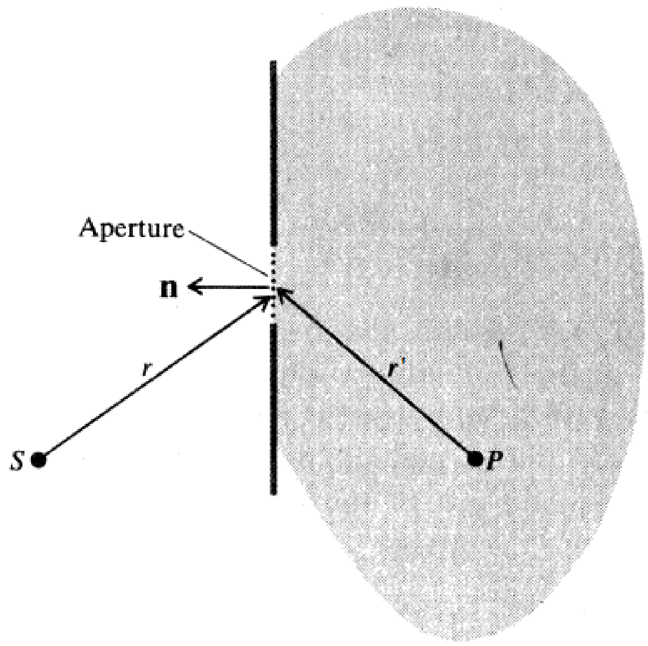

Figure A.2: Study of diffraction of a wave emitted from source S through a one-slit diffraction wall.

$grad_n U$ contribute negligibly to the total integral when taken outside the aperture itself, and that the values of both U and $grad_n U$ are not changed by the presence of the diffraction wall. Those are again results that are in agreement with experimental observations and work withing the scalar approximation of the diffraction theory.

The mathematical treatment of wave diffraction distinguishes between two general cases, named the 'Fraunhofer diffraction' or the 'Fresnel diffraction'. Fraunhofer diffraction theory is applicable when both the incoming and diffracted waves can be *taken to be effectively plane.* In our discussion we assume to be working in the Fraunhofer diffraction regime. In this regime, the equation relating the wanted 'wave disturbance' $U(P)$ in a point $P(r)$, resulting from the diffraction of a plane wave in the form $\exp(i\vec{k} \bullet \vec{r})$ that makes an angle θ with an N-slits diffraction wall equivalent to that of Fig. A.1, can be derived from approximations of Eq. A.1 and takes the simple form:

$$U(P) = \int dx \exp(ik_x x) \exp(ik'_x x) = \int dx \exp(i(k \sin(\theta) + k' \sin(\theta'))x) \tag{A.2}$$

where x *is only varied over the slits on the diffraction wall.* In Eq. (A.2), $\vec{k'}$ represents the wave vector of the resulting diffracted beam, and θ' is the angle of diffraction. With this we have that, for our N-slits diffraction grating:

$$U(P) = U(k_x, k'_x) = \int_0^b + \int_h^{h+b} + \ldots + \int_{(N-1)h}^{(N-1)h+b} \exp\left(i(k_x + k'_x)x\right)dx \tag{A.3}$$

from which we can derive that, after straightforward integration:

$$U(P) = U(k_x, k'_x) = b\exp\left(i\beta\right)\exp\left(i(N-1)\gamma\right)\left(\frac{\sin\beta}{\beta}\right)\left(\frac{\sin N\gamma}{\sin\gamma}\right) \tag{A.4}$$

where $\beta = \frac{1}{2}b(k_x + k'_x)$ and $\gamma = \frac{1}{2}h(k_x + k'_x)$.

The wave intensity distribution function associated to the resulting diffracted wave amplitude given by Eq. (A.4) is written as:

$$I = I_0\left(\frac{\sin\beta}{\beta}\right)^2\left(\frac{\sin N\gamma}{N\sin\gamma}\right)^2 \tag{A.5}$$

where a factor of N have been introduced to normalize the expression. We have then that $I = I_0$ when $\theta = 0$.

In Fig.A.3 is shown the behavior of the quantity $\frac{I}{I_0}$ as we vary the diffraction angle θ' (and therefore the parameter γ) and for growing values for the number N of slits of the diffraction wall. We see by the figure that the diffraction pattern generated by the incoming plane wave consists of various equally spaced peaks of wave intensity, existing for periodic values of the diffraction angle θ' and representing what is called the various *orders of diffraction*. The intensity peaks are enveloped by the sinusoidal term of the form $\left(\frac{\sin\beta}{\beta}\right)^2$. It is apparent that the width and definition of each of the wave intensity peaks increase with increasing values for N. In the limit where $N \to \infty$, the incoming wave will only be diffracted into very specific periodic values for the diffraction angle θ'.

We can extend these results so we can calculate what will be the diffraction pattern for the case where the incoming wave is in a *Gaussian beam form*. Firstly we notice that, like any other beam form, a Gaussian beam can be decomposed and represented by a (infinite) sum of standard plane waves. For the specific case of a Gaussian beam, the coefficients of the decomposition are also Gaussian distributions. Each of the plane-wave components of the so decomposed Gaussian beam will be diffracted independently when sent through the N-slits diffraction grating, in the manner just as we have discussed above and generating a diffracted wave in the exact form of Eq. (A.4). In this manner, *by integrating the product between the result of Eq. (A.4) for the diffraction of a plane wave on the diffraction wall*

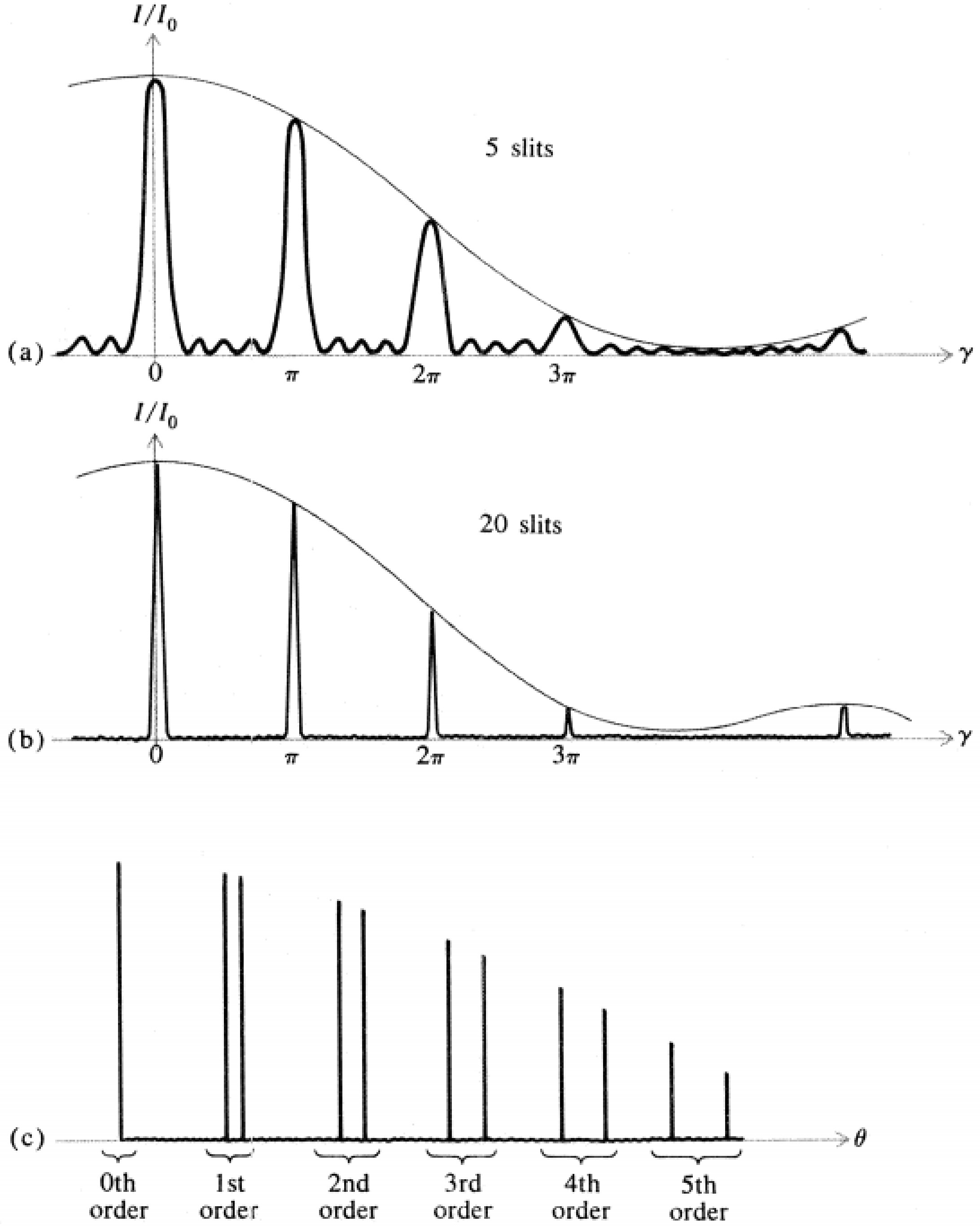

Figure A.3: The Fraunhofer diffraction pattern originating from a multiple slit aperture, or N-slits diffraction grating. Graphs (a) and (b) are derived from the diffraction of monochromatic incoming beams. Graph (c) is originated from when we have a large number N of slits and for the case of two incoming wavelengths. *Image extracted from reference [11].*

and a Gaussian distribution of wave vectors k_x, we are able to calculate what will be the final diffraction pattern $U_T(k'_x)$ for a diffracting Gaussian beam as:

$$U_T(k'_x) = \int dk_x G(k_x) U(k_x, k'_x), \tag{A.6}$$

where

$$G(k_x) = \frac{2\alpha}{\pi}^{\frac{1}{4}} \exp\left(-\alpha^2 k_x^2\right) \tag{A.7}$$

is a (normalized) Gaussian distribution in $\vec{k_x}$ centered in zero.

We solve the integral of Eq. (A.6) for the limit case where $N \to \infty$, using the expressions in Eq. (A.4). For this, we make use of a limit representation of the Dirac delta function, which can be written as:

$$\delta(x) = \lim_{N\to\infty} \frac{\sin Nx}{\pi x}. \tag{A.8}$$

In possession of this expression, it is possible to write the following equality:

$$\lim_{N\to\infty} \left(\frac{\sin N\gamma}{\sin\gamma}\right) = \pi \sum_{m,-\infty}^{\infty} (-1)^m \delta(\gamma - m\pi). \tag{A.9}$$

Finally, we substitute the expressions of Eq. (A.4) and (A.9) into (A.6) to get:

$$U_T(k'_x) = \int dk_x b\pi \exp\left(i\beta\right) \exp\left(i(N-1)\gamma\right) \left(\frac{\sin\beta}{\beta}\right) \sum_{m,-\infty}^{\infty} ((-1)^m \delta(\gamma - m\pi)) G(k_x). \tag{A.10}$$

The integral of Eq. (A.10) will only have non zero values for $U_T(k'_x)$ in the cases when we have that $\gamma = m\pi, m = \ldots -2, -1, 0, 1, 2, \ldots$. This condition can be expressed in terms of the relation between the arrival and diffraction angles θ and θ':

$$\begin{aligned} \gamma &= m\pi, m = \ldots -2, -1, 0, 1, 2, \ldots \\ k_x + k'_x &= \frac{2m\pi}{h} \\ \sin\theta' &= \frac{2m\pi}{kh} - \sin\theta. \end{aligned} \tag{A.11}$$

Again, the diffraction pattern consists of peaks of wave intensity, existing for the periodic values of the diffraction angle θ' that follow the proper conditions. The intensity peaks are in the same manner enveloped by a sinusoidal function term $\left(\frac{\sin\beta}{\beta}\right)^2$. However, the peaks representing the various orders of diffracted waves are *now also in Gaussian beam forms*, in the form of:

$$U(T)(k'_x) \propto \sum_{m,-\infty}^{\infty} (-1)^m \left(\frac{\sin\left(\frac{b}{h}m\pi\right)}{\frac{b}{h}m\pi}\right) \exp\left[-\alpha\left(\frac{2\gamma}{h}m\pi - k'_x\right)^2\right]. \tag{A.12}$$

.

Bibliography

[1] Y. Aharonov, A. Botero, S. Nussinov, S. Popescu, J. Tollaksen, and L. Vaidman. The classical limit of quantum optics: not what it seems at first sight. *New Journal of Physics*, 15:093006, 2013.

[2] M. Cagnet, M. Francon, and J.C. Thier. *Atlas of Optical Phenomena*, volume 1. Springer-Verlag, Berlin, 1962.

[3] M. Sands, R. Feynman, and R. B. Leighton. *The Feynman's Lectures on Physics*, volume 3. Addison–Wesley, New York, 1964.

[4] A. Tonomura, J. Endo, T. Matsuda, T. Kawasaki, and H. Ezawa. Demonstration of single-electron buildup of an interference pattern. *American Journal of Physics*, 57:117, 1989.

[5] M. S. Chapman, C. R. Ekstrom, T. D. Hammond, R. A. Rubenstein, J. Schmiedmayer, S. Wehinger, and D. E. Pritchard. Optics and Interferometry with Na2 Molecules. *Physical Review Letters*, 74:4783, 1995.

[6] V. Jacques, E. Wu, F. Grosshans, F. Treussart, P. Grangier, A. Aspect, and J.-F. Roch. Experimental Realization of Wheeler's Delayed-Choice Gedanken Experiment. *Science*, 315:966, 2007.

[7] M. O. Scully, B. G. Englert, and H. Walther. Quantum Optical Tests of Complementarity. *Nature*, 351:111, 1991.

[8] S. P. Walborn, M. O. Terra Cunha, S. Pádua, and C. H. Monken. Quantum eraser. *Physical Review A*, 65:337, 2002.

[9] G. Gronniger, B. Barwick, and H. Batelaan. A three-grating electron interferometer. *New Journal of Physics*, 8:224, 2006.

[10] R. M. Godun, M. B. D'arcy, G. S. Summy, and K. Burnett. Prospects for atom interferometry. *Contemporary Physics*, 42:77, 2001.

[11] Grant R. Fowles. *Introduction to Modern Optics.* Dover Publications, New York, 2ed. edition, 1968.

[12] A. Pais. *Subtle is the Lord: The Science and the Life of Albert Einstein.* Oxford University Press, Oxford, 1982.

[13] M. F. B. Cenni, R. Correa, and P. L. Saldanha. Quantum Interference of Force (Texto em preparação). 2017.

[14] T. Young. The Bakerian Lecture: On the Theory of Light and Colours. *Phil. Trans.*, 92:12, 1802.

[15] D. ter Haar. On the Law of Distribution of Energy in the Normal Spectrum - A translation of the M. Planck Annalen der Physik Paper of 1900, in "The Old Quantum Theory". Glasgow, 1967. pg.82.

[16] A. B. Aronst and M. B. Peppard. Einsteins Proposal of the Photon Concept - A translation of the Annalen der Physik Paper of 1905. *American Journal of Physics*, 33:367, 1965.

[17] D. Griffiths. *Introduction to Electrodynamics.* Prentice Hall, New Jersey, 3 edition, 2013.

[18] G. I. Taylor. Interference fringes with feeble light. *Proceedings of the Cambridge Philosophical Society*, 15:114, 1909.

[19] A. J. Dempster and H. F. Batho. Light Quanta and Interference. *Physical Review*, 30:644, 1927.

[20] N. Bohr. On the Constitution of Atoms and Molecules. *Philos. Mag.*, 26:12, 1913.

[21] A. F. Kracklauer. *"On the Theory of Quanta", a translation of "Recherches sur la Theorie des Quanta" by L.-V. de Broglie.* Al Kracklauer, California, 2007.

[22] L.-V. de Broglie. The Wave Nature of the Electron, December 1929. Nobel Lecture.

[23] C. Davisson and L. H. Germer. Diffraction of Electrons by a Crystal of Nickel. *Physical Review*, 30:705, 1927.

[24] R. P. Crease. Physics World, Septemper 2002. 'The Most Beautiful Experiment'.

[25] Mark P. Silverman. *Quantum Superposition: Counter intuitive Consequences of Coherence, Entanglement and Interference*. Springer, Berlin, 2008.

[26] W. Schollkopf and J. P. Toennies. Nondestructive Mass Selection of Small van der Waals Clusters. *Science*, 266:1345, 1994.

[27] M. Arndt, O. Nairz, J. Vos-Andreae, C. Keller, G. van der Zouw, and A. Zeilinger. Wave–particle duality of C60 molecules. *Nature*, 401:680, 1999.

[28] N. Bohr. Can quantum mechanical description of physical reality be considered complete? *Physical Review*, 48:777, 1935.

[29] P. A. Schilpp. *Albert Einstein: Philosopher-Scientist, Living Philosophers Vol. VII.* MJF Books, New York, 3ed. edition, 1969.

[30] M. Schlosshauer. Decoherence, the measurement problem, and interpretations of quantum mechanics. *Review of Modern Physics*, 76:1267, 2005.

[31] A. Bassi, K. Lochan, S. Satin, T. P. Singh, and H. Ulbricht. Models of wave-function collapse, underlying theories, and experimental tests. *Review of Modern Physics*, 85:471, 2013.

[32] D. Aerts and M. S. de Bianchi. The extended Bloch representation of quantum mechanics and the hidden-measurement solution to the measurement problem. *Annals of Physics*, 351:975, 2014.

[33] J. A. Wheeler. The "Past" and the 'Delayed Choice' Double-Slit experiment, in A.R. Marlow Mathematical Foundations of Quantum Theory. New York, 1978. pg.9.

[34] J. A. Wheeler and W. H. Zurek. *Quantum Theory and Measurement*, page 182. Princeton University Press, New Jersey, 1984.

[35] M. O. Scully and K. Drühl. Quantum eraser: A proposed photon correlation experiment concerning observation and "delayed choice" in quantum mechanics. *Physical Review A*, 25:2208, 1982.

[36] S. P. Walborn, M. O. Terra Cunha, S. Pádua, and C. H. Monken. Double-slit quantum eraser. *American Scientistt*, 91:033818, 2003.

[37] P. G. Kwiat, K. Mattle, H. Weinfurter, A. Zeilinger, A. V. Sergienko, and Y. Shih. New High-Intensity Source of Polarization-Entangled Photon Pairs. *Physical Review Letters*, 75:4337, 1995.

[38] W. H. Zurek. Decoherence, einselection, and the quantum origins of the classical. *Reviews of Modern Physics*, 75:715, 2003.

[39] W. H. Zurek. Decoherence and the Transition from Quantum to Classical — Revisited. *Nos Alamos Science*, 27, 2002.

[40] J. R. Anglin, J. P. Paz, and W. H. Zurek. Deconstructing Decoherence. *Physical Review A*, 5:4041, 1997.

[41] A. C. Oliveira. Classical limit of quantum mechanics induced by continuous measurements. *Physica A: Statistical Mechanics and its Applications*, 393:655, 2013.

[42] R. Correa and P. L. Saldanha. Photon reflection by a quantum mirror: A wave-function approach. *Physical Review A*, 93:023803, 2016.

[43] R. Gilmore. *Alice in Quantumland: A Charming Illustrated Allegory of Quantum Mechanics.* Copernicus, New York, 1994.

[44] M. Aspelmeyer, T. J. Kippenberg, and F. Marquardt. Cavity Optomechanics. *Reviews of Modern Physics*, 86:1391, 2014.

[45] E. Wolf and L. Mandel. *Optical Coherence and Quantum Optics*, volume 1. Cambridge University Press, Berlin, 1995.

[46] R. W. Boyd. Intuitive explanation of the phase anomaly of focused light beams. *Journal of the Optical Society of America*, 70:877, 2017.

[47] L. E. Ballentine. *Quantum Mechanics: A Modern Development*, volume 1. Simon Fraser University, London, 1998.

[48] D. W. Keith, C. R. Ekstrom, Q. A. Turchette, , and D. Pritchard. An interferometer for atoms. *Physical Review Letters*, 66:2693, 1991.

[49] L. Marton. Electron Interferometer. *Physical Review*, 85:1057, 1952.

[50] L. Marton, J. A. Simpson, and J. A. Suddeth. Electron Beam Interferometer. *Physical Review*, 90:490, 1953.

[51] P. Sonnentag and F. Hasselbach. Decoherence of electron waves due to induced charges moving through a nearby resistive material. *Brazillian Journal of Physics*, 35:385, 2005.

[52] A. Tonomura, N. Osakabe, T. Matsuda, T. Kawasaki, and J. Endo. Evidence for aharonov-bohm effect with magnetic field completely shielded from electron wave. *Physical Review Letters*, 56:795, 1986.

[53] H. C. Sow, K. Harada, A. Tonomura, G. Crabtree, and D. G. Grier. Measurement of the vortex pair interaction potential in a type-ii superconductor. *Physical Review Letters*, 80:2693, 1998.

[54] A. Tonomura, T. Matsuda, T. Kawasaki, J. Endo, and N. Osakabe. Sensitivity-enhanced electron-holographic interferometry and thickness-measurement applications at atomic scale. *Physical Review Letters*, 54:60, 1985.

[55] C. R. Ekstrom, J. Schmiedmayer, M. S. Chapman, T. D. Hammond, and D. E. Pritchard. Measurement of the electric polarizability of sodium with an atom interferometer. *Physical Review A*, 51:3883, 1995.

[56] A. Miffre, R. Delhuille, B. V. de Lesegno, M. Buchner, C. Rizzo, and J. Vigue. The three-grating Mach–Zehnder optical interferometer: a tutorial approach using particle optics. *European Journal of Physics*, 23:623, 2002.